NAVAL POSTGRADUATE SCHOOL
Monterey, California

THESIS

THE USE OF FILTERS IN DIGITAL COHERENT
RECEIVERS OPERATING IN A JAMMING
AND NOISE ENVIRONMENT

by

Damian Macone

June 1985

Thesis Advisor: D. Bukofzer

Approved for public release; distribution unlimited

REPORT DOCUMENTATION PAGE		READ INSTRUCTIONS BEFORE COMPLETING FORM
1. REPORT NUMBER	2. GOVT ACCESSION NO.	3. RECIPIENT'S CATALOG NUMBER
4. TITLE (and Subtitle) The Use of Filters in Digital Coherent Receivers Operating in a Jamming and Noise Environment		5. TYPE OF REPORT & PERIOD COVERED Master's Thesis June 1985
		6. PERFORMING ORG. REPORT NUMBER
7. AUTHOR(s) Damian Macone		8. CONTRACT OR GRANT NUMBER(s)
9. PERFORMING ORGANIZATION NAME AND ADDRESS Naval Postgraduate School Monterey, California 93943-5100		10. PROGRAM ELEMENT, PROJECT, TASK AREA & WORK UNIT NUMBERS
11. CONTROLLING OFFICE NAME AND ADDRESS Naval Postgraduate School Monterey, California 93943-5100		12. REPORT DATE June 1985
		13. NUMBER OF PAGES 132
14. MONITORING AGENCY NAME & ADDRESS(if different from Controlling Office)		15. SECURITY CLASS. (of this report) Unclassified
		15a. DECLASSIFICATION/DOWNGRADING SCHEDULE

16. DISTRIBUTION STATEMENT (of this Report)

Approved for public release; distribution unlimited

17. DISTRIBUTION STATEMENT (of the abstract entered in Block 20, if different from Report)

18. SUPPLEMENTARY NOTES

19. KEY WORDS (Continue on reverse side if necessary and identify by block number)

Jamming; Digital Receivers, Filtering

20. ABSTRACT (Continue on reverse side if necessary and identify by block number)

The effectiveness of the use of front-end bandstop filters in coherent digital receivers versus previously derived optimum jammer waveforms is analyzed. The receivers studied are the binary frequency shift key (FSK) and binary phase shift key (PSK) coherent (correlator) receivers. The filters analyzed for use against an optimum jammer are a single bandstop region ideal filter, and a second order single bandstop region real filter.

DD FORM 1473 1 JAN 73 EDITION OF 1 NOV 65 IS OBSOLETE
S/N 0102-LF-014-6601

1 UNCLASSIFIED

#20 - ABSTRACT - (CONTINUED)

General expressions in frequency domain form, are
derived for the probability of error of coherent receivers
with a front-end filter, then applied specifically
to the performance of receivers operating in the
presence of noise, jamming, and PSK or FSK modulation.
Finally these results are presented in graphical form
and, additionally, analyzed and interpreted.

The Use of Filters in Digital Coherent
Receivers Operating in a Jamming
and Noise Environment

by

Damian Macone
B.S., Tufts University, 1978

Submitted in partial fulfillment of the
requirements for the degree of

MASTER OF SCIENCE IN ELECTRICAL ENGINEERING

from the

NAVAL POSTGRADUATE SCHOOL
June 1985

ABSTRACT

The effectiveness of the use of front-end bandstop filters
in coherent digital receivers versus previously derived optimum
jammer waveforms is analyzed. The receivers studied are the
binary frequency shift key (FSK) and binary phase shift key
(PSK) coherent (correlator) receivers. The filters analyzed
for use against an optimum jammer are a single bandstop region
ideal filter, and a second order single bandstop region real
filter. General expressions in frequency domain form, are
derived for the probability of error of coherent receivers
with a front-end filter, then applied specifically to the
performance of receivers operating in the presence of noise,
jamming, and PSK or FSK modulation. Finally these results are
presented in graphical form and, additionally, analyzed and
interpreted.

4

TABLE OF CONTENTS

5

LIST OF FIGURES

8

ACKNOWLEDGEMENTS

I wish to thank Prof. Daniel Bukofzer for his support and guidance in the preparation of this thesis.

I. INTRODUCTION

This thesis investigates the use of filtering techniques as an electronic counter countermeasure (ECCM) to overcome the effects of the optimum jammer operating against coherent phase shift key (PSK) and frequency shift key (FSK) receivers. These receivers are well-known solutions to the problem of optimum detection of known signals in the presence of additive white Gaussian noise (WGN) [Ref. 1]. The structure of such receivers is shown in Figure A.1. These two receivers represent the optimum signal processing algorithms for the discrimination of the digital signals $s_1(t)$ and $s_0(t)$ representing digital "one" and "zero" logical states respectively. To reduce the effectiveness of these optimum receivers, Ref. 2 and Ref. 3 developed optimum jammers to be used against the PSK and FSK coherent receivers. From the resultant jammer waveforms derived in these references, this thesis investigates the use of front-end filters inserted in these receivers as shown in Figure A.2 as a method for reducing jammer effectiveness.

From Ref. 2, the optimum power constrained jammer for either the coherent PSK or FSK receiver is a signal proportional to the correlator signal, shown in Figure A.2 as $s_d(t)$. This correlator signal (see Ref. 1) is proportional to the difference of $s_1(t)$ and $s_0(t)$, the digital "one" and "zero" signals. Though the correlator signal can take different forms

10

in these receivers depending on the modulation used, the theory used to develop these receivers shows that a jammer waveform, proportional to the difference of $s_1(t)$ and $s_0(t)$, is optimal.

The jammer, therefore, takes the form of a continuous wave (cw) or tone centered at the frequencies of $s_1(t)$ and $s_0(t)$. In the case of the PSK coherent receiver, the jammer is a single tone centered at the signaling frequency. For the FSK case, the jammer waveform consists of the difference of two tones at the frequencies of $s_1(t)$ and $s_0(t)$. The use of tones or cw jammers in angle modulated analog or digital receivers is discussed in Ref. 4.

Given these forms of jammer signals, an obvious choice for the front-end filter is a band reject or bandstop filter. The filters chosen for analysis in this thesis are the ideal bandstop filter and a single zero second order bandstop filter. Though the ideal filter is not realizable, the analysis involving its use will provide both insight into the problem and approximate results before investigating the use of the more complex second order filter. For the PSK coherent receiver, the bandstop regions of both the ideal and second order filters are centered at the frequency of $s_1(t)$ which is also equal to the frequency of $s_0(t)$. Since in this thesis a filter with only a single bandstop region will be analyzed, the bandstop region of the ideal and second order filters used in the FSK coherent receiver will be centered midway between the frequencies of $s_1(t)$ and $s_0(t)$.

11

The analysis of the two forms will begin with the statistics of G, the output of the coherent receiver. From Ref. 2, G is a conditional Gaussian random variable with conditional statistics depending on whether $s_1(t)$ or $s_0(t)$ was transmitted. The analysis will then focus on determining the statistics of the random variable G', the output of the receiver with a front-end filter as shown in Figure A.2. The mean and variance, conditioned on whether $s_1(t)$ or $s_0(t)$ was transmitted will then be determined using frequency domain analysis techniques. Finally, the general analysis will conclude with the determination of an expression for the probability of error of the coherent digital receiver using a front-end filter to counter the optimum jammer. Next, the specific frequency domain forms of the PSK and FSK signals and jammers will be developed and used to calculate the probability of error performance for these receivers with and without front-end filters.

To determine the Fourier transforms of the jammers, this thesis will first assume that the jammer waveform is a time truncated function. Since in References 1, 2, and 3, the correlator signal $s_d(t)$ is defined over the interval $(0,T)$, and the optimum jammer (from Ref. 3) is proportional to $s_d(t)$, the optimum jammer will be treated as defined in the interval $(0,T)$ also. Since from a practical standpoint, the jammer is a cw signal, the analysis will be modified in the sequel to account for this interpretation of the jammer.

In Chapter II, a development of the mathematical expressions in the form of frequency domain equations for the statistics

12

of G' (the output of the coherent receiver of Figure A.2) is undertaken. From these statistics, the expression for the receiver probability of error is developed. Chapter III demonstrates the application of these general expressions to the binary PSK (BPSK) coherent receiver problem with both ideal and second order front-end filters. Chapter IV presents similar analysis to that in Chapter III, applied now to the binary FSK (BFSK) coherent receiver. Chapter V presents quantitative and graphical analysis of the four receiver/ filter combinations, under the assumptions of both the cw and time truncated jammer forms.

II. ANALYSIS OF DIGITAL COHERENT RECEIVERS WITH FRONT END FILTERS

In order to investigate the effects of filtering at the front-end of digital coherent receivers, it is necessary to review the operation and performance of digital coherent receivers in the presence of noise and jamming without the use of filters to notch out the jammer. As previously pre-sented in Ref. 2, the structure of the receiver to be analyzed is shown in Figure A.1. In the absence of a jamming signal this receiver is optimum for determining whether a "one" signal or a "zero" signal was transmitted in a given interval (0,T), with minimum probability of error [Ref. 1].

Following the analysis of Ref. 3, which assumes that the jammer is a deterministic waveform unknown to the receiver, the input signal r(t) to the receiver front-end is mathematically modeled as

$$r(t) = s_i(t) + n(t) + n_j(t) \quad 0 \leq t \leq T, \quad i = 0,1 \quad (2.1)$$

where the $s_i(t)$ (i = 0,1) are used to transmit the digital "one" and "zero" data, n(t) is a sample function of a white Gaussian noise process with power spectral density level of $N_0/2$ watts/hertz, and as stated previously $n_j(t)$ is the jammer waveform. From the analysis of Ref. 2, the output of the receiver is given by

$$G = (r, s_d) + \frac{1}{2}[||s_0||^2 - ||s_1||^2] \qquad (2.2)$$

where

$$(x,y) = \int_a^T x(t)y(t)\,dt \quad \text{and} \quad ||x||^2 = (x,x)$$

Since G is a (conditional) Gaussian random variable, the statistics are completely determined when the conditional mean and variance are found. The conditional mean is given by

$$E[G|s_i \text{ transmitted}] = (s_i, s_d) + (n_j, s_d)$$
$$+ \frac{1}{2}[||s_0||^2 - ||s_1||^2] \qquad (2.3)$$
$$i = 0,1$$

and the conditional variance is given by

$$\text{VAR}[G|s_i(t) \text{ transmitted}] = \frac{N_0}{2} ||s_d||^2, \quad i = 0,1 . \qquad (2.4)$$

A. FILTERING EFFECTS ON THE MEAN AND VARIANCE

The effect of placing a filter at the front-end of the receiver is now analyzed by evaluating the conditional mean and variance of the receiver output. Figure A.2 shows the placement of the filter at the receiver front-end. It can be seen that G becomes G' where

15

$$G' = (r', s_d) + \frac{1}{2}[||s_0||^2 - ||s_1||^2]$$

$$(2.5)$$

$$r' = r * h = \int_{-\infty}^{\infty} h(t-\alpha) r(\alpha) d\alpha$$

and $h(t)$ is the front-end filter impulse response. Since

$$r'(t) = s_i'(t) + n'(t) + n_j'(t) \quad i = 0,1 \quad (2.6)$$

it is simple to see that

$$E[G'|s_i(t) \text{ transmitted}] = (s_i', s_d) + (n_j', s_d)$$

$$+ \frac{1}{2}[||s_0||^2 - ||s_1||^2] \quad (2.7)$$

$$i = 0,1$$

where

$$s_i'(t) = s_i(t) * h(t)$$

$$n_j'(t) = n_j(t) * h(t)$$

It is much more convenient to specify filters in the frequency domain because convolutions in the time domain become multiplications in the frequency domain. Thus looking specifically at the term (s_i', s_d) where

$$(s_i', s_d) = \int_0^T s_i'(t) s_d(t) dt \quad i = 0,1 \quad (2.8)$$

16

or

$$(s_i', s_d) = \int_{-\infty}^{\infty} s_i'(t) s_{dp}(t) dt \qquad i = 0,1 \qquad (2.9)$$

where

$$s_{dp}(t) = s_d(t) \cdot p(t)$$

with

$$p(t) = \begin{cases} 1, & 0 \le t \le T \\ 0, & \text{elsewhere} \end{cases}$$

and replacing $s_{dp}(t)$ by its inverse Fourier transform equivalent $(s_{dp}(t) \iff S_{dp}(\omega))$, namely

$$s_{dp}(t) = \frac{1}{2\pi} \int_{-\infty}^{\infty} S_{dp}(\omega) e^{j\omega t} d\omega \qquad (2.10)$$

yields

$$(s_i', s_d) = \int_{-\infty}^{\infty} s_i'(t) [\frac{1}{2\pi} \int_{-\infty}^{\infty} S_{dp}(\omega) e^{j\omega t} d\omega] dt \qquad (2.11)$$

Interchanging the order of integration yields

17

$$(s_i', s_d) = \frac{1}{2\pi} \int_{-\infty}^{\infty} S_{dp}(\omega) [\int_{-\infty}^{\infty} s_i'(t) e^{j\omega t} dt] d\omega \quad i = 0, 1 \qquad (2.12)$$

and recognizing the fact that

$$\int_{-\infty}^{\infty} s_i'(t) e^{j\omega t} dt = S_i'(-\omega) \quad i = 0, 1$$

results in

$$(s_i', s_d) = \frac{1}{2\pi} \int_{-\infty}^{\infty} S_{dp}(\omega) S_i'(-\omega) d\omega \quad i = 0, 1 \qquad (2.13)$$

Furthermore, since

$$s_i'(t) = s_i(t) * h(t) \quad i = 0, 1$$

$S_i'(\omega)$ is given by

$$S_i'(\omega) = S_i(\omega) H(\omega) \quad i = 0, 1$$

and therefore

$$(s_i', s_d) = \frac{1}{2\pi} \int_{-\infty}^{\infty} S_{dp}(\omega) S_i(-\omega) H(-\omega) d\omega \quad i = 0, 1 \qquad (2.14)$$

Replacing $s_d(t)$ with $s_{dp}(t)$ as in Equation 2.9, the term (n_j', s_d) becomes

$$(n_j', s_d) \quad = \quad \int_{-\infty}^{\infty} n_j'(t) s_{dp}(t) \, dt \qquad (2.15)$$

and using Equation 2.10 in Equation 2.15 yields

$$(n_j', s_d) \quad = \quad \int_{-\infty}^{\infty} n_j'(t) \left[\frac{1}{2\pi} \int_{-\infty}^{\infty} S_{dp}(\omega) e^{j\omega t} d\omega\right] dt \qquad (2.16)$$

As done in Equations 2.11-2.13, interchanging the order of integration and using

$$N_j'(-\omega) \quad = \quad \int_{-\infty}^{\infty} n_j'(t) e^{j\omega t} dt \qquad (2.17)$$

with

$$N_j'(\omega) \quad = \quad N_j(\omega) H(\omega)$$

finally yields

$$(n_j', s_d) \quad = \quad \frac{1}{2\pi} \int_{-\infty}^{\infty} S_{dp}(\omega) N_j(-\omega) H(-\omega) \, d\omega \qquad (2.18)$$

The conditional mean of g', given that $s_i(t)$ is transmitted, is

$$E[G' | s_i(t) \text{ transmitted}] = \frac{1}{2\pi} \int_{-\infty}^{\infty} S_{dp}(\omega) S_i(-\omega) H(-\omega) d\omega$$

$$+ \frac{1}{2\pi} \int_{-\infty}^{\infty} S_{dp}(\omega) N_j(-\omega) H(-\omega) d\omega$$

$$+ \frac{1}{2}[||s_o||^2 - ||s_1||^2] \qquad (2.19)$$

$$i = 0,1$$

The variance of g' given that $s_i(t)$ is transmitted can be shown to take on the form

$$VAR[G' | s_i \text{ transmitted}] = E[(n'(t), s_d(t))^2] \qquad (2.20)$$

The right hand side of this equation becomes

$$E[(n'(t), s_d(t))^2]$$

$$= E[\int_{-\infty}^{\infty} n'(t) s_{dp}(t) dt \int_{-\infty}^{\infty} n'(\tau) s_{dp}(\tau) d\tau] \qquad (2.21)$$

Equation 2.21 can now be written as

$$E[(n'(t), s_d(t))^2]$$

$$= \int_{-\infty}^{\infty} \int_{-\infty}^{\infty} E[n'(t) n'(\tau)] s_{dp}(t) s_{dp}(\tau) dt d\tau \qquad (2.22)$$

20

Recognizing that the expected value operation in the integral is the autocorrelation function of the filtered white Gaussian noise, $R_{n'}(t-\tau)$, Equation 2.21 can be written as

$$E[(n',s_d)^2]$$

$$= \int_{-\infty}^{\infty} \int_{-\infty}^{\infty} R_{n'}(t-\tau) s_{dp}(t) s_{dp}(\tau) \, dt \, d\tau \qquad (2.23)$$

Again, it is much more convenient to continue the analysis in the frequency domain. Using the inverse Fourier transform for the frequency domain representation of $R_{n'}(t-\tau)$ and substituting into Equation 2.23 yields

$$E[(n',s_d)^2]$$

$$= \int_{-\infty}^{\infty} \int_{-\infty}^{\infty} [\frac{1}{2\pi} \int_{-\infty}^{\infty} S_{n'}(\omega) e^{j\omega(t-\tau)} d\omega] s_{dp}(t) s_{dp}(\tau) \, dt \, d\tau$$

$$(2.24)$$

where $s_{dp}(t)$ is defined by Equation 2.9. Interchanging the order of integration, Equation 2.24 becomes

$$E[(n',s_d)^2]$$

$$= \frac{1}{2\pi} \int_{-\infty}^{\infty} S_{n'}(\omega) \, d\omega \int_{-\infty}^{\infty} s_{dp}(t) e^{j\omega t} dt \int_{-\infty}^{\infty} s_{dp}(\tau) e^{-j\omega \tau} d\tau$$

$$(2.25)$$

It is easily recognized that

21

$$\int_{-\infty}^{\infty} s_{dp}(t) e^{j\omega t} dt \;=\; S_{dp}(-\omega) \;=\; S_{dp}^{*}(\omega)$$

and

$$\int_{-\infty}^{\infty} s_{dp}(\tau) e^{-j\omega \tau} d\tau \;=\; S_{dp}(\omega)$$

Therefore in the frequency domain, VAR($G' \mid s_i$ transmitted) becomes

$$\text{VAR}[G' \mid s_i(t) \text{ transmitted}] \;=\; \frac{1}{2\pi} \int_{-\infty}^{\infty} S_{n'}(\omega) \, |S_{dp}(\omega)|^2 \, d\omega \qquad (2.26)$$

Finally since $n'(t) = n(t) * h(t)$, it is well known that

$$S_{n'}(\omega) \;=\; S_{n}(\omega) \, |H(\omega)|^2$$

Since $n(t)$ is a sample function of a random process that was assumed to have power spectral density $S_n(\omega) = N_0/2$, for all ω,

$$\text{Var}[G' \mid s_i(t) \text{ transmitted}] \;=\; \frac{N_0}{2\pi} \int_{0}^{\infty} |H(\omega)|^2 \, |S_{dp}(\omega)|^2 \, d\omega \qquad (2.27)$$

where the fact that $|H(\omega)|^2 |S_{dp}(\omega)|^2$ is an even symmetric function has been used to reduce the limits of integration to half the real line.

22

In summary, G' is a (conditional) Gaussian random variable with conditional mean and variance given by

$$E[G'|s_i(t) \text{ transmitted}]$$

$$= \frac{1}{2\pi} \int_{-\infty}^{\infty} S_{dp}(\omega) S_i(-\omega) H(-\omega) d\omega$$

$$+ \frac{1}{2\pi} \int_{-\infty}^{\infty} S_{dp}(\omega) N_j(-\omega) H(-\omega) d\omega + \frac{1}{2}[||s_0||^2 - ||s_1||^2]$$

$$i = 0,1 \qquad\qquad (2.28)$$

and

$$VAR[G'|s_i(t) \text{ transmitted}]$$

$$= \frac{N_0}{2\pi} \int_0^{\infty} |H(\omega)|^2 |S_{dp}(\omega)|^2 d\omega \qquad i = 0,1 \qquad (2.29)$$

B. PROBABILITY OF ERROR PERFORMANCE

The analysis thus far has been concerned with determining the statistics of the random variable G', the output of the coherent receiver. The next step is to determine the probability of error from the decision process, where the amplitude of G' is compared with a threshold γ. Referring to Figure A.2, if the value of G' is greater than γ, the receiver decides that a "one" or $s_1(t)$ was transmitted, and conversely if the value of G' is less than γ the receiver decides that a "zero" or $s_0(t)$ was transmitted. The quantity, γ, is determined in the derivation of the optimum receiver for detecting known signals

23

in additive white noise [see Ref. 1]. That analysis determines the threshold of the correlator (coherent) receiver as

$$\gamma = \frac{N_0}{2} \ln \eta + \frac{1}{2} \int_0^T [y_1^2(t) - y_0^2(t)] dt \qquad (2.30)$$

However the receiver of Figure A.2 treats the second term of Equation 2.30 as a bias, thus the threshold becomes

$$\gamma = \frac{N_0}{2} \ln \eta \qquad (2.31)$$

where $N_0/2$ is the power spectral density level of the white Gaussian noise process. Here, η is determined by the specific decision rule applied. In this case, the receiver strategy is to detect $s_1(t)$ or $s_0(t)$ with minimum probability of error, so from Ref. 1

$$\eta = \frac{P\{s_1(t) \text{ was transmitted}\}}{P\{s_0(t) \text{ was transmitted}\}} \qquad (2.32)$$

All further analysis in this thesis will assume that the probability that $s_1(t)$ was transmitted is equal to that of $s_0(t)$ being transmitted, so the decision threshold is

$$\gamma = \frac{N_0}{2} \ln 1 = 0 \qquad (2.33)$$

Now, the receiver can make two types of errors. Specifically, deciding that $s_0(t)$ was transmitted when in fact $s_1(t)$

was transmitted (defined as error 1), and deciding that $s_1(t)$ was transmitted when $s_0(t)$ was actually transmitted (defined as error 2). The receiver decides that $s_0(t)$ was transmitted when G' is less than the threshold γ, and that $s_1(t)$ was transmitted when G' is greater than γ. So, the probability of error 1 occurring is the probability that G' is less than γ when $s_1(t)$ is transmitted. Since G' is a Gaussian random variable with conditional probability desnity functions dependent on whether $s_1(t)$ or $s_0(t)$ was transmitted

$$P_{error\ 1} = \int_{-\infty}^{\gamma} \frac{1}{\sqrt{2\pi v_g}} e^{-\frac{(g'-m_1)^2}{2v_g}} dg' \qquad (2.34)$$

where $m_1 = E[G'|s_1(t)$ was transmitted$]$ and $v_g = VAR[G'|s_1(t)$ was transmitted$]$. By letting $x = g'-m_1/\sqrt{v_g}$, Equation 2.34 becomes the integral of the standard Gaussian probability density function also known as the error function (erf(x)) of the form

$$P_{error\ 1} = \int_{-\infty}^{-m_1/\sqrt{v_g}} \frac{1}{\sqrt{2\pi}} e^{-x^2/2} dx \qquad (2.35)$$

The probability of error 2 occurring is the probability that G' is greater than γ when $s_0(t)$ is transmitted. Therefore

$$P_{error\ 2} = \int_{\gamma}^{\infty} \frac{1}{\sqrt{2\pi v_g}} e^{-(g'-m_0)^2/2v_g} dg' \qquad (2.36)$$

25

where

$$m_0 = E[G' | s_i(t) \text{ transmitted}].$$

Using a similar change of variables as in Equation 2.35
yields

$$P_{\text{error 2}} = \int_{-m_0/\sqrt{v_g}}^{\infty} \frac{1}{\sqrt{2\pi}} e^{-x^2/2} \, dx \tag{2.37}$$

where γ is zero from Equation 2.33. Finally, the average
probability of error becomes

$$P_e = p \, P_{\text{error 1}} + (1-p) \, P_{\text{error 2}} \tag{2.38}$$

where $p = P\{s_1(t) \text{ was transmitted}\}$ and $1-p = P\{s_0(t) \text{ was}$
transmitted$\}$. Since $p = 1/2$ and substituting Equations 2.35
and 2.37 into 2.38, the average probability of error is

$$P_e = \frac{1}{2} \left[\int_{-\infty}^{-m_1/\sqrt{v_g}} \frac{1}{\sqrt{2\pi}} e^{-x^2/2} \, dx \right.$$

$$+ \left. \int_{-m_0/\sqrt{v_g}}^{\infty} \frac{1}{\sqrt{2\pi}} e^{-x^2/2} \, dx \right] \tag{2.39}$$

26

III. PHASE SHIFT KEY COHERENT RECEIVER
WITH A FRONT-END FILTER

A. PHASE SHIFT KEY WITH AN IDEAL FRONT-END FILTER

Using the equations for the mean and variance of the con-
ditional Gaussian random variable G' (Equations 2.28 and 2.29),
along with the probability of error equation (Equation 2.39),
it is possible to investigate the effect of a front-end filter
on the probability of error performance of the coherent receiver.
The receiver analyzed in this case is the optimum receiver for
binary phase shift key modulated signals with an ideal band-
stop filter in the front-end. The filter will be characterized
as having a gain of unity over all frequencies, with the excep-
tion of the regions from $\omega = \pm\omega_0 - B/2$ to $\omega = \pm\omega_0 + B/2$ where
the gain is zero. The bandwidth of the filter is B radians/
second and the center frequency is ω_0 radians/second. Although
this filter is not realizable, it serves both as a good approxi-
mation to a higher order bandstop filter, and as a simple
example so as to gain insight to the receiver performance.

Using Figure A.2 as a reference, the generic coherent
digital receiver can be made into a BPSK receiver by setting

$$s_d(t) \ = \ 2A \cos \omega_0 t \qquad 0 \le t \le T \tag{3.1}$$

and modeling the input PSK signals as

$$s_i(t) = A \cos(\omega_0 t + \theta_i(t)) \quad 0 \le t \le T, \quad i = 0,1 \qquad (3.2)$$

where

$$\theta_i(t) = \begin{cases} \pi & \text{for} \quad i = 0 \\ 0 & \text{for} \quad i = 1 \end{cases}$$

Thus $s_i(t)$ $(i = 0,1)$ can be expressed as

$$s_0(t) = -A \cos \omega_0 t$$
$$0 \le t \le T \qquad (3.3)$$
$$s_1(t) = A \cos \omega_0 t .$$

The jammer waveform is set to

$$n_j(t) = \sqrt{P_{nj}} \sqrt{2/T} \cos \omega_0 t \quad 0 \le t \le T \qquad (3.4)$$

since in Ref. 2 it was shown to be optimum against BPSK trans-mission. Here P_{nj} is the jammer output power. Finally the noise input into the receiver of Figure A.2 is a white Gaussian random process with power spectral density level of $N_0/2$ watts/hertz.

1. Calculation of the Variance

From Equation 2.27, the variance of G' conditioned on $s_i(t)$ being transmitted is given by

VAR[G'$\mid s_i$(t) transmitted]

$$= \frac{N_0}{2\pi} \int_0^\infty |H(\omega)|^2 |S_{dp}(\omega)|^2 d\omega \qquad i = 0,1 \qquad (3.5)$$

Since the front-end filter is ideal, Equation 3.5 can be modified to become

VAR[G'$\mid s_i$(t) transmitted]

$$= \frac{N_0}{2\pi} [\int_0^\infty |S_{dp}(\omega)|^2 d\omega - \int_{\omega_0 - B/2}^{\omega_0 + B/2} |S_{dp}(\omega)|^2 d\omega \qquad (3.6)$$

$$i = 0,1$$

since $|H(\omega)|^2$ is unity except over the bandstop region.

In order to calculate $|S_{dp}(\omega)|^2$, since $s_{dp}(t) = s_d(t)p(t)$ where

$$p(t) = \begin{cases} 1 & 0 \le t \le T \\ 0 & \text{elsewhere} \end{cases}$$

then

$$s_{dp}(t) = 2A \, p(t) \, \cos \rho_0 t \qquad (3.7)$$

The Fourier transform identity $f(t) \cdot g(t) \iff (1/2\pi) \times F(\omega) * G(\omega)$ will be used in order to calculate $S_{dp}(\omega)$. Since $P(\omega)$ is

29

$$P(\omega) = T \, Sa(\omega T/2) e^{-j\omega T/2} \qquad (3.8)$$

and

$$S_d(\omega) = 2A\pi[\delta(\omega-\omega_0) + \delta(\omega+\omega_0)]$$

$S_{dp}(\omega)$ is the convolution of these Fourier transforms, result-
ing in

$$S_{dp}(\omega) = AT[Sa(\omega-\omega_0)\frac{T}{2}e^{-j(\omega-\omega_0)T/2}$$
$$+ Sa(\omega+\omega_0)\frac{T}{2}e^{-j(\omega+\omega_0)T/2}] \qquad (3.9)$$

From this, $|S_{dp}(\omega)|^2$ is obtained by multiplying $S_{dp}(\omega)$ by
$S_{dp}(-\omega)$ which results in

$$|S_{dp}(\omega)|^2 = A^2T^2 \cdot [Sa^2(\omega-\omega_0)\frac{T}{2} + Sa^2(\omega+\omega_0)\frac{T}{2}] \qquad (3.10)$$

where the product of $Sa(\omega+\omega_0)T/2$ and $Sa(\omega-\omega_0)T/2$ has been
ignored because it is essentially zero for practical values
of ω_0 and T.

Since the variance consists of an integral from $\omega = 0$
to infinity, for large ω_0 the contribution of the $Sa(\omega+\omega_0)T/2$
term is negligible. Therefore, substituting into Equation 3.6
yields

Var$[G'|s_i(t)$ transmitted]

$$= A^2 T^2 \frac{N_0}{2\pi} [\int_0^\infty Sa^2(\omega-\omega_0) \frac{T}{2} d\omega - \int_{\omega_0-B/2}^{\omega_0+B/2} Sa^2(\omega-\omega_0) \frac{T}{2} d\omega] \qquad (3.11)$$

$$i = 0,1$$

In this form Equation 2.11 is unmanageable due to its complexity and the number of variables present. To simplify, the follow-ing substitutions will be made:

1. $x = (\omega-\omega_0) T/2$, $2/Tdx = d\omega$

2. for $\omega = 0$, $x = -\omega_0 T/2$ which for large values of $\omega_0 T$
    becomes approximately $-\infty$

3. for $\omega = \infty$, $x = \infty$

4. for $\omega = \omega_0 \pm B/2$, $x = \pm BT/4$

Equation 3.11 now becomes

VAR$[G'|s_i(t)$ transmitted]

$$= \frac{A^2 TN_0}{\pi} [\int_{-\infty}^\infty Sa^2(x) dx - \int_{-BT/4}^{BT/4} Sa^2(x) dx] \qquad (3.12)$$

$$i = 0,1$$

Finally the $Sa^2(x)$ is a symmetric function about $x = 0$ and $\int_0^\infty Sa^2(x) dx = \pi/2$ from math tables. Thus the variance of G'

can be written as

$$\text{VAR}[G' \mid s_i(t) \text{ transmitted}]$$

$$= N_0 A^2 T \frac{2}{\pi} [\frac{\pi}{2} - \int_0^{BT/4} Sa^2(x)\,dx] \qquad i = 0,1 \tag{3.13}$$

2. Calculation of the Conditional Mean

The conditional mean of G' is given by Equation 2.7 and shown here for convenience,

$$E[G' \mid s_i(t) \text{ transmitted}]$$

$$= (s_i', s_d) + (n_j', s_d) + \frac{1}{2}[||s_0||^2 - ||s_1||^2] \qquad i = 0,1$$

and consists of three terms. The frequency domain forms of (s_i', s_d) and (n_j', s_d) are given by Equations 2.14 and 2.18 respectively. The term $\frac{1}{2}[||s_0||^2 - ||s_1||^2]$ (recall that $||s_0||^2 = \int_0^T s_0^2(t)\,dt$), represents the difference between the energy contained in $s_0(t)$ and $s_1(t)$. Since our signals are equal energy signals, the term in question becomes zero. Thus the conditional mean becomes

$$E[G' \mid s_i(t) \text{ transmitted}] = (s_i', s_d) + (n_j', s_d) \qquad i = 0,1 \tag{3.14}$$

Looking first at the term (n_j', s_d) and recalling that $H(\omega)$ is an ideal filter, Equation 2.18 can be modified to

32

$$(n_j', s_d) = \frac{1}{2\pi} [\int_{-\infty}^{\infty} S_{dp}(\omega) N_j(-\omega) d\omega$$

$$- \int_{\omega_0-B/2}^{\omega_0+B/2} S_{dp}(\omega) N_j(-\omega) d\omega - \int_{-\omega_0-B/2}^{-\omega_0+B/2} S_{dp}(\omega) N_j(-\omega) d\omega]$$

(3.15)

In order to evaluate Equation 3.15, the product $N_j(-\omega) S_{dp}(\omega)$ must be calculated using $n_j(t)$ as given by Equation 3.4. However, since the model of the coherent receiver in Figure A.2 contains a finite time integrator, $n_j(t)$ is effectively truncated to the interval $0 < t < T$, or equivalently, the new term $n_{jp}(t)$ replaces $n_j(t)$ where $n_{jp}(t) = n_j(t) p(t)$ and $p(t)$ is as previously defined. Thus, $N_{jp}(\omega)$ becomes

$$N_{jp}(\omega) = \sqrt{P_{nj}} \sqrt{2/T} \frac{T}{2}$$

$$\cdot [Sa(\omega-\omega_0)\frac{T}{2}e^{-j(\omega-\omega_0)T/2} + Sa(\omega+\omega_0)T/2e^{-j(\omega+\omega_0)T/2}] \quad (3.16)$$

Multiplying $N_{jp}(-\omega)$ and $S_{dp}(\omega)$ yields four terms: two Sa terms centered at ω_0 and $-\omega_0$ and two terms that involve the product of $Sa(\omega+\omega_0)T/2$ and $Sa(\omega-\omega_0)T/2$. It can easily be seen that for large ω_0 this product is essentially zero. Substituting into Equation 3.15 it is also easy to see that the contribution of the $Sa(\omega+\omega_0)T/2$ term in the integral with limits of $+\omega_0\pm B/2$ is negligible, so that (n_j', s_d) becomes

33

$$(n_j', s_d) \;=\; \frac{1}{2\pi} \frac{AT^2}{2} \sqrt{P_{nj}} \; \sqrt{2/T}$$

$$\cdot \left[\left(\int_{-\infty}^{\infty} Sa^2(\omega-\omega_0)\, \frac{T}{2} d\omega \;-\; \int_{\omega_0-B/2}^{\omega_0+T/2} Sa^2(\omega+\omega_0)\, \frac{T}{2} d\omega \right) \right.$$

$$\left. +\; \left(\int_{-\infty}^{\infty} Sa^2(\omega+\omega_0)\, \frac{T}{2} - \int_{-\omega_0-B/2}^{-\omega_0+B/2} Sa^2(\omega+\omega_0)\, \frac{T}{2} d\omega \right) \right] \tag{3.17}$$

Recognizing that the integrals of $Sa^2(\omega+\omega_0)T/2$ and $Sa^2(\omega-\omega_0)T/2$ are equal, performing the same change of variables as in Equation 3.11, (n_j', s_d) becomes

$$(n_j', s_d) \;=\; \frac{AT}{\pi} \sqrt{P_{nj}} \; \sqrt{2/T}$$

$$\cdot \left[\int_{-\infty}^{\infty} Sa^2(x)\, dx \;-\; \int_{-BT/4}^{BT/4} Sa^2(x)\, dx \right] \tag{3.18}$$

Finally, recognizing symmetry about $x = 0$ and using $\int_0^{\infty} Sa^2(x)\, dx = \pi/2$, we obtain

$$(n_j', s_d) \;=\; AT \sqrt{P_{nj}} \; \sqrt{2/T} \; \frac{2}{\pi} \left[\frac{\pi}{2} \;-\; \int_0^{BT/4} Sa^2(x)\, dx \right] \tag{3.19}$$

Looking now at the term (s_i', s_d), recalling again that $H(\omega)$ is an ideal filter, (s_i', s_d) can be written as

34

$$(s_i', s_d) = \frac{1}{2\pi}[\int_{-\infty}^{\infty} S_{dp}(\omega) S_i(-\omega) d\omega - \int_{\omega_0-B/2}^{\omega_0+B/2} S_{dp}(\omega) S_i(\omega) d\omega$$

$$- \int_{-\omega_0-B/2}^{-\omega_0-B/2} S_{dp}(\omega) S_i(-\omega) d\omega] \qquad (3.20)$$

$$i = 0,1$$

The signal models for $s_0(t)$ and $s_1(t)$ given by Equation 3.3 can be Fourier transformed to yield

$$S_0(\omega) = -\frac{AT}{2}[Sa(\omega-\omega_0)\frac{T}{2}e^{-j(\omega-\omega_0)T/2}$$

$$+ Sa(\omega+\omega_0)\frac{T}{2}e^{-j(\omega+\omega_0)T/2}] \qquad (3.21)$$

and

$$S_1(\omega) = \frac{AT}{2}[Sa(\omega-\omega_0)e^{-j(\omega-\omega_0)T/2}$$

$$+ Sa(\omega+\omega_0)\frac{T}{2}e^{-j(\omega+\omega_0)T/2} \qquad (3.22)$$

To calculate the specific case of (s_i', s_d), first form the product of $S_{dp}(\omega) S_0(-\omega)$. This yields four terms as in (n_j', s_d), where two are Sa terms centered at $\pm\omega_0$ and two are products of $Sa(\omega+\omega_0)T/2$ and $Sa(\omega-\omega_0)T/2$. The latter products can be neglected for large ω_0. Also, with respect to Equation 3.20, the contribution of the $Sa(\omega+\omega_0)T/2$ term to the integral whose limits are $+\omega_0+B/2$ is negligible. Therefore, substituting $S_{dp}(\omega) S_0(-\omega)$ into Equation 3.20 yields

$$(s_0', s_d) = \frac{-A^2 T^2}{2} \frac{1}{2\pi} [(\int_{-\infty}^{\infty} Sa^2(\omega - \omega_0) T/2 \; d\omega$$

$$- \int_{\omega_0 - B/2}^{\omega_0 + B/2} Sa^2(\omega - \omega_0) \frac{T}{2} d\omega) + (\int_{-\infty}^{\infty} Sa^2(\omega + \omega_0) \frac{T}{2} d\omega$$

$$- \int_{-\omega_0 - B/2}^{-\omega_0 - B/2} Sa^2(\omega + \omega_0) \frac{T}{2} d\omega)] \tag{3.23}$$

It is easily seen that the integrals involving $Sa^2(\omega + \omega_0) T/2$ are equal to the integrals involving the $Sa^2(\omega - \omega_0) T/2$ term. Making use of this observation and the same change of variables used in Equation 3.9, it is easily seen that

$$(s_0', s_d) = -A^2 T \frac{2}{\pi} [\int_{-\infty}^{\infty} Sa^2(x) dx - \int_{-BT/4}^{BT/4} Sa^2(x) dx] \tag{3.24}$$

and by using the symmetry of the $Sa^2(x)$ function, (s_0', s_d) becomes

$$(s_0', s_d) = -A^2 T \frac{2}{\pi} [\frac{\pi}{2} - \int_0^{BT/4} Sa^2(x) dx] \tag{3.25}$$

By similar analysis it can be shown that

$$(s_1', s_d) = A^2 T \frac{2}{\pi} [\frac{\pi}{2} - \int_0^{BT/4} Sa^2(x) dx] \tag{3.26}$$

In general terms, (s_i', s_d) $(i = 0,1)$ can be written as

$$(s_i', s_d) = -1^{(i+1)} A^2 T \frac{2}{\pi} [\frac{\pi}{2} - \int_0^{BT/4} Sa^2(x) dx] \quad i = 0,1 \quad (3.27)$$

so that the conditional mean of G' can be expressed as

$E[G' | s_i(t) \text{ transmitted}]$

$$= [AT\sqrt{P_{nj}} \sqrt{2/T} + -1^{(i+1)} A^2 T] [\frac{2}{\pi}(\frac{\pi}{2} - \int_0^{BT/4} Sa^2(x) dx)] \quad (3.28)$$

$$i = 0,1$$

3. Probability of Error Calculation

With the conditional mean and variance of G' given by Equations 3.28 and 3.13, it is now possible to compute the probability of error performance of the BPSK coherent receiver with an ideal front-end filter. Assuming the probability of the transmitter sending a "one" or a "zero" signal is the same $(P(s_1(t)) = P(s_0(t)) = 1/2))$, Equation 2.39 shows that the average probability of error P_e is

$$P_e = \frac{1}{2}[\int_{-m_0/\sqrt{V_g}}^{\infty} \frac{1}{\sqrt{2\pi}} e^{-x^2/2} dx + \int_{-\infty}^{-m_1/\sqrt{V_g}} e^{-x^2/2} dx] \quad (3.29)$$

where the threshold setting given by Equation 2.33 has been utilized.

In order to compute P_e, all that is needed is the specific conditional mean divided by the square root of the conditional variance and using this ratio in the limit of the appropriate error function integral. First, for a "zero" transmitted,

$$\frac{-m_0}{\sqrt{v_g}} = \frac{[AT\sqrt{P_{nj}}\sqrt{2/T}-A^2T] \, [\frac{2}{\pi}(\frac{\pi}{2} - \int_0^{BT/4} Sa^2(x)\,dx)]}{\sqrt{A^2TN_0 \frac{2}{\pi}[\frac{\pi}{2} - \int_0^{BT/4} Sa^2(x)\,dx]}} \qquad (3.30)$$

Recognizing that $A^2T/2 = E$, the average energy per bit and substituting this in Equation 3.30 one obtains

$$\frac{-m_0}{\sqrt{v_g}} = \frac{[\sqrt{4EP_{nj}} - 2E] \, [\frac{2}{\pi}(\frac{\pi}{2} - \int_0^{BT/4} Sa^2(x)\,dx)]}{\sqrt{2EN_0 \frac{2}{\pi}(\frac{\pi}{2} - \int_0^{BT/4} Sa^2(x)\,dx)}} \qquad (3.31)$$

Finally

$$\frac{-m_0}{\sqrt{v_g}} \; \sqrt{2E/N_0}\,(1-\sqrt{P_{nj}/E}) \sqrt{\frac{2}{\pi}(\frac{\pi}{2} - \int_0^{BT/4} Sa^2(x)\,dx}} \qquad (3.32)$$

and similarly

$$\frac{-m_1}{\sqrt{v_g}} = -\sqrt{2E/N_0}\,(1 + \sqrt{P_{nj}/E}) \sqrt{\frac{2}{\pi}(\frac{\pi}{2} - \int_0^{BT/4} Sa^2(x)\,dx}} \qquad (3.33)$$

38

By using Equations 3.32 and 3.33 as the limits of integration in Equation 3.29, the probability of error performance can now be determined versus E/N_0, the signal to noise ratio; P_{nj}/E, the jammer to signal ratio; and BT, the relationship of the filter bandwidth to the inverse of the signal bandwidth.

Several items of note can be observed in the calculation of P_e. First, as BT approaches zero, the term $2/\pi (\pi/2 - \int_0^{BT/4} Sa^2(x) dx)$ becomes unity and Equation 3.29 becomes the receiver probability of error under optimum jamming [See Ref. 2] for BPSK modulation. Furthermore, when both BT and P_{nj}/E, the jammer to signal ratio, go to zero, Equation 3.29 becomes the well-known result for performance of a coherent BPSK receiver operating in additive white Gaussian noise [see Ref. 1].

B. COHERENT PSK USING A SECOND ORDER FRONT-END FILTER

Instead of choosing a filter transfer function that approaches the ideal case, the effect of a second order front-end filter on the probability of error performance of the coherent BPSK receiver will be investigated. The general coherent receiver structure becomes the BPSK coherent receiver by using Equations 3.1 and 3.3 in place of $s_d(t)$ and $s_i(t)$ (i = 0,1) respectively. The filter will be characterized as having a single notch at the center frequency of the jammer. The filter transfer function H(s), is derived from a first order, low pass prototype given by

$$H(s) = \frac{1}{1+s} \qquad (3.34)$$

39

To transform this into a bandstop filter centered at ω_0, the frequency transformation

$$s = \frac{s(\omega_U - \omega_L)}{s^2 + \omega_U \omega_L} \qquad (3.35)$$

will be substituted in Equation 3.34. Here, ω_U and ω_L represent the upper and lower 3 dB frequencies of the bandstop region. Before substitution, it can be seen that for ω_L approximately equal to ω_U, or equivalently $\omega_U - \omega_L$ small compared to $\omega_U \omega_L$, $\omega_U \omega_L$ and $\omega_U - \omega_L$ are approximately equal to ω_0^2 and B respectively. Note that B is the half power bandwidth of the bandstop region. Thus, Equation 3.35 becomes

$$s = \frac{Bs}{s^2 + \omega_0^2} \qquad (3.36)$$

Substituting finally into Equation 3.34 and also setting $s = j\omega$ in order to arrive at the frequency domain form, the filter transfer function is

$$H(\omega) = \frac{\omega_0^2 - \omega^2}{\omega_0^2 - \omega^2 + j\omega B} \qquad (3.37)$$

This filter will prove somewhat cumbersome to work with when put into Equations 2.14, 2.18 and 2.27. Therefore a more convenient form of this filter will be sought later.

Looking at Equations 2.14, 2.18, and 2.27, the products $S_{dp}(\omega) S_i(-\omega)$, $S_{dp}(\omega) N_j(-\omega)$ and $|S_{dp}(\omega)|^2$ (calculated in the

derivation of Equations 3.10, 3.18, 3.23) are Foureir trans-
forms of a time limited signal multiplied by a $\cos(\omega_0 t)$. The
time domain forms of these products are of the general form

$$c(t) = a(t)\cos(\omega_0 t) \qquad 0 \le t \le T \qquad (3.38)$$

which is essentially an "AM" modulated signal. This is not
surprising because each signal in the coherent BPSK receiver
model is of constant phase over a bit interval $(0 < t < T)$.
Reference 5 shows that the effect of filtering a modulated
cosine wave can be determined by calculating the effect of the
modulation being passed through an equivalent baseband filter.
The baseband equivalent of the bandstop filter will be in this
case a high pass filter.

The equivalent high pass filter model can be derived by
applying the transformation

$$s = \frac{\Omega_U}{s} \qquad (3.39)$$

to the low pass prototype of Equation 3.34, and letting Ω_U,
the upper cutoff frequency be equal to B/2. The resulting
filter in the frequency domain is

$$H'(\omega) = \frac{j\omega}{B/2 + j\omega} \qquad (3.40)$$

When Equation 3.37 is evaluated under the assumptions of
large ω_0 and small B compared to ω_0, the filter of Equation

3.40 can be seen as an equivalent, frequency shifted version
of the filter of Equation 3.37. Using the filter of Equation
3.40 and just the "modulation" spectra of the products, the
effect of a second order bandstop filter in the front-end of
the BPSK receiver can be evaluated with respect to the proba-
bility of error performance.

   1.   Calculation of the Conditional Mean

        The conditional mean of G' is given by Equation 2.7
where (n'_j, s_d) and (s'_i, s_d) are given by Equations 2.14 and
2.18, with the added fact that $1/2(||s_0||^2 - ||s_1||^2)$ is zero.
There is now enough information to determine the conditional
mean of G' namely

$$E[G'|s_i \text{ transmitted}] = (n'_j, s_d) + (s'_i, s_d) \quad i = 0,1$$

Taking each term individually, (n'_j, s_d) will be calculated
first. Equation 2.18, repeated here for clarity,

$$(n'_j, s_d) = \frac{1}{2\pi} \int_{-\infty}^{\infty} S_{dp}(\omega) N_j(-\omega) H(-\omega) d\omega$$

shows that the product $S_{dp}(\omega) N_j(-\omega)$ and $H(-\omega)$ will be needed.
The product $S_{dp}(\omega) N_j(-\omega)$ was previously found (in the derivation
of Equation 3.17) to be

$$S_{dp}(\omega) N_j(-\omega) = \frac{AT^2}{2} \sqrt{P_{nj}} \sqrt{2/T} [Sa^2(\omega-\omega_0)\frac{T}{2} + Sa^2(\omega+\omega_0)\frac{T}{2}] \qquad (3.41)$$

42

Before multiplying this by $H(-\omega)$ and substituting into Equation 2.18, it can be seen that Equation 3.41 can be written in the form

$$S_{dp}(\omega)N_j(-\omega)$$

$$= AT\sqrt{P_{nj}}\ \sqrt{2/T}\ TSa^2(\omega)\frac{T}{2}\ *\ \pi[\delta(\omega-\omega_0)+\delta(\omega+\omega_0)] \qquad (3.42)$$

which in the time domain is of the form of Equation 3.38. Thus the baseband equivalents of $S_{dp}(\omega)N_j(-\omega)$ and $H(-\omega)$ can be substituted into Equation 2.18. Therefore (n_j',s_d) becomes

$$(n_j',s_d)\ =\ \frac{1}{2\pi}AT\sqrt{P_{nj}}\sqrt{2/T}\ \int_{-\infty}^{\infty}TSa^2(\omega T/2)H'(-\omega)d\omega \qquad (3.43)$$

where $TSa^2(\omega T/2)$ is the modulation spectrum and $H'(-\omega)$ is the equivalent high pass filter Finally, substituting Equation 3.40 into Equation 3.43 yields

$$(n_j',s_d)\ =\ \frac{1}{2\pi}AT\sqrt{P_{nj}}\sqrt{2/T}\ \int_{-\infty}^{\infty}TSa^2(\omega T/2)\cdot\frac{-j\omega}{-j\omega+B/2}\ d\omega \qquad (3.44)$$

Now taking advantage of the simplified expressions for the filter, the "modulation" term, and the respective time domain forms, Equation 3.44 can be evaluated using Parseval's theorem. Parseval's theorem states that if $f_1(t)$ and $f_2(t)$ are time functions with Fourier transforms $F_1(\omega)$ and $F_2(\omega)$ then

43

$$\int_{-\infty}^{\infty} f_1(t) f_2(t) \, dt \quad = \quad \frac{1}{2\pi} \int_{-\infty}^{\infty} F_1(\omega) F_2(-\omega) \, d\omega$$

By letting $-j\omega/(-j\omega+B/2)$ equal $F_2(-\omega)$, it is easy to show the impulse response of the baseband filter $h'(t)$ is

$$h'(t) \quad = \quad \delta(t) - \frac{B}{2} e^{-Bt/2} \mu(t) \tag{3.45}$$

Before using Parseval's theorem, the inverse Fourier transform of $T(Sa^2(\omega)T/2$ must be found. This is easily determined from tables to be

$$\mathcal{F}^{-1}[TSa^2(\omega T/2)] \quad = \quad \begin{cases} \dfrac{t}{T} + 1, & -T \le t \le 0 \\[2mm] -\dfrac{t}{T} + 1, & 0 \le t \le T \end{cases} \tag{3.46}$$

Putting (n'_j, s_d) into the equivalent time domain integral form using Parseval's theorem, yields

$$(n'_j, s_d) \quad = \quad AT \sqrt{P_{nj}} \sqrt{2/T} \int_0^T \left(-\frac{t}{T} + 1\right) \left(\delta(t) - \frac{B}{2} e^{-Bt/2} \mu(t)\right) dt \tag{3.47}$$

due to the fact that the filter is causal (only defined for $t > 0$) and that $\mathcal{F}^{-1}(TSa^2(\omega)T/2)$ is defined from $-T < t < T$. Evaluating Equation 3.47 consists simply of the task of evaluating the sum of four integrals with limits from zero to T. It is easily demonstrated that

44

$$(n_j',s_d) \quad = \quad AT \; \sqrt{P_{nj}} \; \sqrt{2/T} \, [\tfrac{2}{BT}(1 - e^{-BT/2})] \qquad (3.48)$$

The second term that must be evaluated is (s_i',s_d), $(i = 0,1)$ in order to be able to determine the conditional mean of G'. From Equation 2.14 repeated here for convenience,

$$(s_i',s_d) \quad = \quad \frac{1}{2\pi} \int_{-\infty}^{\infty} S_{dp}(\omega) S_i(-\omega) H(-\omega) \, d\omega \quad i = 0,1$$

It is apparent that the products of $S_{dp}(\omega)$ and $S_i(-\omega)$ $(i = 0,1)$ have been determined in the derivation of Equation 3.24 and can easily be put in the form of Equation 3.42. Therefore, the baseband equivalents of the filter and the product are substituted into Equation 2.14 which yields

$$(s_0',s_d) \quad = \quad - \frac{A^2 T}{2\pi} \int_{-\infty}^{\infty} T Sa^2(\omega T/2) \, \frac{-j\omega}{-j\omega + B/2} \, d\omega \qquad (3.49)$$

It is easily seen that the integral in this equation is of the same form as Equation 3.44, thus Parseval's theorem can be applied directly and for the specific case of (s_0',s_d) yields

$$(s_0,s_d) \quad = \quad -A^2 T \int_0^T (\tfrac{-t}{T} + 1)(\delta(t) - \tfrac{B}{2} e^{-BT/2} \mu(t)) \, dt \qquad (3.50)$$

Here the limits of the integral are 0 and T because the filter impulse response h'(t) is causal. Since the integral has

45

already been evaluated, we obtain

$$(s_0', s_d) = -A^2 T[\frac{2}{BT}(1 - e^{-BT/2})] \qquad (3.51)$$

and similarly

$$(s_1', s_d) = A^2 T[\frac{2}{BT}(1 - e^{-BT/2})] \qquad (3.52)$$

Finally, the conditional mean of G' under the assumption that a "one" or a "zero" signal was transmitted is

$$E[G' | s_i \text{ transmitted}]$$

$$= [AT \sqrt{P_{nj}} \sqrt{2/T} + -1^{-i+1} A^2 T][\frac{2}{BT}(1 - e^{-BT/2})] \qquad (3.53)$$
$$i = 0,1$$

2. Calculation of the Conditional Variance

In order to calculate the conditional variance of G', it will be more convenient to use Equation 2.27 due to the fact that Parseval's theorem can be applied to its evaluation. The conditional variance of G' is

$$VAR[G' | s_i(t) \text{ transmitted}]$$

$$= \frac{N_0}{4\pi} \int_{-\infty}^{\infty} |H(\omega)|^2 |S_{dp}(\omega)|^2 d\omega \qquad i = 0,1 \qquad (3.54)$$

The term $|S_{dp}(\omega)|^2$ has been calculated and is given by Equation 3.10, and as shown here, it is of a form similar to Equation

3.41, namely

$$|S_{dp}(\omega)|^2 = A^2 T^2 [Sa^2(\omega-\omega_0)T/2 + Sa^2(\omega+\omega_0)T/2] \qquad (3.55)$$

Therefore the baseband equivalent of $|S_{dp}(\omega)|^2$, that is

$$|S'_{dp}(\omega)|^2 = 2A^2 T^2 [Sa^2(\omega T/2)] \qquad (3.56)$$

will be used along with the baseband equivalent filter $H'(\omega)$.
$|H'(\omega)|^2$ is calculated by multiplying $H'(\omega)$ by $H'(-\omega)$, producing
the following result

$$|H'(\omega)|^2 = \frac{\omega^2}{(B/2)^2 + \omega^2} \qquad (3.57)$$

Thus the conditional variance of G' becomes

$$\text{VAR}[G'|s_i \text{ transmitted}] = \frac{N_0 2A^2 T}{4\pi}$$

$$\cdot \int_{-\infty}^{\infty} TSa^2(\omega T/2)[\frac{\omega^2}{(B/2)^2 + \omega^2}]d\omega \quad i = 0,1 \qquad (3.58)$$

by substituting Equations 3.56 and 3.57 into 3.54.

Use of Parseval's theorem in order to compute the
conditional variance of G' requires the inverse Fourier trans-
forms of $TSa^2(\omega T/2)$ and $\omega^2/((B/2)^2 + \omega^2)$. The first inverse
transform has already been determined and is

47

$$F^{-1}[TSa^2(\omega T/2)] = \begin{cases} \dfrac{t}{T} + 1, & -T \le t \le 0 \\[2ex] -\dfrac{t}{T} + 1, & 0 \le t \le T \end{cases} \tag{3.59}$$

Next, the inverse Fourier transform of $|H'(\omega)|^2$ must be deter-
mined. Since $|H'(\omega)|^2$ was obtained by multiplying $H'(\omega)$ by
$H'(-\omega)$, $F^{-1}\{|H'(\omega)|^2\}$ can be written in the following form

$$F^{-1}[|H'(\omega)|^2] = F^{-1}[H'(\omega)] \ast F^{-1}[H'(-\omega)] \tag{3.60}$$

Now, using the Fourier transform identity $F^{-1}\{H(-\omega)\} \Leftrightarrow h(-t)$,
Equation 3.60 becomes

$$F^{-1}[|H'(\omega)|^2] = [\delta(t) - \frac{B}{2}e^{-Bt/2}\mu(t)] \ast [\delta(-t)\frac{B}{2}e^{Bt/2}\mu(-t)]$$

$$\tag{3.61}$$

where the necessary inverse Fourier transform has been deter-
mined in Equation 3.45. Substituting this into the convolution
integral yields

$$F^{-1}[|H'(\omega)|^2] = \int_{-\infty}^{\infty} [\delta(t-x) - \frac{B}{2}e^{-B(t-x)}\mu(t-x)]$$

$$\cdot [\delta(-x) - \frac{B}{2}e^{-B(-x)/2}]\,dx \tag{3.62}$$

and performing the convolution specified in Equation 3.62,
the inverse Fourier transform of $|H'(\omega)|^2$ is

48

$$F^{-1}[|H'(\omega)|^2] = \delta(t) - \frac{B}{4}e^{-B|t|/2} \qquad (3.63)$$

Using Parseval's theorem, the conditional variance of G' becomes

$$VAR[G'|s_i \text{ transmitted}] = A^2TN_0$$

$$\cdot \left[\int_{-T}^{0} (\frac{t}{T}+1)(\delta(t) - \frac{B}{4}e^{BT/2})dt + \int_{0}^{T} (\frac{-t}{T}+1)(\delta(t) - \frac{B}{4}e^{-Bt/2})dt \right]$$

$$i = 0,1 \qquad (3.64)$$

The evaluation of Equation 3.64 is fairly straightforward, with the exception that care must be taken when integrating the $\delta(t)$ over $-T$ to zero and from zero to T. There is only one singularity present at $t = 0$ with an area of one, so that each integral of $\delta(t)$ can be treated as being equal to 1/2. Therefore, the conditional variance of G' is

$$VAR[G'|s_i(t) \text{ transmitted}]$$

$$= A^2TN_0[\frac{2}{BT}(1 - e^{-BT/2})] \qquad i = 0,1 \qquad (3.65)$$

3.   <u>Probability of Error Calculation</u>

With the conditional mean and variance of G' specified by Equations 3.53 and 3.64, it is now possible to compute the probability of error performance of the BPSK coherent receiver with a second order front-end filter. Assuming the probability

of the transmitter sending a "one" or a "zero" signal are
equal $(P(s_1(t)) = P(s_0(t)) = 1/2))$, Equation 2.39 shows that
the average probability of error P_e is

$$P_e = \frac{1}{2}[\int_{-m_0/\sqrt{v_g}}^{\infty} \frac{1}{\sqrt{2\pi}}e^{-x^2/2}dx$$

$$+ \int_{-\infty}^{-m_1\sqrt{v_g}} \frac{1}{\sqrt{2\pi}} e^{-x^2/2} dx] \tag{3.66}$$

where the threshold setting given by Equation 2.33 has been
utilized.

To compute P_e, all that is needed is the specific
conditional mean divided by the square root of the conditional
variance and using this ratio in the limit of the appropriate
error function. First, for a zero transmitted

$$\frac{-m_0}{\sqrt{v_g}} = \frac{[A^2T - AT\sqrt{P_{nj}} \sqrt{2/T}](1 - e^{-BT/2})2/BT}{\sqrt{A^2TN_0(1 - e^{-BT/2})2/BT}} \tag{3.67}$$

Recognizing that $A^2T/2 = E$, the average energy per bit, and
substituting this in Equation 3.67 yields

$$\frac{-m_0}{\sqrt{v_g}} = \sqrt{2E/N_0} - \sqrt{(2E/N_0)(P_{nj}/E)} \left(\sqrt{(1 - e^{-BT/2})2/BT} \right)$$

$$\tag{3.68}$$

Finally

$$\frac{-m_0}{\sqrt{v_g}} = \sqrt{2E/N_0}\,(1 - \sqrt{P_{nj}/E})\,\left(\sqrt{(1 - e^{-BT/2})\frac{2}{BT}}\right) \qquad (3.69)$$

and similarly

$$\frac{-m_1}{\sqrt{v_g}} = -\sqrt{2E/N_0}\,(\sqrt{P_{nj}/E} + 1)\,\sqrt{(1 - e^{-BT/2})\frac{2}{BT}} \qquad (3.70)$$

The probability of error performance can now be determined versus E/N_0, the signal to noise ratio; P_{nj}/E, the jammer to signal ratio; and BT, the relationship of the filter bandwidth to the inverse of the signal bandwidth, by using Equations 3.69 and 3.70 as the limits of integration in Equation 3.66.

To evaluate the probability of error performance of the BPSK coherent receiver as the filter bandwidth approaches zero, L'Hôpital's rule must be utilized. Applying this rule to Equations 3.53 and 3.65 and then substituting the results into Equation 3.67 shows that, as the filter bandwidth (multiplied by the bit length T) goes to zero, the probability of error performance of the filtered coherent BPSK receiver becomes that of the coherent BPSK receiver in the presence of noise and jamming derived in Ref. 2. Furthermore when the jammer to signal ratio goes to zero, the probability of error performance is the same as that of a coherent BPSK receiver in the presence of noise along as derived in Ref. 1.

As one more check, when the filter bandwidth approaches infinity both Equations 3.69 and 3.70 become zero and the

probability of error is one half. This exhibits similar

behavior in the limits of BT as in the calculations performed

using the ideal filter. In a follow-on chapter, the behavior

of the BPSK receiver with either type of front-end filter

will be compared over the complete range of variables.

IV. FREQUENCY SHIFT KEY COHERENT RECEIVER
WITH A FRONT-END FILTER

A. FSK WITH A SINGLE IDEAL FILTER

As done with the BPSK receiver, the FSK receiver will be
evaluated using an ideal front-end filter, first to gain in-
sight into the problem and second to obtain an approximation
to the performance achieved using a higher order filter. In
the first case, the front-end filter will be modelled by an
ideal bandstop filter with a center frequency $\pm\omega_c$ radians/
second and the bandstop region defined from $\pm\omega_c - B/2$ to $\pm\omega_c + B/2$
where B is the bandwidth in radians/second.

In order to obtain a coherent FSK receiver from the
generic coherent receiver of Figure A.2, $s_d(t)$ is set to

$$s_d(t) = -2A \sin\frac{1}{2}(\omega_1 - \omega_0)t \, \sin\frac{1}{2}(\omega_1 + \omega_0)t \qquad (4.1)$$

$$0 \leq t \leq T$$

The input FSK signals are

$$s_1(t) = A \cos\omega_1 t \qquad 0 \leq t \leq T$$

and

$$s_0(t) = A \cos\omega_0 t \qquad 0 \leq t \leq T \qquad (4.2)$$

53

The optimum jammer derived in Ref. 2 for use against the coherent FSK receiver (without a front-end filter) is

$$n_j(t) = -\sqrt{P_{nj}} \frac{2}{\sqrt{T}} \sin \frac{1}{2}(\omega_1 - \omega_0)t \sin \frac{1}{2}(\omega_1 + \omega_0)t \qquad (4.3)$$

$$0 \leq t \leq T$$

Finally, the additive noise is modeled as a white Gaussian noise process with a power spectral density level of $N_0/2$ watts/hertz.

The first step in determining the probability of error performance (as previously done) involves determining the statistics of the random variable G' at the output of the receiver. Since it can be shown that G' is a conditional Gaussian random variable, all that is needed are the conditional mean and variance under the assumption that a "one" or a "zero" are transmitted. Finally, the probability of error performance will be calculated by applying these statistics to Equation 2.39.

1. Calculation of the Conditional Mean

In order to determine the conditional mean, Equation 2.7 becomes the starting point. Equation 2.7 is repeated here for convenience, that is

$$E[G|s_i(t) \text{ transmitted}] = (s_i', s_d) + (n_j', s_d) + \frac{1}{2}[||s_0||^2 - ||s_1||^2]$$

It has already been shown in the PSK system analysis that for equal duration, equal amplitude signals, the term

54

$1/2(||s_0||^2 - ||s_1||^2)$ is zero. The frequency domain equations

for (s_i', s_d) and (n_j', s_d) are given by Equations 2.14 and 2.18

respectively. Modifying Equation 2.14 in order to account

for the fact that $H(\omega)$ is an ideal filter, (s_i', s_d) becomes

$$(s_i', s_d) = \frac{1}{2\pi}[\int_{-\infty}^{\infty} S_i(-\omega)S_{dp}(\omega)d\omega -$$

$$\int_{-\omega_c-B/2}^{\omega_c+B/2} S_i(-\omega)S_{dp}(\omega)d\omega - \int_{-\omega_c-B/2}^{-\omega_c-B/2} S_i(-\omega)S_{dp}(\omega)d\omega]$$

$$i = 0,1 \qquad\qquad (4.4)$$

In order to calculate (s_i', s_d), Equation 4.4 shows that the

product of $S_i(-\omega)$ and $S_{dp}(\omega)$ is needed. Since $s_i(t)$ is defined

over $0 < t < T$, it can be shown that $S_i(\omega)$ given by

$$S_i(\omega) = \frac{AT}{2}[Sa(\omega-\omega_i)\frac{T}{2}e^{-j(\omega-\omega_i)T/2}$$

$$+ Sa(\omega+\omega_i)\frac{T}{2}e^{-j(\omega+\omega_i)T/2}] \qquad i = 0,1 \qquad (4.5)$$

$S_{dp}(\omega)$ is determined to be

$$S_{dp}(\omega) = \frac{AT}{2}[Sa(\omega-\omega_1)\frac{T}{2}e^{-j(\omega-\omega_1)T/2} + Sa(\omega+\omega_1)\frac{T}{2}e^{-j(\omega+\omega_1)T/2}$$

$$- Sa(\omega-\omega_0)\frac{T}{2}e^{-j(\omega-\omega_0)T/2} - Sa(\omega+\omega_0)\frac{T}{2}e^{-j(\omega-\omega_0)T/2}] \qquad (4.6)$$

Before investigating the specific case (s_0', s_d), it

will be convenient to look at the relationship between the

center frequency of the filter and the signal and jammer fre-
quencies. Since the filter contains a single bandstop region
and the jammer has a spectrum similar to that of $S_{dp}(\omega)$, the
filter center frequency should be located between the jammer
frequencies in order to notch out the jammer. Also, the
filter should have a bandwidth sufficient to cover both ω_0
and ω_1. Although the midpoint of ω_0 and ω_1 is given by
$(\omega_0+\omega_1)/2$, it will prove to be much more convenient to define
ω_1 and ω_0 in terms of ω_c, that is

$$\omega_1 = \omega_c + \omega_d$$

$$(4.7)$$

$$\omega_0 = \omega_c - \omega_d$$

where $\omega_d = (\omega_1-\omega_0)/2$ and $\omega_c = (\omega_1+\omega_0)/2$.

Substituting Equation 4.7 for ω_1 and ω_0 and multiplying
$S_{dp}(\omega)$ by $S_0(-\omega)$ yields

$$S_{dp}(\omega)S_0(-\omega) = \frac{A^2T^2}{4}$$

$$\cdot [Sa(\omega-\omega_c+\omega_d)\frac{T}{2}Sa(\omega-\omega_c+\omega_d)\frac{T}{2}e^{j\omega_dT} + Sa(\omega+\omega_c-\omega_d)\frac{T}{2}Sa(\omega+\omega_c+\omega_d)\frac{T}{2}e^{-j\omega_dT}$$

$$-Sa^2(\omega-\omega_c+\omega_d)\frac{T}{2} - Sa^2(\omega+\omega_c-\omega_d)\frac{T}{2}] \qquad (4.8)$$

Before the substitution of Equation 4.8 into Equation
4.4 is made, some simplification can be achieved. The contribu-
tion of the $Sa^2(x)$ functions with arguments of $(\omega \pm \omega_c \pm \omega_d)$, to

56

the integrals with limits of $\pm\omega_c \pm B/2$ is negligible for large ω_c and small B compared to ω_c. This also holds true for the products $Sa(\omega+\omega_c+\omega_d)T/2 \cdot Sa(\omega+\omega_c-\omega_d)T/2$ and $Sa(\omega-\omega_c+\omega_d)T/2 \cdot S(\omega-\omega_c-\omega_d)T/2$. Therefore substituting Equation 4.8 into Equation 4.4 yields

$$
(s_0', s_d) = \frac{1}{2\pi}\frac{A^2T^2}{4}[e^{j\omega_d T}(\int_{-\infty}^{\infty} Sa(\omega-\omega_c+\omega_d)\frac{T}{2}Sa(\omega-\omega_c-\omega_d)\frac{T}{2}d\omega
$$

$$
- \int_{\omega_c-B/2}^{\omega_c+B/2} Sa(\omega-\omega_c+\omega_d)\frac{T}{2}Sa(\omega-\omega_c-\omega_d)\frac{T}{2}d\omega)
$$

$$
+ e^{j\omega_d T}(\int_{-\infty}^{\infty} Sa(\omega+\omega_c-\omega_d)\frac{T}{2}Sa(\omega+\omega_c+\omega_d)\frac{T}{2}d\omega
$$

$$
- \int_{-\omega_c-B/2}^{-\omega_c+B/2} Sa(\omega+\omega_c-\omega_d)\frac{T}{2}Sa(\omega+\omega_c+\omega_d)\frac{T}{2}d\omega)
$$

$$
- (\int_{-\infty}^{\infty} Sa^2(\omega-\omega_c+\omega_d)\frac{T}{2}d\omega - \int_{\omega_c-B/2}^{\omega_c+B/2} Sa^2(\omega-\omega_c+\omega_d)\frac{T}{2}d\omega)
$$

$$
- (\int_{-\infty}^{\infty} Sa^2(\omega+\omega_c-\omega_d)\frac{T}{2}d\omega - \int_{-\omega_c-B/2}^{-\omega_c+B/2} Sa^2(\omega+\omega_c-\omega_d)\frac{T}{2}d\omega)] \qquad (4.9)
$$

Equation 4.9 is certainly cumbersome, but both the number of variables and the complexity can be reduced by making the following change of variables on the positive frequency integrals:

1)   let $x = (\omega - \omega_c)T/2$ then $(2/T)dx = d\omega$

2)   when $\omega = \pm\infty$, $x = \pm\infty$

3)   when $\omega = \omega_c \pm B/2$, $x = \pm BT/4$.

For the negative frequency integrals the following substitutions will be made:

1)   let $x = (\omega + \omega_c)T/2$, then $(2/T)dx = d\omega$

2)   when $\omega = \pm\infty$, $x = \pm\infty$

3)   when $\omega = -\omega_c \pm B/2$, $x = \pm BT/4$.

After performing these substitutions, it is seen that the first two integrals are equal in amplitude, but have opposite phase angles. As a result of this, (s_0', s_d) becomes

$$
(s_0', s_d) = \frac{-A^2 T}{4\pi}\left[\left(\int_{-\infty}^{\infty} Sa^2(x - \omega_d T/2)\,dx\right.\right.
$$

$$
\left. - \int_{-BT/4}^{BT/4} Sa^2(x - \omega_d T/2)\,dx\right)
$$

$$
+ \left(\int_{-\infty}^{\infty} Sa^2(x + \omega_d T/2)\,dx - \int_{-BT/4}^{BT/4} Sa^2(x - \omega_d T/2)\,dx\right)
$$

$$
-2\cos\omega_0 T\left(\int_{-\infty}^{\infty} Sa(x + \omega_d T/2)\,Sa(x - \omega_d T/2)\,dx\right.
$$

$$
\left. - \int_{-BT/4}^{BT/4} Sa(x + \omega_d T/2)\,Sa(x - \omega_d T/2)\,dx \right. \tag{4.10}
$$

By similar analysis

$$(s_1', s_d) = \frac{A^2 T}{4\pi} [(\int_{-\infty}^{\infty} Sa^2(x-\omega_d T/2) \, dx - \int_{-BT/4}^{BT/4} Sa^2(x-\omega_d T/2) \, dx)$$

$$+ (\int_{-\infty}^{\infty} Sa^2(x-\omega_d T/2) \, dx - \int_{-BT/4}^{BT/4} Sa^2(x+\omega_d T/2) \, dx)$$

$$-2\cos\omega_0 T (\int_{-\infty}^{\infty} Sa(x+\omega_d T/2) Sa(x-\omega_d T/2) \, dx$$

$$- \int_{-BT/4}^{BT/4} Sa(x+\omega_d T/2) Sa(x-\omega_d T/2) \, dx)] \qquad (4.11)$$

The next term in the conditional mean is (n_j', s_d) which is given by Equation 2.18. As previously done, this equation is modified to become

$$(n_j', s_d) = \frac{1}{2\pi} [\int_{-\infty}^{\infty} S_{dp}(\omega) N_j(-\omega) \, d\omega$$

$$- \int_{\omega_c - B/2}^{\omega_c + B/2} S_{dp}(\omega) N_j(-\omega) \, d\omega$$

$$- \int_{-\omega_c - B/2}^{-\omega_c + B/2} S_{dp}(\omega) N_j(-\omega) \, d\omega] \qquad (4.12)$$

Since $H(\omega)$ is an ideal filter, in order to form the product of $N_j(-\omega)$ and $S_{dp}(\omega)$, the spectrum of $n_j(t)$ must be found. The equation for $n_j(t)$ (see Equation 4.3) shows a truncated process similar to that found for the BPSK case. Thus $N_j(\omega)$ is determined to be

$$N_j(\omega) = \sqrt{P_{nj}/T}\,\frac{T}{2}[\mathrm{Sa}(\omega-\omega_1)\frac{T}{2}e^{-j(\omega-\omega_1)T/2}$$

$$+ \mathrm{Sa}(\omega+\omega_1)\frac{T}{2}e^{-j(\omega+\omega_1)T/2}$$

$$- \mathrm{Sa}(\omega-\omega_0)\frac{T}{2}e^{-j(\omega-\omega_0)T/2} - \mathrm{Sa}(\omega+\omega_0)\frac{T}{2}e^{-j(\omega-\omega_0)T/2}] \qquad (4.13)$$

Now, multiplying $N_j(-\omega)$ by $S_{dp}(\omega)$, where $S_{dp}(\omega)$ is given by Equation 4.9 yields eight terms. Four are on the positive side of the $\omega = 0$ axis and four are on the negative side of the $\omega = 0$ axis. For convenience just the positive frequency terms are shown here

$$N_j(-\omega)S_{dp}(\omega) = \frac{AT^2}{4}\sqrt{P_{nj}/T}[\mathrm{Sa}^2(\omega-\omega_0)\frac{T}{2}$$

$$- 2\cos\omega_d T\mathrm{Sa}(\omega-\omega_0)\frac{T}{2}\mathrm{Sa}(\omega+\omega_1)\frac{T}{2} + \mathrm{Sa}^2(\omega-\omega_1)\frac{T}{2}] \qquad (4.14)$$

Expressing ω_0 and ω_1 as $\omega_c\pm\omega_d$ as before, and substituting Equation 4.14 into Equation 4.12 under the assumptions stated in the development of (s_i', s_d), yields an expression similar to Equation 4.9. The difference here is that the $\mathrm{Sa}(\omega-\omega_c+\omega_d)T/2\mathrm{Sa}(\omega-\omega_c-\omega_d)T/2$ terms are multiplied by $2\cos\omega_d T$ rather than $e^{j\omega_d T}$. By making the same change of variables as in Equation 4.10 and recognizing that Equation 4.14 covers only half of the frequency spectrum (which is symmetrical), (n_j', s_d) becomes

$$(n_j', s_d) = \frac{1}{2\pi} AT \sqrt{P_{nj}/T} \left[\left(\int_{-\infty}^{\infty} Sa^2(x-\omega_d T/2)\, dx \right. \right.$$

$$- \int_{-BT/4}^{BT/4} Sa^2(x-\omega_d T/2)\, dx \left) \left(\int_{-\infty}^{\infty} Sa^2(x+\omega_d T/2) \right. \right.$$

$$- \int_{-BT/4}^{BT/4} Sa^2(x+\omega_d T/2)\, dx \right)$$

$$-2\cos\omega_d T \left(\int_{-\infty}^{\infty} Sa(x+\omega_d T/2) Sa(x-\omega_d T/2)\, dx \right.$$

$$- \int_{-BT/4}^{BT/4} Sa(x+\omega_d T/2) Sa(x-\omega_d T/2)\, dx \right] \qquad (4.15)$$

Finally, with (s_i', s_d), (n_1', s_d) and $\frac{1}{2}(||s_0||^2 - ||s_1||^2)$ determined, the conditional mean of G' can be expressed as

$$E[G' | s_i \text{ transmitted}] = [AT\sqrt{P_{nj}/T} + -1^{-i+1} \frac{A^2 T}{2}] \frac{1}{2\pi}$$

$$\cdot \left[\left(\int_{-\infty}^{\infty} Sa^2(x+\omega_d T/2)\, dx - \int_{-BT/4}^{BT/4} Sa^2(x+\omega_d T/2)\, dx \right) \right.$$

$$+ \left(\int_{-\infty}^{\infty} Sa^2(x-\omega_d T/2)\, dx - \int_{-BT/4}^{BT/4} Sa^2(x-\omega_d T/2)\, dx \right)$$

$$-2\cos\omega_d T \left(\int_{-\infty}^{\infty} Sa(x-\omega_d T/2) Sa(x+\omega_d T/2)\, dx \right.$$

$$- \int_{-BT/4}^{BT/4} Sa(x-\omega_d T/2) Sa(x+\omega_d T/2)\, dx \right)], \quad i = 0,1 \qquad (4.16)$$

61

2. Calculation of the Conditional Variance

The conditional variance of G' in the frequency domain is given by Equation 2.27, which can be modified to take on the following form

$$
\text{VAR}[G' | s_i(t) \text{ transmitted}] = \frac{N_0}{2\pi}
$$

$$
\cdot [\int_0^\infty |S_{dp}(\omega)|^2 d\omega - \int_{\omega_c - B/2}^{\omega_c + B/2} |S_{dp}(\omega)|^2 d\omega], \quad i = 0,1 \quad (4.17)
$$

due to the fact that $H(\omega)$ is assumed to be an ideal filter. Therefore in order to calculate the conditional variance, all that is needed is the determination of $|S_{dp}(\omega)|^2$. Since $|S_{dp}(\omega)|^2 = S_{dp}(\omega) S_{dp}(-\omega)$ and $S_{dp}(\omega)$ is given by Equation 4.8, the terms on the right hand side of the $\omega = 0$ axis are given by

$$
|S_{dp}(\omega)|^2 = \frac{A^2 T^2}{4} [Sa^2(\omega - \omega_c + \omega_d)\frac{T}{2} + Sa^2(\omega - \omega_c - \omega_d)\frac{T}{2}
$$

positive
frequency
terms
$$
- 2\cos\omega_d T Sa(\omega - \omega_c + \omega_d)\frac{T}{2} Sa(\omega - \omega_c - \omega_d)\frac{T}{2}] \quad (4.18)
$$

where $\omega_0 = \omega_c - \omega_d$ and $\omega_1 = \omega_c + \omega_d$.

Since the limits of the integrals in Equation 4.17 are on the right hand side of the $\omega = 0$ axis, for large ω_c and small B compared to ω_c, the terms of $|S_{dp}(\omega)|^2$ on the left hand side of the $\omega = 0$ axis can be neglected. By substituting Equation 4.18 into 4.17 it is quickly recognized that the integrals are of the same form as Equations 4.9, 4.10 and 4.14.

So, instead of repeating the steps which have been demonstrated before, the conditional variance is shown here without further development

$$
\text{VAR}[G' \,|\, s_i(t) \text{ transmitted}] = \frac{A^2 T}{2\pi} \Big[\big(\int_{-\infty}^{\infty} Sa^2(x - \omega_d T/2)\, dx
$$

$$
- \int_{-BT/4}^{BT/4} Sa^2(x - \omega_d T/2)\, dx \big) + \big(\int_{-\infty}^{\infty} Sa^2(x + \omega_d T/2)\, dx
$$

$$
\cdot \int_{-BT/4}^{BT/4} Sa^2(x + \omega_d T/2)\, dx \big)
$$

$$
- 2\cos\omega_d T \big(\int_{-\infty}^{\infty} Sa(x - \omega_d T/2)\, Sa(x + \omega_d T/2)\, dx
$$

$$
- \int_{-BT/4}^{BT/4} Sa(x - \omega_d T/2)\, Sa(x + \omega_d T/2)\, dx \big) \Big], \quad i = 0,1 \tag{4.19}
$$

3. Probability of Error Calculation

With the conditional mean and variance of G' given by Equations 4.16 and 4.19, it is now possible to compute the probability of error performance of the BFSK coherent receiver with an ideal front-end filter. Assuming that the probability of the transmitter sending a "one" or a "zero" signal are equal $(P(s_1(t)) = P(s_0(t)) = 1/2))$, Equation 2.39 shows that the average probability of error P_e is

$$
P_e = \frac{1}{2} \Big[\int_{-m_0/\sqrt{v_g}}^{\infty} \frac{1}{\sqrt{2\pi}} e^{-x^2/2}\, dx + \int_{-\infty}^{-m_1/\sqrt{v_g}} \frac{1}{\sqrt{2\pi}} e^{-x^2/2}\, dx \Big] \tag{4.20}
$$

63

where the threshold setting given by Equation 2.33 has been utilized.

In order to compute P_e, all that is needed is the specific conditional mean divided by the square root of the conditional variance and using this ratio in the limit of the appropriate error function integral. Recognizing that $A^2T/2 = E$, the average energy per bit, and making the appropriate cancellations, $m_0/\sqrt{v_g}$ is determined to be

$$\frac{-m_0}{\sqrt{v_g}} = \sqrt{E/N_0}\,(1 - \sqrt{2Pn_j/E})\,\sqrt{\text{Filter Factor}} \qquad (4.21)$$

and $m_1/\sqrt{v_g}$ becomes

$$\frac{-m_1}{\sqrt{v_g}} = -\sqrt{E/N_0}\,(1 + \sqrt{2P_{nj}/E})\,\sqrt{\text{Filter Factor}} \qquad (4.22)$$

where the Filter Factor is defined as

$$\text{Filter Factor} = \frac{1}{2\pi}$$

$$\cdot \left[\left(\int_{-\infty}^{\infty} Sa^2(x-\omega_d T/2)\,dx - \int_{-BT/4}^{BT/4} Sa^2(x-\omega_d T/2)\,dx \right) \right.$$

$$+ \left(\int_{-\infty}^{\infty} Sa^2(x-\omega_d T/2)\,dx - \int_{-BT/4}^{BT/4} Sa^2(x-\omega_d T/2)\,dx \right)$$

$$- 2\cos\omega_d T \left(\int_{-\infty}^{\infty} Sa\,(x-\omega_d T/2)\,Sa\,(x+\omega_d T/2)\,dx \right.$$

$$\left. - \int_{-BT/4}^{BT/4} Sa\,(x-\omega_d T/2)\,Sa\,(x+\omega_d T/2)\,dx \right) \Big] \qquad (4.23)$$

64

The probability of error performance can now be determined
versus E/N_0, the signal to noise ratio; P_{nj}/E, the jammer to
signal ratio; and BT, the relationship of the filter bandwidth
to the inverse of the signal bandwidth, by using Equations
4.21 and 4.22 as the limits of integration in Equation 4.20.

It is desirable to compare these results with those
previously obtained for both the jamming problem and for
the general FSK coherent receiver. In order to compare the
results for the probability of error performance of the coher-
ent FSK receiver with no filtering, it is necessary to analyze
how those results were obtained. For the coherent receiver
operating in just additive white Gaussian noise alone, the
probability of error from Ref. 1 is

$$P_e = \int_{\sqrt{E/N_0}}^{\infty} \frac{1}{\sqrt{2\pi}} e^{-u^2/2} \, du \qquad (4.24)$$

This result is obtained when the energy per bit is $A^2T/2$
and the normalized cross correlation $\bar{\rho}$ is zero, where (see
Ref. 1)

$$E = \frac{1}{2} \int_{t_0}^{t_f} [y_0^2(t) + y_1^2(t)] \, dt \qquad (4.25)$$

$$\bar{\rho} = \frac{1}{E} \int_{t_0}^{t_f} y_0(t) y_1(t) \, dt \qquad (4.26)$$

65

and t_0, t_f are replaced by 0, T respectively. From these expressions it is easy to show that $\omega_1 T$ must equal $n\pi$ and $\omega_0 T = k\pi$ (where n and k are integers) for $E = A^2 T/2$. For the FSK modulation $\bar{\rho}$ is

$$\bar{\rho} = Sa(\omega_1 + \omega_0)T + Sa(\omega_1 - \omega_0)T \qquad (4.27)$$

For large $(\omega_1 + \omega_0)T$ the $Sa(\omega_1 + \omega_0)T$ is negligible and $\bar{\rho}$ is zero when $(\omega_1 - \omega_0)T$ is equal to $m\pi$ (where m is an integer). When this is substituted into Equation 4.23, recalling that $\omega_d T = (\omega_1 - \omega_0)T/2$, it can be seen that when BT is zero the Filter Factor of Equation 4.23 is 1.0. For values of $\omega_d T$ that are odd multiplies of $\pi/2$ the Filter Factor is exactly equal to 1.0, but for even multiples it becomes 1 plus a small quantity that is negligible. So again, as in the PSK ideal front-end filter case, for BT equal to zero, Equations 4.53 and 4.54 are in agreement with the results of Ref. 2 for the coherent FSK receiver operating against the optimum jammer. For P_{nj}/E equal to zero these results correspond to the results of Ref. 1 for the coherent FSK receiver operating in additive white Gaussian noise alone.

B. FSK WITH A SECOND ORDER FRONT-END FILTER

In order to evaluate the effect of a second order band-stop filter on the probability of error performance of a coherent FSK receiver, the filter specified by Equation 3.37 will be utilized. The use of the equivalent baseband filter,

along with Parseval's theorem will not greatly aid in the determination of the conditional mean and variance of G' (the output of the receiver of Figure A.2). For convenience, the parameters of the coherent FSK receiver model are repeated here (see Equations 4.1 and 4.2)

$$s_2(t) = -2A \sin \tfrac{1}{2}(\omega_1 - \omega_0)t \, \sin \tfrac{1}{2}(\omega_1 + \omega_0)t$$

$$s_0(t) = A \cos \omega_0 t$$

$$s_1(t) = A \cos \omega_1 t \qquad 0 \le t \le T$$

The optimum jammer derived in Ref. 2 is

$$n_j(t) = -\sqrt{P_{nj}} \, \frac{2}{\pi} \sin \tfrac{1}{2}(\omega_1 - \omega_0)t \, \sin \tfrac{1}{2}(\omega_1 + \omega_0)t \qquad 0 \le t \le T$$

and the filter of Equation 3.37 is

$$H(\omega) = \frac{\omega_0^2 - \omega^2}{\omega_0^2 - \omega^2 + j\omega B}$$

where ω_0 will be replaced by ω_c as in the FSK calculations involving the ideal filter case.

1. Calculation of the Conditional Mean

As before, Equation 2.7 will be used to determine the conditional mean of G'. Since the FSK signals are equal energy signals, all that is needed from Equation 2.7 are the

terms (n_j', s_d) and (s_i', s_d) with $i = 0,1$. These terms are given by Equations 2.14 and 2.18. First (s_i', s_d) will be calculated by evaluating the product of $S_i(-\omega)$ with $S_{dp}(\omega)$ along with $H(-\omega)$ and then substituting into Equation 2.18 which is repeated here for convenience

$$(s_i', s_d) = \frac{1}{2\pi}[\int_{-\infty}^{\infty} S_i(-\omega)S_{dp}(\omega)H(-\omega)d\omega \qquad i = 0,1$$

Investigating the particular case of (s_0', s_d), the product of $S_0(-\omega)$ and $S_{dp}(\omega)$ is given by Equation 4.8 where $\omega_c+\omega_d$ and $\omega_c-\omega_d$ were substituted for ω_1 and ω_0 respectively. Thus, substituting Equation 4.8 into Equation 2.18 yields

$$(s_0', s_d) = \frac{1}{2\pi}\frac{A^2T^2}{4}$$

$$\cdot [e^{j\omega_d T}(\int_{-\infty}^{\infty} Sa(\omega-\omega_c+\omega_d)\frac{T}{2}Sa(\omega-\omega_c-\omega_d)\frac{T}{2}H(-\omega)d\omega)$$

$$\cdot e^{-j\omega_d T}(\int_{-\infty}^{\infty} Sa(\omega+\omega_c-\omega_d)\frac{T}{2}Sa(\omega+\omega_c+\omega_d)\frac{T}{2}H(-\omega)d\omega)$$

$$- \int_{-\infty}^{\infty} Sa^2(\omega-\omega_c+\omega_d)\frac{T}{2}H(-\omega)d\omega - \int_{-\infty}^{\infty} Sa^2(\omega+\omega_c-\omega_d)\frac{T}{2}H(-\omega)d\omega] \qquad (4.28)$$

to further determine (s_0', s_d) it is necessary to investigate both $H(-\omega_c-2x/T)$ and $H(\omega_c-2x/T)$. By substituting ω_c-2X/T for ω in Equation 3.37, expanding, and multiplying numerator and denominator by $T/4\omega_c$ results in

68

$$H(\omega_c - 2x/T) = \frac{x - \dfrac{x^2}{\omega_c T}}{(x - \dfrac{x^2}{\omega_c T}) + \dfrac{jBT}{4} - \dfrac{jBx}{2\omega_c}} \tag{4.30}$$

The filter transfer function was derived under the assumption that $\omega_c \gg B$ so $H(\omega_c - 2x/T)$ becomes

$$H(\omega_c - 2x/T) = \frac{x - \dfrac{x^2}{\omega_c T}}{(x + \dfrac{x^2}{\omega_c T}) + \dfrac{jBT}{4}} \tag{4.31}$$

and similarly

$$H(-\omega_c - 2x/T) = \frac{x + \dfrac{x^2}{\omega_c T}}{(x + \dfrac{x^2}{\omega_c T}) + \dfrac{jBT}{4}} \tag{4.32}$$

For ease of notation let $H_1(x) = H(\omega_c - 2x/T)$ and $H_2(x) = H(-\omega_c - 2x/T)$. Then separating $H_1(x)$ and $H_2(x)$ into real and imaginary parts yields

$$\mathrm{Re}\{H_1(x)\} = \frac{(x - \dfrac{x^2}{\omega_c T})^2}{(x - \dfrac{x^2}{\omega_c T})^2 + (\dfrac{BT}{4})^2} \tag{4.33}$$

$$\mathrm{Im}\{H_1(x)\} = \frac{\dfrac{-BT}{4}(x - \dfrac{x^2}{\omega_c T})}{(x - \dfrac{x^2}{\omega_c T})^2 + (\dfrac{BT}{4})^2} \tag{4.34}$$

69

$$\text{Re}\{H_2(x)\} = \frac{(x + \frac{x^2}{\omega_c T})}{(x + \frac{x^2}{\omega_c T})^2 + (\frac{BT}{4})^2} \tag{4.35}$$

$$\text{Im}\{H_2(x)\} = \frac{\frac{-BT}{4}(x + \frac{x^2}{\omega_c T})}{(x + \frac{x^2}{\omega_c T})^2 + (\frac{BT}{4})^2} \tag{4.36}$$

With Equations 4.33 through 4.36 it is now possible to expand Equation 4.29 into real and imaginary parts which yields

$$(s_0', s_d) = \frac{A^2 T}{4\pi}[\cos\omega_d T [\int_{-\infty}^{\infty} \text{Sa}(x-\omega_d T/2)\text{Sa}(x+\omega_d T/2)$$

$$[\text{Re}\{H_1(x)\}+\text{Re}\{H_2(x)\}]dx$$

$$+ j \int_{-\infty}^{\infty} \text{Sa}(x-\omega_d T/2)\text{Sa}(x+\omega_d T/2)(\text{Im}\{H_1(x)\}+\text{Im}\{H_2(x)\})dx]$$

$$+ \sin\omega_d T[\int_{-\infty}^{\infty} \text{Sa}(x-\omega_d T/2)\text{Sa}(x+\omega_d T/2)(\text{Im}\{H_1(x)\}-\text{Im}\{H_2(x)\})dx$$

$$+ j \int_{-\infty}^{\infty} \text{Sa}(x-\omega_d T/2)\text{Sa}(x+\omega_d T/2)(\text{Re}\{H_1(x)\}-\text{Re}\{H_2(x)\})dx]$$

$$- [\int_{-\infty}^{\infty} \text{Sa}^2(x+\omega_d T/2)\text{Re}\{H_1(x)\}dx + \int_{-\infty}^{\infty} \text{Sa}^2(x-\omega_d T/2)\text{Re}\{H_2(x)\}dx$$

$$+ j \int_{-\infty}^{\infty} \text{Sa}^2(x+\omega_d T/2)\text{Im}\{H_1(x)\}+\text{Sa}^2(x-\omega_d T/2)\text{Im}\{H_2(x)\}dx]] \tag{4.37}$$

With the real and imaginary parts of $H_1(x)$ and $H_2(x)$ as given by Equations 4.33 through 4.36, it is easy to see that the imaginary terms integrate to zero because of the odd symmetry about $x = 0$ that the functions of Equation 4.37 exhibit. Thus (s_0', s_d) becomes

$$
(s_0', s_d) = \frac{-A^2 T}{4\pi} [\int_{-\infty}^{\infty} Sa^2(x+\omega_d T/2) Re\{H_1(x)\} dx
$$

$$
+ \int_{-\infty}^{\infty} Sa^2(x+\omega_d T/2) Re\{H_2(x)\} dx
$$

$$
- \cos\omega_d T \int_{-\infty}^{\infty} Sa(x-\omega_d T/2) Sa(x+\omega_d T/2) (Re\{\dot{H}_1(x)\}+Re\{H_2(x)\}) dx
$$

$$
- \sin\omega_d T \int_{-\infty}^{\infty} Sa(x-\omega_d T/2) Sa(x+\omega_d T/2) (Im\{H_1(x)\}-Im\{H_2(x)\}) dx]
$$

$$(4.38)$$

and by similar analysis

$$
(s_1', s_d) = \frac{A^2 T}{4\pi} [\int_{-\infty}^{\infty} Sa^2(x+\omega_d T/2) Re\{H_1(x)\} dx
$$

$$
+ \int_{-\infty}^{\infty} Sa^2(x-\omega_d T/2) Re\{H_2(x)\} dx
$$

$$
- \cos\omega_d T \int_{-\infty}^{\infty} Sa(x-\omega_d T/2) Sa(x+\omega_d T/2) (Re\{H_1(x)\}+ Re\{H_2(x)\}) dx
$$

$$
- \sin\omega_d T \int_{-\infty}^{\infty} Sa(x-\omega_d T/2) Sa(x+\omega_d T/2) (Im\{H_1(x)\}-Im\{H_2(x)\} dx]
$$

$$(4.39)$$

71

The next term that must be computed is (n'_j, s_d), given by Equation 2.18 and repeated here for convenience

$$(n'_j, s_d) = \frac{1}{2\pi} \int_{-\infty}^{\infty} S_{dp}(\omega) N_j(-\omega) H(-\omega) d\omega$$

As before, the calculation of this term starts with the product of $N_j(-\omega)$ and $S_{dp}(\omega)$. This product when fully expanded contains sixteen terms. Eight are products of $Sa(x)$ functions centered on opposite sides of the $\omega = 0$ axis and, for large ω_1 ω_0, are essentially equal to zero. By expressing ω_0 as $\omega_c - \omega_d$ and ω_1 as $\omega_c + \omega_d$, substituting into Equation 2.18, and performing the same change of variables as in the expansion of (s'_i, s_d), it can be shown that (n'_j, s_d) becomes

$$(n'_j, s_d) = \frac{AT}{4\pi} \sqrt{P_{nj}/T} \left[\int_{-\infty}^{\infty} Sa^2(x + \omega_d T/2) (H(\omega_c - 2x/T) + H(-\omega_c - 2x/T)) dx \right.$$

$$+ \int_{-\infty}^{\infty} Sa^2(x - \omega_d T/2) [H(\omega_c - 2x/T) + H(-\omega_c - 2x/T)) dx$$

$$- 2 \int_{-\infty}^{\infty} Sa(x - \omega_d T/2) Sa(x + \omega_d T/2) [e^{-j\omega_d T} H(\omega_c - 2x/T)$$

$$+ e^{j\omega_d T} H(-\omega_c - 2x/T)) dx] \tag{4.40}$$

The integrals in Equation 4.40 are now of the same form as those in Equation 4.29. Therefore, the same change of

variables operation can be performed as done in the derivation
of Equation 4.40.   This results in

$$
(n_j', s_d) = \frac{AT}{4\pi}\sqrt{P_{nj}/T}\,[\int_{-\infty}^{\infty} Sa^2(x-\omega_d T/2)\,(Re\{H_1(x)\}+Re\{H_2(x)\})\,dx
$$

$$
+ \int_{-\infty}^{\infty} Sa^2(x+\omega_d T/2)\,(Re\{H_1(x)\}+Re\{H_2(x)\})\,dx
$$

$$
- 2\cos\omega_d T \int_{-\infty}^{\infty} Sa(x-\omega_d T/2)\,Sa(x+\omega_d T/2)\,(Re\{H_1(x)\}+Re\{H_2(x)\})\,dx
$$

$$
- 2\sin\omega_d T \int_{-\infty}^{\infty} Sa(x-\omega_d T/2)\,Sa(x+\omega_d T/2)\,(Im\{H_1(x)\}-Im\{H_2(x)\}\,dx]
$$

$$
(4.41)
$$

where $Re\{H_1(x)\}$, $Re\{H_2(x)\}$, $Im\{H_1(x)\}$ and $Im\{H_2(x)\}$ are defined
by Equations 4.33 to 4.36.   The conditional mean of G' under
the assumption that $s_0(t)$ or $s_1(t)$ was transmitted can be
expressed as the sum of Equation 4.38 or 4.39 with Equation
4.41.

   2.   Calculation of the Conditional Variance

      The conditional variance of G' is given by Equation
2.27 and repeated here for convenience

$$
VAR[G'|s_i(t)\ transmitted] = \frac{N_0}{4\pi}\int_{-\infty}^{\infty} |S_{dp}(\omega)|^2 |H(\omega)|^2 d\omega
$$

by recognizing that $|H(\omega)|^2$ is $H(\omega)H(-\omega)$, for real h(t),
Equation 2.27 can be expressed as

73

$$\text{VAR}[G'|s_i(t) \text{ transmitted}] = \frac{N_0}{4\pi} \int_{-\infty}^{\infty} |S_{dp}(\omega)|^2 H(\omega) H(-\omega) \, d\omega \quad (4.42)$$

In order to begin the calculation of the conditional variance, as for the ideal filter case, $|S_{dp}(\omega)|^2$ must be determined by multiplying $S_{dp}(\omega)$ by $S_{dp}(-\omega)$. This product contains sixteen terms as encountered in the product of $N_j(-\omega)$ and $S_{dp}(\omega)$. Fortunately, $|S_{dp}(\omega)|^2$ only differs from $N_j(-\omega) S_{dp}(\omega)$ by a constant. Therefore it is possible to perform a similar set of operations as done in the derivation of Equation 4.29 so as to arrive at

$$\text{VAR}[G'|s_i \text{ transmitted}] = \frac{N_0 A^2 T}{4\pi}$$

$$\cdot \left[\int_{-\infty}^{\infty} \text{Sa}^2(x-\omega_d T/2) \left[H(2x/T-\omega_c) H(\omega_c-2x/T) + H(-2x/T-\omega_c) H(\omega_c+2x/T) \right) dx \right.$$

$$+ \left[\int_{-\infty}^{\infty} \text{Sa}^2(x+\omega_d T/2) \left(H(2x/T-\omega_c) H(\omega_c-2x/T) + H(\omega_c+2x/T) H(-\omega_c-2x/T) \right) dx \right.$$

$$- 2 \int_{-\infty}^{\infty} \text{Sa}(x+\omega_d T/2) \text{Sa}(x-\omega_d T/2) (e^{j\omega_d T} H(2x/T-\omega_c) H(\omega_c-2x/T)$$

$$+ e^{-j\omega_d T} H(2x/T+\omega_c) H(-2x/T-\omega_c)) dx] \quad i = 0,1 \quad (4.43)$$

where $H(-\omega_c-2x/T)$ and $H(\omega_c-2x/T)$ are given by Equations 4.31 and 4.32. It can be demonstrated that $H(2x/T-\omega_c)$ and $H(2x/T+\omega_c)$ are given by

$$H(2x/T+\omega_c) = \frac{(x + \frac{x^2}{\omega_c T})}{(x + \frac{x^2}{\omega_c T}) - \frac{jBT}{4}} \qquad (4.44)$$

and

$$H(2x/T-\omega_c) = \frac{(x - \frac{x^2}{\omega_c T})}{(x - \frac{x^2}{\omega_c T}) - \frac{jBT}{4}} \qquad (4.45)$$

By substituting Equations 4.30, 4.31, 4.44 and 4.45 into Equation 4.42 and expanding it into real and imaginary parts the conditional variance of G' becomes

$$VAR[G'|s_i \text{ transmitted}] = \frac{N_0 A^2 T}{4\pi}$$

$$\cdot \int_{-\infty}^{\infty} Sa^2(x-\omega_d T/2) \left[\frac{(x - \frac{x^2}{\omega_c T})}{(x - \frac{x^2}{\omega_c T})^2 + (\frac{BT}{2})^2} + \frac{(x + \frac{x^2}{\omega_c T})^2}{(x + \frac{x^2}{\omega_c T})^2 + (\frac{BT}{2})^2} \right.$$

$$+ \int_{-\infty}^{\infty} Sa(x+\frac{\omega_d T}{2}) \left[\frac{(x - \frac{x^2}{\omega_c T})^2}{(x - \frac{x^2}{\omega_c T})^2 + (\frac{BT}{2})^2} + \frac{(x + \frac{x^2}{\omega_c T})^2}{(x + \frac{x^2}{\omega_c T})^2 + (\frac{BT}{2})^2} \right] dx$$

$$-2\cos\omega_d T \int_{-\infty}^{\infty} Sa(x-\frac{\omega_d T}{2}) S (x+\frac{\omega_d T}{2}) \left[\frac{(x - \frac{x^2}{\omega_c T})^2}{(x - \frac{x^2}{\omega_c T})^2 + (\frac{BT}{2})^2} + \frac{(x + \frac{x^2}{\omega_c T})^2}{(x + \frac{x^2}{\omega_c T})^2 + (\frac{BT}{4})^2} \right] dx$$

$$-2\cos\omega_d T \int_{-\infty}^{\infty} Sa\left(x-\frac{\omega_d T}{2}\right) Sa\left(x+\frac{\omega_d T}{2}\right) \left[\frac{\left(x-\frac{x^2}{\omega_c T}\right)^2}{\left(x-\frac{x^2}{\omega_c T}\right)^2+\left(\frac{BT}{2}\right)^2} + \frac{\left(x+\frac{x^2}{\omega_c T}\right)^2}{\left(x+\frac{x^2}{\omega_c T}\right)^2+\left(\frac{BT}{2}\right)^2}\right] dx\}$$

$$i = 0,1 \qquad (4.47)$$

3. Probability of Error Calculation

The conditional mean of G' is given by the sum of Equation 4.41 with either Equation 4.38 or 4.39 depending whether $s_0(t)$ or $s_1(t)$ were transmitted, respectively. The conditional variance is Equation 4.47. With the conditional mean and variance determined it is now possible to compute the probability of error performance of the FSK coherent receiver with an ideal front-end filter. Assuming the probability of the transmitter sending a "one" or a "zero" signal are equal $(P(s_1(t)) = P(s_0(t)) = 1/2))$, Equation 2.39 shows that the average probability of error P_e is

$$P_e = \frac{1}{2}\left[\int_{-m_0/\sqrt{v_g}}^{\infty} \frac{1}{\sqrt{2\pi}} e^{-x^2/2} dx + \int_{-\infty}^{-m_1/\sqrt{v_g}} \frac{1}{\sqrt{2\pi}} e^{-x^2/2} dx\right]$$

$$(4.48)$$

where the threshold setting given by Equation 2.33 has been utilized.

In order to compute P_e, all that is needed is the specific conditional mean divided by the square root of the conditional variance since this ratio must be used in the limit

of the appropriate error function. However, the integrals of
Equation 4.47 do not match those of the conditional mean, as
found in every case investigated thus far. So before going
on to compute the limits of the error functions of Equation
4.48, the behavior of the conditional means and the variances
will be investigated with respect to $\omega_c T$. Referring to Equa-
tions 4.33 through 4.36 and 4.44 to 4.45, each has a term of
the form $x^2/\omega_c T$ in both the numerator and denominator.
Remembering that the filter was derived using an assumption
of large ω_c, the effect of the $x^2/\omega_c T$ terms can become negligi-
ble when used in the integrals involving products of two $Sa(x)$
functions, since these functions decrease rapidly with increas-
ing x. Therefore for large $\omega_c T$, a Filter Factor can be defined
as

$$\text{Filter Factor} = \int_{-\infty}^{\infty} Sa(x+\frac{\omega_d T}{2}) + Sa(x-\frac{\omega_d T}{2})]\,(\frac{x^2}{x^2+(\frac{BT}{2})^2})\,dx$$

$$- 2\cos\omega_d T \int_{-\infty}^{\infty} Sa(x-\frac{\omega_d T}{2})\,Sa(x+\frac{\omega_d T}{2})\,(\frac{x^2}{x^2+(\frac{BT}{2})^2})\,dx \qquad (4.49)$$

Thus the conditional variance becomes

$$\text{Var}[G'|s_i \text{ transmitted}] = \frac{A^2 T N_0}{2\pi} \times \text{Filter Factor} \qquad (4.50)$$
$$i = 0,1$$

and the conditional mean becomes

$$E[G'|s_i \text{ transmitted}] = [AT\sqrt{P_{nj}/T} - 1^{i+1} \frac{A^2 T}{2}]$$

$$\times \frac{1}{2\pi} \times \text{Filter Factor} \quad i = 0,1 \qquad (4.51)$$

The Filter Factor was computed via numerical integration
methods and compared with the complete expressions of Equation
4.47 for $\omega_c T$ as small as 50 and as large as 1000 with negligi-
ble errors. An example of a large $\omega_c T$ would be a communications
system operating at 1.0 MHz with a bit length of 13.3 milli-
seconds (75 baud). The $\omega_c T$ term would have a value of 13,300
which further supports dropping the $x^2/\omega_c T$ term from the equations.

Evaluating now $m_0/\sqrt{v_g}$ by dividing Equation 4.51 by
the square root of Equation 4.50 where the Filter Factor is
defined by Equation 4.49, $m_0/\sqrt{v_g}$ becomes

$$\frac{m_0}{\sqrt{v_g}} = \frac{[AT\sqrt{P_{nj}/T} - A^2 T/2] \times \frac{1}{2\pi} \times \text{Filter Factor}}{\sqrt{A^2 T N_0} \times \frac{1}{2\pi} \times \text{Filter Factor}} \qquad (4.52)$$

Recognizing that $A^2 T/2 = E$, the average energy per bit, and
substituting this in Equation 4.52 yields

$$\frac{-m_0}{\sqrt{v_g}} = \sqrt{E/N_0}(1 - \sqrt{2P_{nj}/E} \sqrt{1/2\pi \times \text{Filter Factor}} \qquad (4.53)$$

and similarly

$$\frac{-m_1}{\sqrt{v_g}} = -\sqrt{E/N_0}(1 + \sqrt{2P_{nj}/E}) \sqrt{1/2\pi \times \text{Filter Factor}} \qquad (4.54)$$

The probability of error performance can now be determined

versus E/N_0, the signal to noise ratio; P_{nj}/E, the jammer

to signal ratio; and BT (the relationship of the filter band-

width to the inverse of the signal bandwidth), by using

Equations 4.53 and 4.54 as the limits of integration in

Equation 4.48.

As with the ideal filter case, in order to compare the

results for the probability of error performance of the

coherent FSK receiver with no filtering, it is necessary to

remember that those results were obtained using $\bar{\rho} = 0$ and

$E = A^2 T/2$, where $\bar{\rho}$ and E are defined by Equations 4.26 and

4.25 respectively. Therefore, for large $(\omega_1 + \omega_0)T$, the

$Sa(\omega_1 + \omega_0)T$ term is negligible and $\bar{\rho}$ is zero when $(\omega_1 - \omega_0)T$ is

equal to m . When this is substituted in Equation 4.23,

recalling that $\omega_d T = (\omega_1 - \omega_0)T/2$, it can be seen that when BT

is zero the Filter Factor is 2π. For values of $\omega_d T$ that are

odd multiples of $\pi/2$ the Filter Factor is exactly equal to

2π, but for even multiples it is equal to 2 plus a quantity

which is negligible. So again, as in the FSK ideal front-end

filter case, for BT equal to zero, Equations 4.53 and 4.54 are

in agreement with the results of Ref. 2 for the coherent FSK

receiver operating against the optimum jammer. For P_{nj}/E

equal to zero, these results correspond to the results of Ref.

1 for the coherent FSK receiver operating in additive white

Gaussian noise alone. Again, as with the coherent BPSK receiver,

as the BT approaches zero, the behavior of the probability of

error performance of the coherent FSK receiver calculated using

a second order front-end filter is similar to the performance
calculated using the ideal front-end filter. Later the per-
formance comparison will be performed throughout the range of
pertinent values for the variable parameters.

V. RESULTS AND DISCUSSION

A. GENERAL

For each of the four receiver configurations (PSK and FSK receivers with both ideal and second order front-end filters), the results for the probability of error performance have been calculated and plotted as functions of P_{nj}/E (jammer to signal ratio), E/N_0 (signal to noise ratio) and BT (the filter bandwidth, bit duration product). The meaning of the jammer to signal and signal to noise ratios are self explanatory. However, the term BT deserves some attention. Since T is the time duration of $s_1(t)$ and $s_0(t)$, the spectra of each have been shown to be functions of the form $Sa(\omega T/2)$ where $Sa(x)$ has been defined as $\sin(x)/x$. The $Sa(\omega T/2)$ function has nulls when the value of $\omega T/2$ is an integer multiple of π or when $\omega = N(2\pi/T)$.

From the $Sa(\omega T/2)$ spectrum it can be shown that the value of $B = 2\pi/T$ represents approximately the 3 dB (or half power) bandwidth of the signal (actually $2\pi/T$ is the 4 dB bandwidth). The term BT can thus be thought of as the ratio of the filter bandwidth to the signal bandwidth for intuitive purposes. It is still convenient to refer in further discussions to the location of the nulls of the $Sa(\omega T/2)$ function.

The analysis of the calculated probability of error performance for each receiver configuration uses three types of plots. The first is the familiar plot of probability of

81

error versus signal to noise ratio, with constant values of BT and P_{nj}/E. The values of P_{nj}/E used are 0, .1, .5, 1, and 10. These values correspond to no jammer present, and jammer to noise ratios of -10 dB, -3 dB, 0 dB, and 10 dB. The particular values of BT depend on the modulation structure analyzed, and will be discussed later. The second type of plot will allow the analysis of the probability of error performance to be viewed as a direct function of BT. That is, for a constant value of signal to noise ratio, the probability of error is plotted versus BT. This plot consists of a family of curves corresponding to values of jammer to signal ratio (J/S) of 0.1 (-10 dB), 0.25 (-6 dB). 0.5 (-3 dB) and 1 (0 dB). Finally the third type of plot used in this analysis is again a probability of error versus signal to noise ratio plot. However this plot will consist of a family of curves for values of BT appropriate to the case analyzed. In these plots the value of J/S used is zero. This corresponds to the case where the jammer waveform is considered not to be time truncated.

The case J/S = 0 represents an alternate to the assumption that $n_j(t)$ is a time truncated process. When $n_j(t)$ is a pure cosine function, $N_j(\omega)$ is a delta function, which can be completely removed by the front-end filter. The resulting plots then describe the effect of the signal being distorted by the front-end filter before it is correlated with $s_d(t)$. The probability of error curves for this analysis is shown by

the set of plots described in the preceding paragraph. This
performance analysis can also be viewed in each of the other
plots with the curve J/S = 0.

B.   PHASE SHIFT KEY RECEIVER ANALYSIS

   1.   General

         The probability of error performance of the BPSK receiver
with both the ideal and second order front-end filters is
analyzed and compared to that of the unfiltered BPSK receiver
in this section.   The results of Equations 3.32 and 3.33 are
substituted into Equation 3.29, yielding the average proba-
bility of error for the BPSK receiver with an ideal front-end
filter.   Substituting Equations 3.69 and 3.70 into Equation
3.66 yields the average probability of error for the BPSK
receiver with a second order front-end filter.   In each case
the plots described in the beginning section of this chapter
are used to analyze the performance.   For PSK modulated sig-
nals, the discrete values of BT are chosen with respect to
the PSK modulation frequency spectrum.   Recalling that the
spectrum (Equation 3.22) is of $Sa(\omega T/2)$ form, the first null
of this spectrum occurs for $\omega = 2\pi/T$.   Thus the null to null
bandwidth is $4\pi/T$.   Therefore, the value of BT = 4π will be
used as a practical limit in this analysis.   The other dis-
crete values of BT are: BT = 0 (no filter), BT = 0.4 (a
small notch), BT = 3.16 (25% of the null to null bandwidth),
BT = 6.28 (50% of the null to null bandwidth), and BT = 12.56
(the full null to null bandwidth).

2. PSK Receiver With An Ideal Front-End Filter

Figures A.3 through A.9 result when the probability of error for the BPSK receiver with a front-end filter is calculated using the ideal filter model. These plots show how the probability of error performance is affected by the signal to noise ratio, jammer to signal ratio and BT. Figure A.3 represents the probability of error performance of the BPSK receiver with no front-end filter. This corresponds to the results derived and plotted in Ref. 2. In fact the J/S = 0 curve in this plot is the well-known result for the coherent BPSK receiver operating in additive white Gaussian noise alone. This curve will serve as a performance reference in the following discussions. Figures A.3 through A.8 allow the probability of error performance to be graphically analyzed for the cases where the jammer is either a truncated process or a continuous time function as discussed in the first section of this chapter.

For the truncated jammer, by following the J/S = 0.1 and 0.5 curves from Figure A.3 to Figure A.8, the curves shift to the right as the value of BT is increased. This means that for a given probability of error, the receiver operating with the larger value of BT requires more signal to noise ratio to achieve a given level of performance. Thus for the optimum jammer (truncated by the receiver process) the front-end filter actually further degrades the probability of error performance for the BPSK receiver. Specifically, (refer to the J/S = 0 curve of Figure A.3) for BT = 3.16 there is 5 dB of degradation, for BT = 6.28 there is 6 dB of degradation and for BT = 12.56

84

there is 9 dB of degradation. The rapid increase of the probability of error as BT increases is seen in Figure A.8. For a fixed value of E/N = 100 (20 dB), the probability of error rapidly increases as BT approaches 4π. As BT increases further, the slope of the probability of error curves become less positive as less energy is incrementally removed from the signal by the filter.

Assuming now that the jammer is not truncated by the receiver process, the analysis of the probability of error curves is performed by comparing the J/S = 0 curves of Figures A.4 to A.8 with that of Figure A.3. These are plotted together in Figure A.9. From Figure A.3, for J/S equal to -10 dB, 5 dB of additional signal to noise ratio is required to achieve the same probability of error performance as with no jammer present. For J/S equal to -3 dB, 10 dB of additional signal to noise ratio is required, and for J/S greater than one, no increase in signal to noise ratio results in improved performance as discussed in Ref. 2. Assuming that the filter completely removes the jammer, Figure A.9 shows the performance penalty associated with the use of the front-end filter. By comparing Figure A.9 with Figure A.3, it is seen that for large values of J/S the receiver probability of error performance is improved by the front-end filter. The specific level of improvement is determined by comparing the curve in Figure A.3 corresponding to a particular J/S value with the curve in Figure A.9 for a fixed value of BT. For the ideal jammer in which the frequency spectrum is a delta function, an infinitely

85

narrow bandwidth filter can be used to counter this jammer.

In a more practical sense, the filter bandwidth should be made

as narrow as possible, and yet completely null the jammer over

its entire spectrum. The sensitivity of the probability of

error performance to the value of BT used for this case is

shown in Figure A.8 with the J/S = 0 curve. Again, there is

a rapid increase of probability of error as BT increases to

the value of 12.56. This further shows that BT should be kept

as small as practically possible.

3.   PSK With A Second Order Front-End Filter

Figures A.10 through A.16 result when the probability

of error for a coherent BPSK receiver with a second order

front-end filter is plotted versus E/N, J/S, and BT. The

probability of error in this case is obtained by substituting

Equations 3.69 and 3.70 into Equation 3.66. Figure A.10

shows the probability of error performance with BT = 0 (actually

BT = 0.0001 for computational purposes). For values of BT

less than 3.16 (approximately equal to π), the probability of

error curves compare closely with the curves plotted for the

BPSK receiver with the ideal filter. This is illustrated by

comparing Figure A.11 with Figure A.4, and Figure A.12 with

Figure A.5. For values of BT greater than 2π the comparison

of Figures A.6 and A.7, with Figures A.13 and A.14, show that

for BT = 6.28 the ideal filter calculations differ from the

second order filter calculations by 1 dB. For BT = 12.56

there is a 2 dB difference in the curves calculated using the

ideal versus the second order filter. The comparison of Figures A.8 and A.15 show that as BT increases, the calculations using the ideal filter are less accurate compared to the second order filter calculations. Again, for the truncated jammer case, no value of BT results in improved probability of error performance in comparison to the unfiltered receiver.

Now, assuming that the receiver process does not truncate the jammer, Figure A.16 shows the probability of error performance achieved for BT = 0, 3.16, 6.28 and 12.56. Comparing Figure A.16 to Figure A.9 shows that there is similarity in the probability of error performance calculated using the ideal filter model with that calculated using the second order filter model, for values of BT less than 3.16. Therefore for values of BT less than π (or B less than 25% of the signal null to null bandwidth), the probability of error can be determined from the results derived for the ideal filter model being used as a front-end filter.

C. COHERENT FREQUENCY SHIFT KEY RECEIVER ANALYSIS

The probability of error performance of the FSK receiver with the two filters, the ideal and second order front-end filters, is analyzed and compared to the unfiltered coherent FSK receiver performance in this section. The results of Equations 4.53 and 4.54 are substituted into Equation 4.48, yielding the average probability of error of the FSK receiver with an ideal front-end filter. Substituting Equations 2.28 and 2.29 into Equation 2.23 yields the average probability of

error for the FSK receiver with a second order front-end filter. In each case the plots described in the beginning section of this chapter are used to analyze performance. For FSK modulated signals, not only must the parameter BT be chosen, but also the frequency separation of the FSK signals must be set. From the general results on performance for the coherent receiver, the probability of error is given by (from Ref. 1 assuming no filters and no jamming present)

$$P_e = \text{erfc}[\frac{\varepsilon(1-\overline{\rho})}{\sqrt{N_0\varepsilon(1-\overline{\rho})}} \tag{5.1}$$

with

$$\text{erfc}(x) = \int_x^\infty \frac{1}{\sqrt{2\pi}} e^{-u^2/2} \, du$$

where ε and $\overline{\rho}$ have been defined by Equations 4.24 and 4.26, respectively. The results of Ref. 2 given by Equation 4.5, with the Filter Factor equal to 2 , use a value of $\overline{\rho}$ of zero. Therefore the comparisons made here will be for values of $\omega_1 - \omega_0$ such that $\overline{\rho}$ is zero. The term used to describe this separation and used in the derivation of the probability of error results is $\omega_d T$, defined in Equation 4.7 as $\omega_d T = (\omega_1 - \omega_0)T/2$. The minimum value of $\omega_d T$ is chosen to be $\pi/2$ because from Equation 4.27 it is seen that the separation $(\omega_1 - \omega_0 = \pi/T)$ is the minimum separation required for the normalized correlation coefficient of $s_0(t)$ and $s_1(t)$ to be zero. The other value of

88

$\omega_d T$ chosen is π, where again with this separation the normalized correlation coefficient is zero.

In Section IV.A.1 the strategy of placing the filter at the midpoint of ω_1 and ω_0 is described. From Equation 4.13, it is seen that the optimum jammer for the coherent FSK receiver consists of Sa(T/2) functions centered at ω_1 and ω_0. Therefore in order to filter out the major portions of the jammer, the bandwidth of the filter must be at least equal to the frequency separation of the FSK signals. This also holds true for the case where the jammer is considered not to be truncated by the receiver process. Given these conditions, for $\omega_d T$ equal to $\pi/2$ the values of BT used will be zero, corresponding to no filter, π corresponding to the difference of the signal frequencies, and finally $\pi + 0.1\pi$ (= 3.46) in order to take into account the non-truncated jammer having non-zero spectral width. Similarly for $\omega_d T = \pi$, the values of BT chosen are BT = 0, BT = 2, and BT = $2\pi + 0.1 \cdot 2\pi$ (= 6.91).

1. FSK Receiver With An Ideal Front-End Filter

Figures A.17 to A.24 result when the probability of error for the coherent FSK receiver with a single ideal front-end filter is plotted as functions of signal to noise ratio, jammer to signal ratio, frequency separation, and BT. Figures A.17 and A.20 present the probability of error for the coherent FSK receiver operating with no front-end filter. Also the J/S = 0 curve in these figures correspond to the probability of error performance for the FSK coherent receiver (with

89

orthogonal signals) operating in white Guassian noise alone.
It is not surprising that Figures A.17 and A.20 are exact
duplicates, because in each case the normalized correlation
coefficient of $s_1(t)$ and $s_0(t)$ is zero, as described in
Section V.C. As with the BPSK analysis, the J/S = 0 curves
of Figures A.17 and A.20 will serve as a performance reference.

Assuming the truncated version of the jammer, first
for $\omega_d T = \pi/2$, Figures A.17 to A.19 show that as BT increases
from 0 to 3.46, the probability of error curves shift to the
right. This indicates that for increasing filter bandwidths,
more signal to noise ratio is required to achieve the same
probability of error performance as with no filter. From
Figure A.17, for a value of BT equal to π, approximately 2
dB of additional signal to noise ratio is required to achieve
the same level of performance as in Figure A.17. This applies
for all values of J/S. From Figure A.19, 2.8 dB of additional
signal to noise ratio is required to achieve the performance
level presented in Figure A.17. The increase in probability
of error with increasing BT for all values of J/S is shown in
Figure A.23.

With $\omega_d T$ equal to π, more filter bandwidth is required
in order to attempt to notch out the jammer. As a result, a
greater amount of the signal energy is removed by the filter
than is the case for the receiver operating with $\omega_d T$ of $\pi/2$.
Therefore, the performance of the FSK receiver with a front-
end filter and $\omega_d T$ set to the value of π, will be worse.
Figures A.20 to A.22 show that for BT increasing from zero to

6.91, more signal to noise ratio is required to achieve the performance level of the receiver operating with an unfiltered jammer. Specifically, 5.6 dB of additional E/N is required for BT = 2π, and 6.6 dB of additional E/N is required for BT = 6.91. Figure A.24 shows the sensitivity of the probability of error performance for increasing values of BT. Focusing on Figures A.17 to A.24, in either case ($\omega_d T = \pi/2$ or 1.57), analysis using the truncated jammer assumption shows that no value of BT causes a decrease in the probability of error for the coherent FSK receiver. Only degradation is observed.

The analysis of the coherent FSK receiver with the ideal front-end filter, assuming the non-truncated jammer, is performed by comparing the J/S = 0 curves on Figures A.17, A.18 and A.19 for $\omega_d T = \pi/2$. For $\omega_d T = \pi$, the J/S = 0 curves on Figures A.20, A.20 and A.22 are compared. As before, the unfiltered J/S = 0 curves (Figures A.17 and A.20) serve as a reference. As in the BPSK case, this analysis shows that for either $\omega_d T = \pi/2$ or π, the J/S = 0 curves still shift to the right as BT is increased indicating that more signal to noise ratio is required in order to achieve the same performance as for the unfiltered case. From the curves for an unfiltered jammer (Figures A.17 and A.20) for values of J/S greater than 0.5, the receiver is essentially inoperable ($P_e \approx 0.5$). However, the J/S = 0 curve of Figure A.18 shows that an increase of E/N_0 of 5.6 dB can bring the performance of the filtered FSK receiver to the same value of P_e as for the unfiltered receiver. Figure A.18 corresponds to $\omega_d T = \pi/2$, BT = π. Figure A.19

shows that for BT = 3.46, 2.8 dB of additional E/N_0 is required
to achieve the unfiltered, unjammed performance. Figures A.18
and A.19 show that for values of J/S greater than .5 (for the
coherent receiver) the use of the ideal filter does show an
improvement on the performance of the FSK receiver when the
filter is used to notch out the cw jammer. The sensitivity
of the probability of error to the value of BT used for the
case of $\omega_d T = \pi/2$, is shown by the J/S = 0 curve of Figure
A.23. As in the BPSK receiver case, this shows that the smallest
possible filter bandwidth should be utilized. For $\omega_d T = \pi$,
similar results are shown in Figures A.21 and A.22. With
BT = 2π, 5.6 dB of additional E/N_0 is required to achieve the
performance level of the unfiltered, unjammed receiver, and
for BT = 6.91, 6.6 dB of additional E/N_0 is required. Figure
A.24 shows the sensitivity of the probability of error for
this case. An important fact to remember is that when using
Figures A.23 and A.24, the ideal filter does not alter the
jammer until BT is at least $2 x \omega_d T$.

2. The FSK Coherent Receiver With A Second Order
   Front-End Filter

Figures A.25 to A.32 result when Equations 4.53 and
4.54 are substituted into Equation 4.48 and are plotted versus
BT, J/S and E/N_0. Figures A.25 and A.28 are the probability
of error curves for the unfiltered FSK coherent receiver
operating with $\omega_d T = \pi/2$ and π, respectively, and with an
unfiltered jammer. As described in the analysis of Figures
A.17 and A.20, Figures A.25 and A.28 are exact duplicates

92

because $\bar{\rho}$ in each case is zero. In general, the curves plotted using the second order filter model match within 1 dB to those calculated using the ideal filter model. Specifically, Figures A.26 and A.27 ($\omega_d T = \pi/2$, BT = π and 3.46 respectively) compare within 1 dB to the results of Figures A.18 and A.19 which are calculated using the ideal filter model. Similarly, for $\omega_d T = \pi$, Figures A.29 and A.30 compare within 1 dB to the results presented in Figures A.21 and A.22 respectively. The sensitivity analysis from Figures A.31 and A.32 ($\omega_d T = \pi/2$ and π) still shows the rapid increase in probability of error with increasing BT. However, compared to similar curves calculated using the ideal filter, Figures A.31 and A.32 have smaller (positive) slope. In all, assuming the truncated jammer, Figures A.25 to A.32 still show that as the front-end filter bandwidth increases, the probability of error increases also. Therefore, as with the ideal filter case, the second order front-end filter only further degrades the performance of the coherent FSK receiver operating against the truncated optimum jammer.

Assuming the non-truncated version of the optimum jammer, it is easily seen that a second order front-end filter such as the one given by Equation 3.37 would not be completely effective against that jammer. By expanding Equation 4.3, it is seen that the jammer spectrum would consist of delta functions centered at ω_1 and ω_0. The filter described in Section III.B has a null only at $\omega = \pm\omega_c$. Therefore the

93

analysis cannot be performed by simply letting J/S = 0 in this case. From the analysis completed for the ideal filter case, it is seen that a higher order filter, or a filter with nulls at ω_1 and ω_0, should be used to defeat the non-truncated optimum jammer.

VI. CONCLUSIONS

A. GENERAL CONCLUSIONS

In this thesis the effectiveness of front-end filtering techniques has been investigated as an electronic counter-countermeasure (ECCM) in order for the coherent digital receiver to be able to operate effectively against the optimum jammer derived in Ref. 2. The specific coherent digital receivers analyzed were the coherent BPSK receiver and the coherent BFSK receiver. The filters placed in the front-end of the receivers, as shown in Figure A.2, were an ideal filter and a second order filter of the form given by Equation 3.37.

Because the analysis of Ref. 2 defines the optimum jammer in the time interval $(0,T)$, the analysis was performed using this interval in the calculation of the Fourier transforms of the jammer models. As a result, Sections V.B.2 and V.B.3 as well as Sections V.C.2 and V.C.3 show that none of the front-end filters resulted in any decrease in the probability of error in comparison to receivers operating without front-end filters for the class of receivers analyzed. This occurs because the resultant jammer consists of a signal that is of the same form as $s_d(t)$, the correlation signal. As a result, the filter affects equal portions of both the signal spectrum as well as the jammer spectrum. Therefore under this analysis, the front-end filters further added to the probability of error

caused by the jammer and the additive noise for both the BPSK
and BFSK coherent receivers.

Taking into account the physical aspect of this problem,
an ambiguity is seen. Both $s_d(t)$ and $n_j(t)$ are defined over
the interval $(0,T)$. However over the next interval $(T,2T)$
these signals remain unchanged. This repeats itself for the
next interval of length T, and so on. In other words, both
$s_d(t)$ and $n_j(t)$ are cw signals. Assuming such a form for
the optimum jammer, the analysis was carried out by substi-
tuting 0 for the value of J/S, for all but the FSK receiver
with the second order front-end filter. Setting J/S = 0 pro-
vides the same result as setting the term (n'_j, s_d) equal to
zero. In the case of the FSK coherent receiver, the second
order filter does not have nulls at the frequencies of the
optimum jammer. This analysis cannot be performed simply by
setting J/S = 0.

When the PSK coherent receiver was analyzed with both
filter models using the cw form of the optimum jammer, the
filter was observed to introduce improvements to the proba-
bility of error performance provided that the receiver was
jammed with a value of J/S of at least 0.5. This is quite
apparent for J/S equal to 1.0, as the unfiltered PSK coherent
receiver becomes essentially inoperative (P = 0.5). When
the filter is introduced in this case, the jammer term
(n'_j, s_d) is set to zero. Therefore the conditional mean of
G', the output of the receiver, is a function of (s'_i, s_d) only.

When this happens, any increase in the probability of error compared to that of the unfiltered, unjammed receiver is caused only by the filter distorting the signal. The use of the filter is not without cost. As shown in Figures A.9 and A.16, additional signal to noise ratio is required to achieve the same probability of error as that of unfiltered unjammed receiver.

The analysis of the FSK coherent receiver with the ideal front-end filter, under the assumption of the cw jammer shows similar results. However, because a single filter, centered at the midpoint frequency between the FSK signals is used, more signal to noise ratio is required to achieve the same probability of error performance as that of unfiltered, un-jammed receiver. This results because the filter bandwidth must be at least equal to the frequency separation of the FSK signals. Due to this observation, the smallest practical frequency separation should be used. Analysis of the second order front-end filter shows that this type of filter centered midway between the FSK signals was not as useful as a filter with nulls at the jammer frequencies.

B. SPECIFIC CONCLUSIONS

Some specific conclusions follow from the analysis performed in this thesis. These are as follows:

1) For the PSK coherent receiver with a front-end filter, the probability of error performance calculated using

the ideal front-end filter matches the performance calculated using the second order filter within 1 dB for values of BT of less than π. Therefore, the analysis can be performed using the ideal filter for small values of BT. So, though this will require computer integration methods, time will be saved by not analyzing complex filter models.

2) Under the assumption of a time truncated jammer, the probability of error for the FSK coherent receiver calculated using the ideal filter compares with the results calculated using the second order filter with BT = $2\omega_d T$. Therefore, the ideal filter can be used for these calculations.

3) The second order front-end filter centered between the FSK signals does not effectively remove the jammer (assuming the non-truncated jammer) and therefore is not as useful as a filter with nulls at the jammer frequencies.

4) It appears that part of the performance degradation introduced by filtering is due to the fact that the filter distorts the signal components $s_1(t)$ and $s_0(t)$, so that the correlator receiver (or equivalently the matched filter receiver) is not matched to the incoming signals. This degradation could be overcome by using a matched filter receiver that is matched to $s_1'(t)$ and $s_0'(t)$. While this has not been investigated in this thesis, it appears that such investigations would be of great interest and worthwhile.
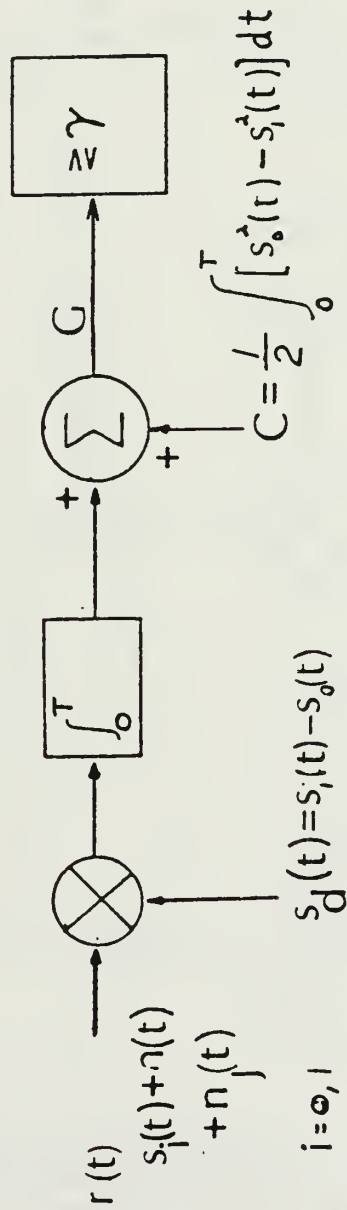
Figure 1. Coherent Receiver
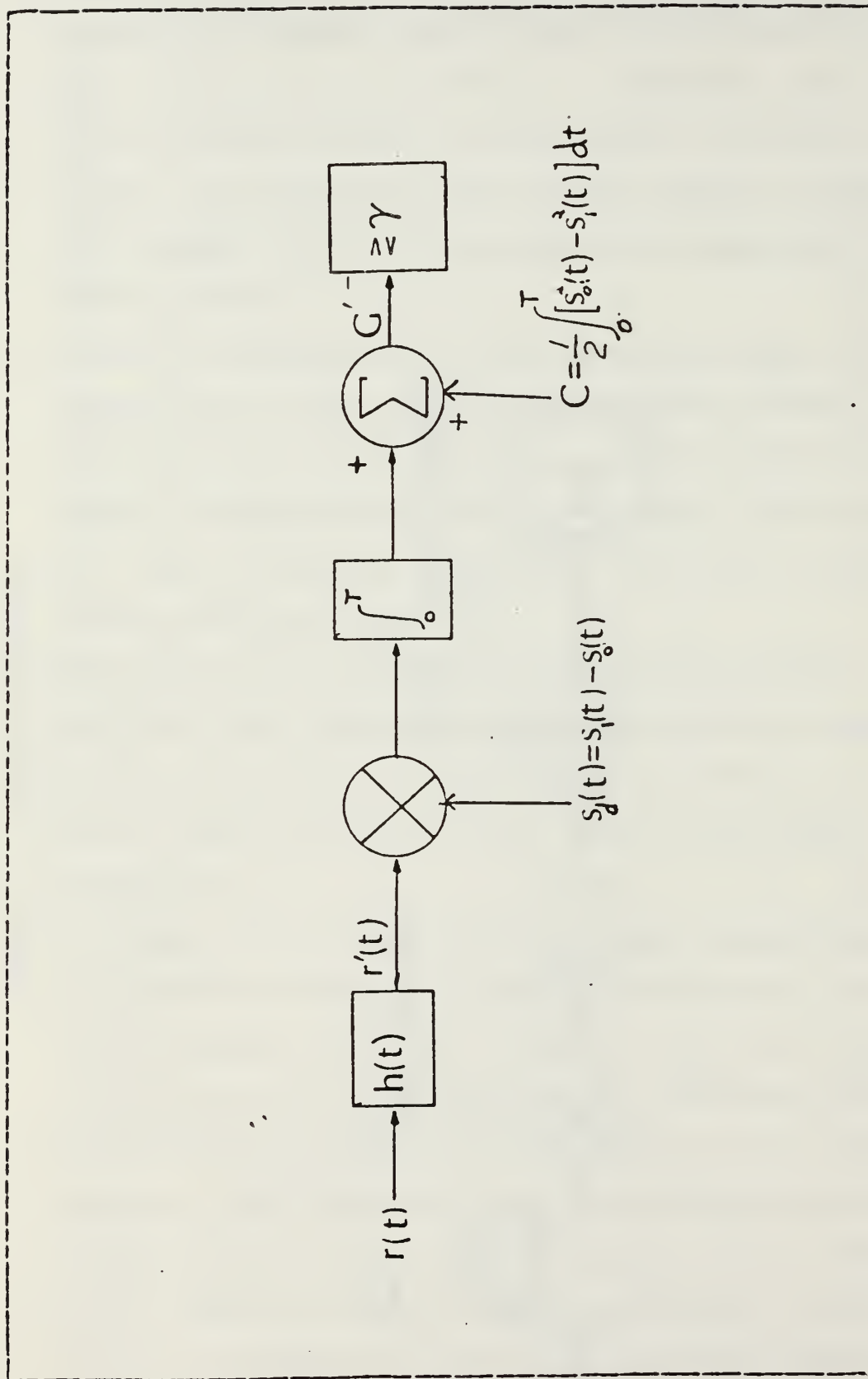
Figure A.2. Coherent Receiver with a Front-End Filter
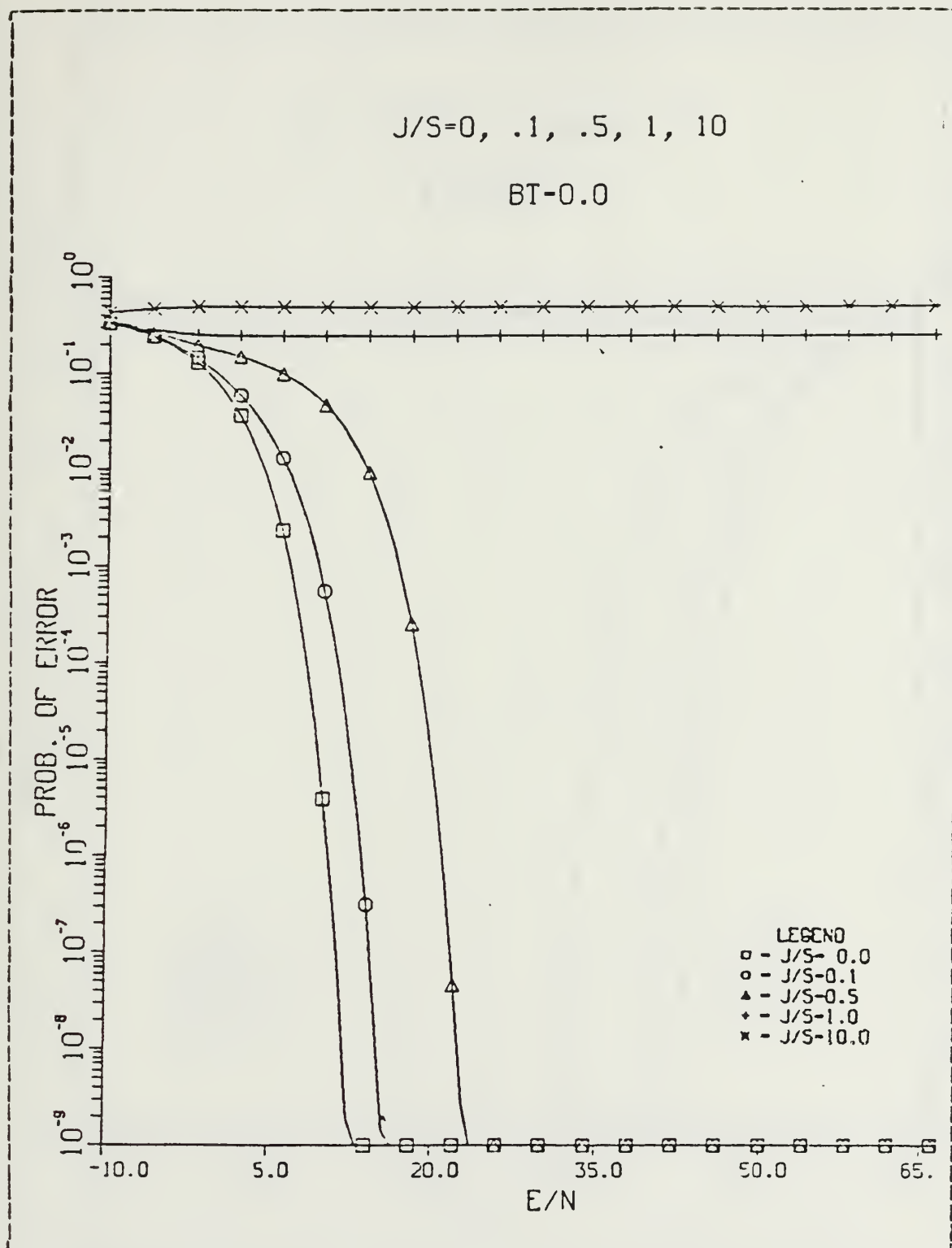
Figure A.3.   Coherent PSK Receiver with an Ideal
             Front-End Filter, BT = 0.0

101
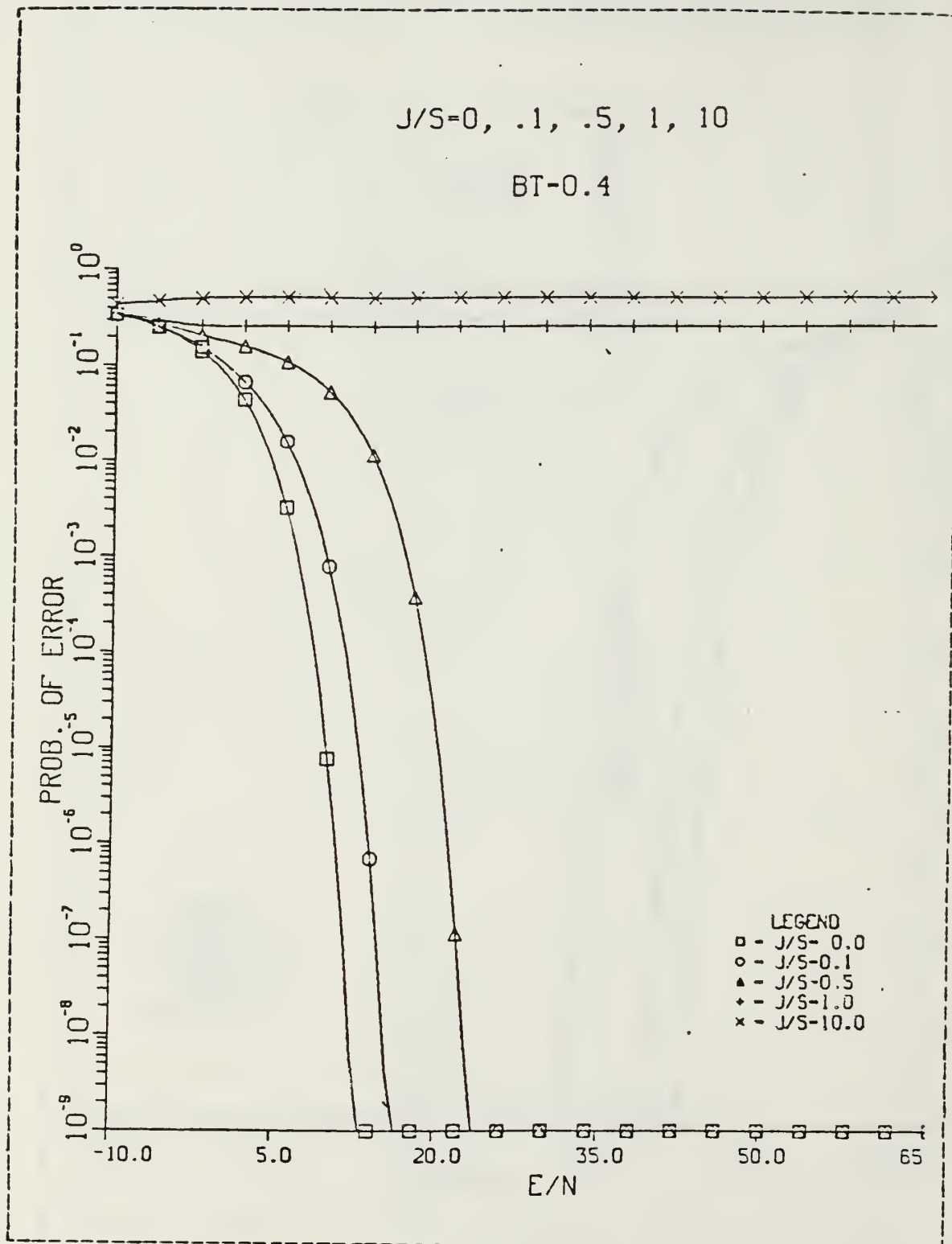
Figure A.4.   Coherent PSK Receiver with an Ideal
               Front-End Filter, BT = 0.4
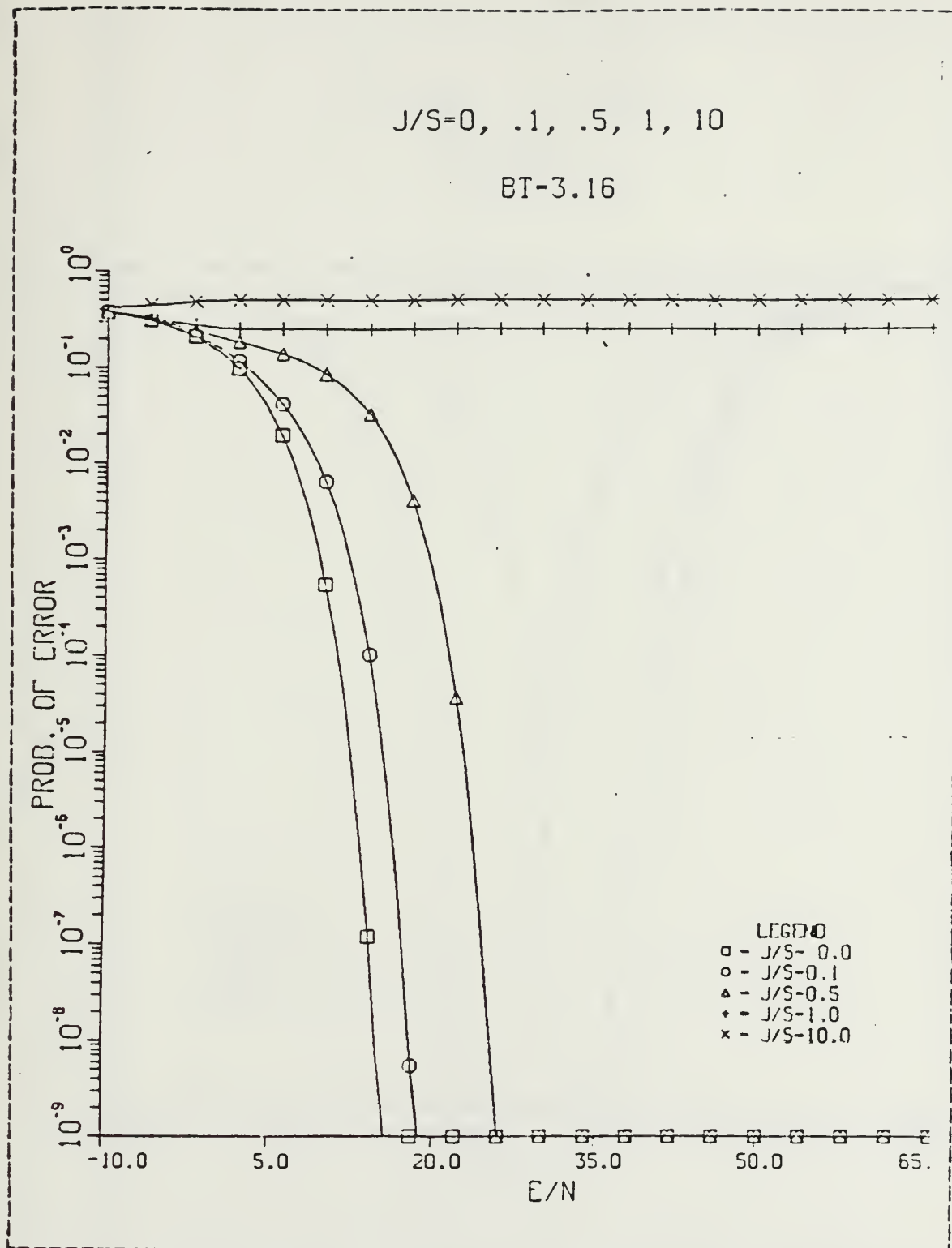
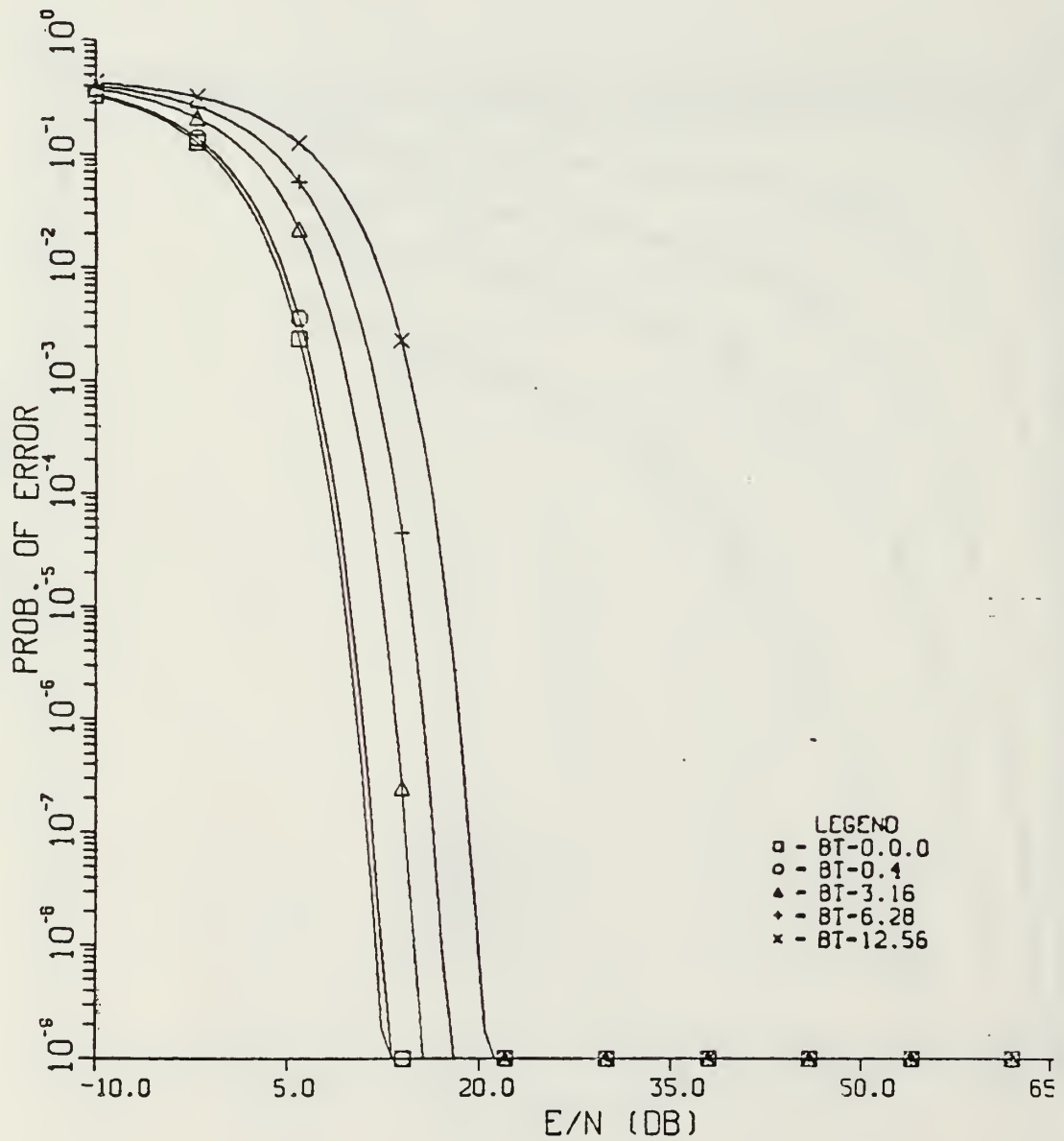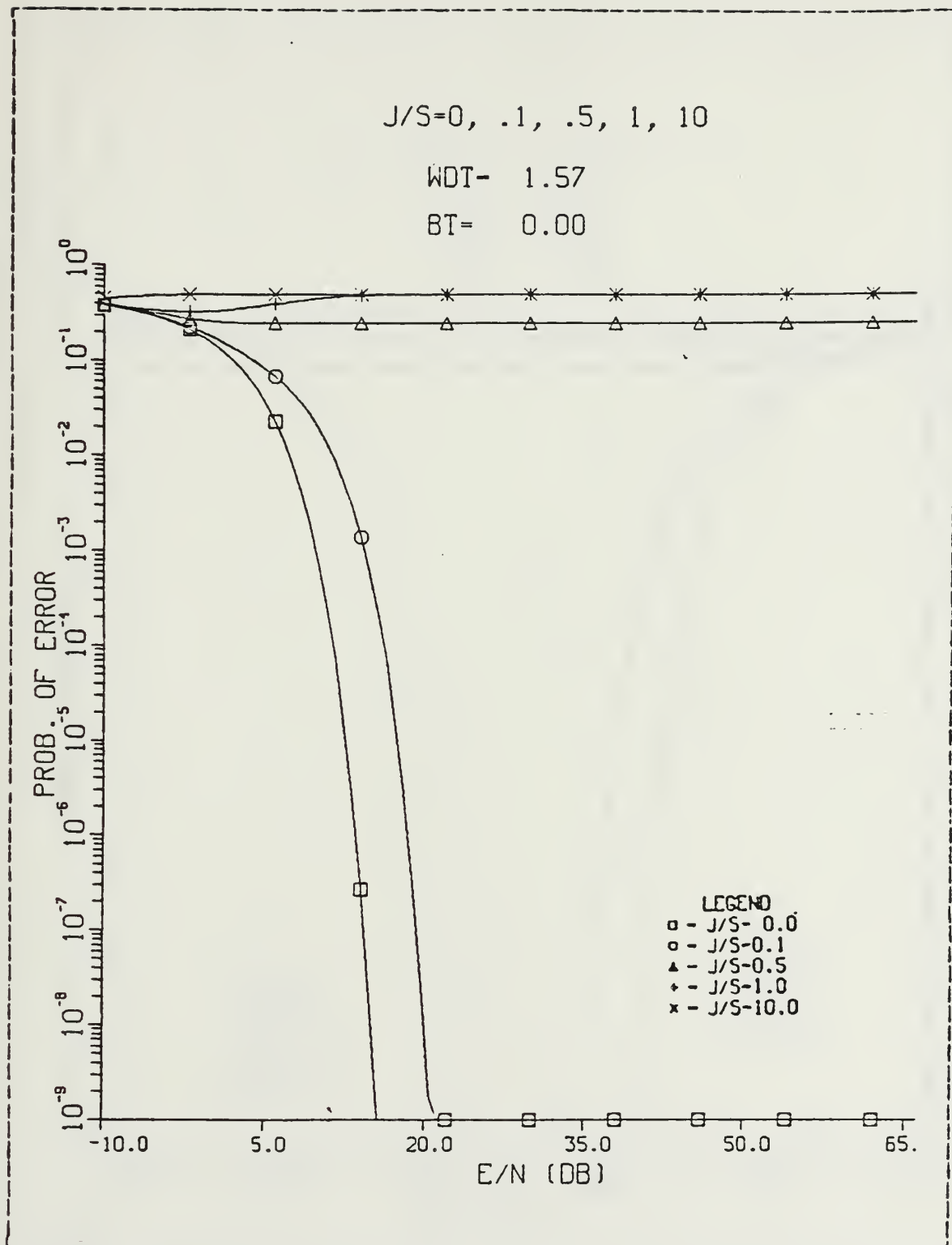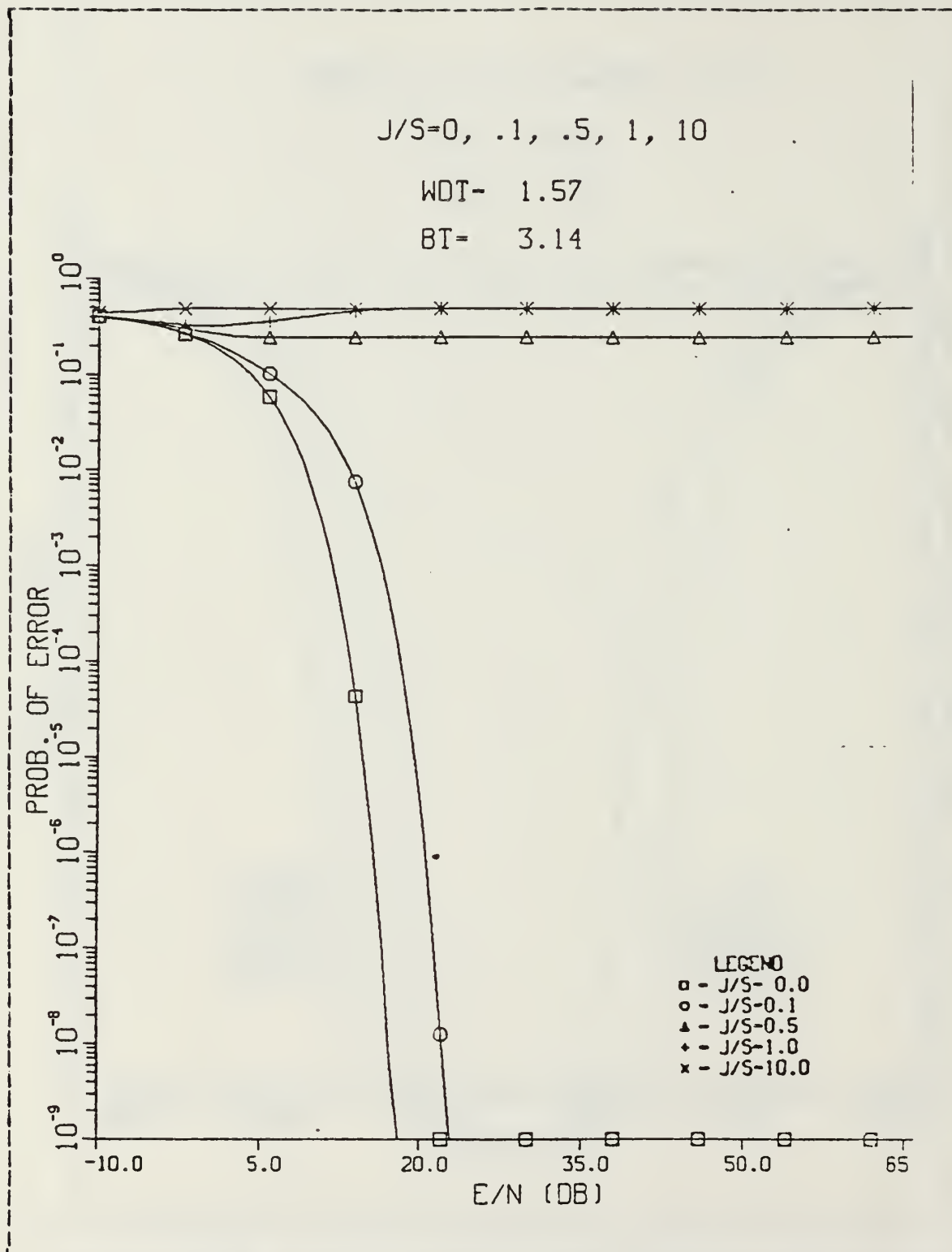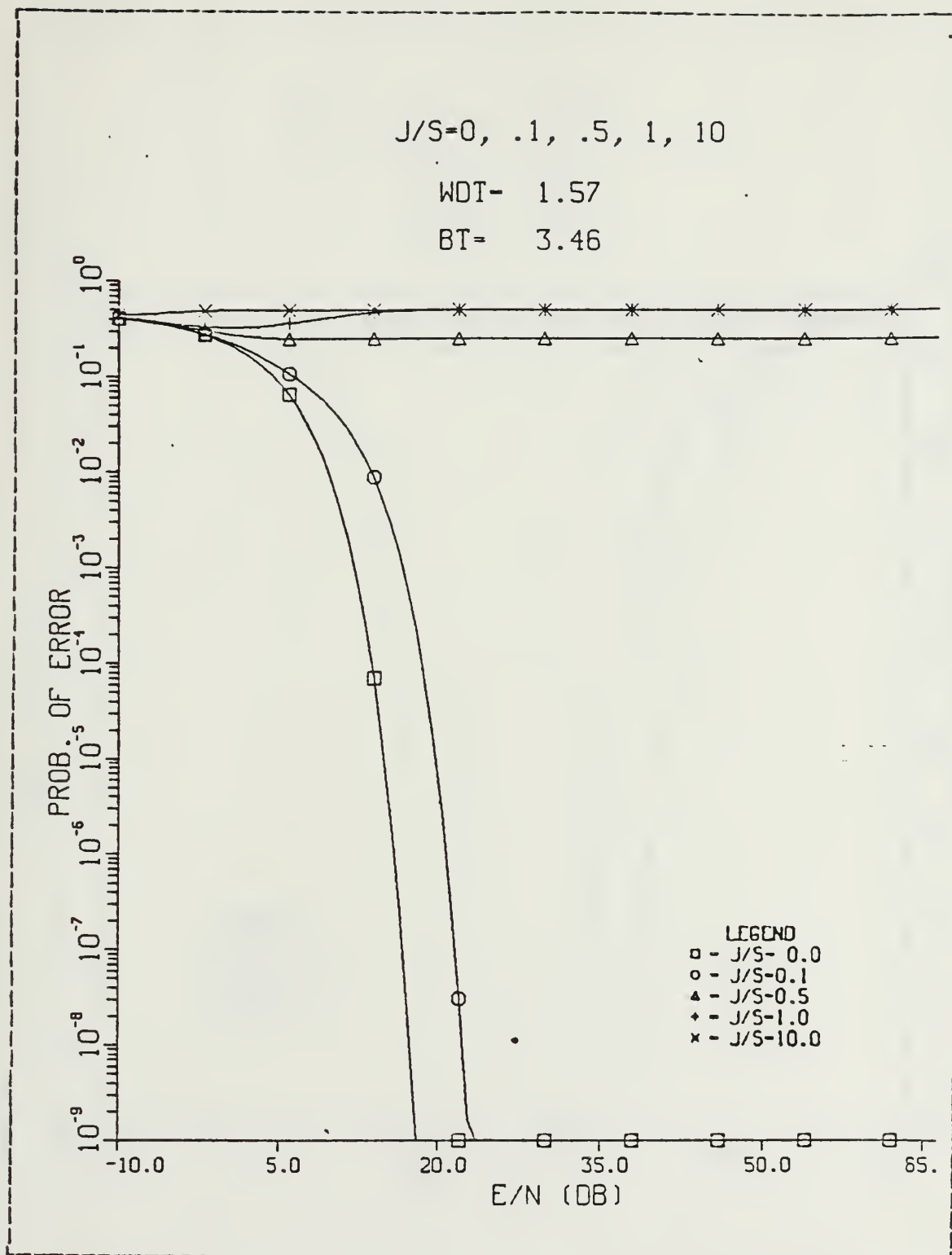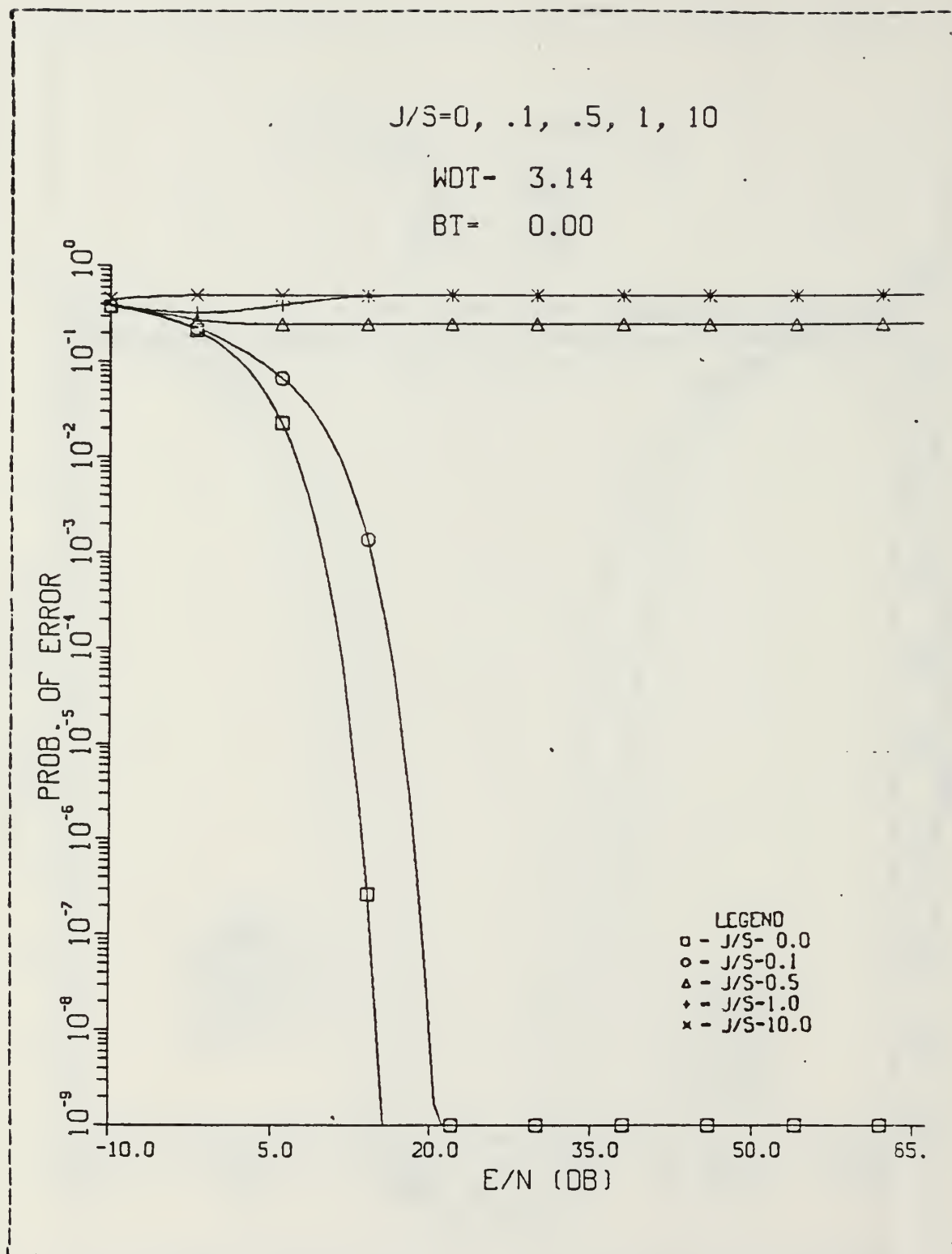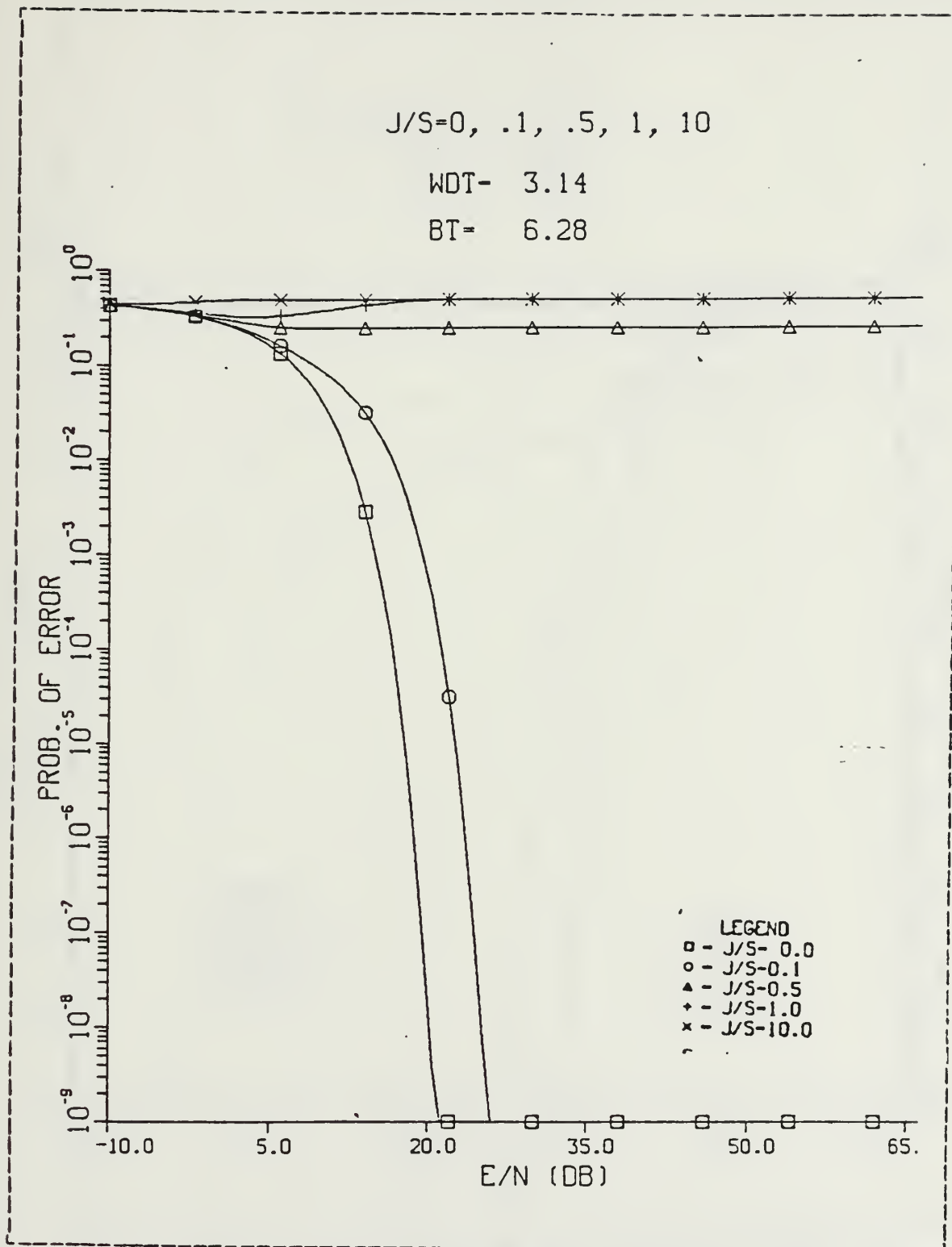Figure A.5. Coherent PSK Receiver with an Ideal
Front-End Filter, BT = 3.16

103
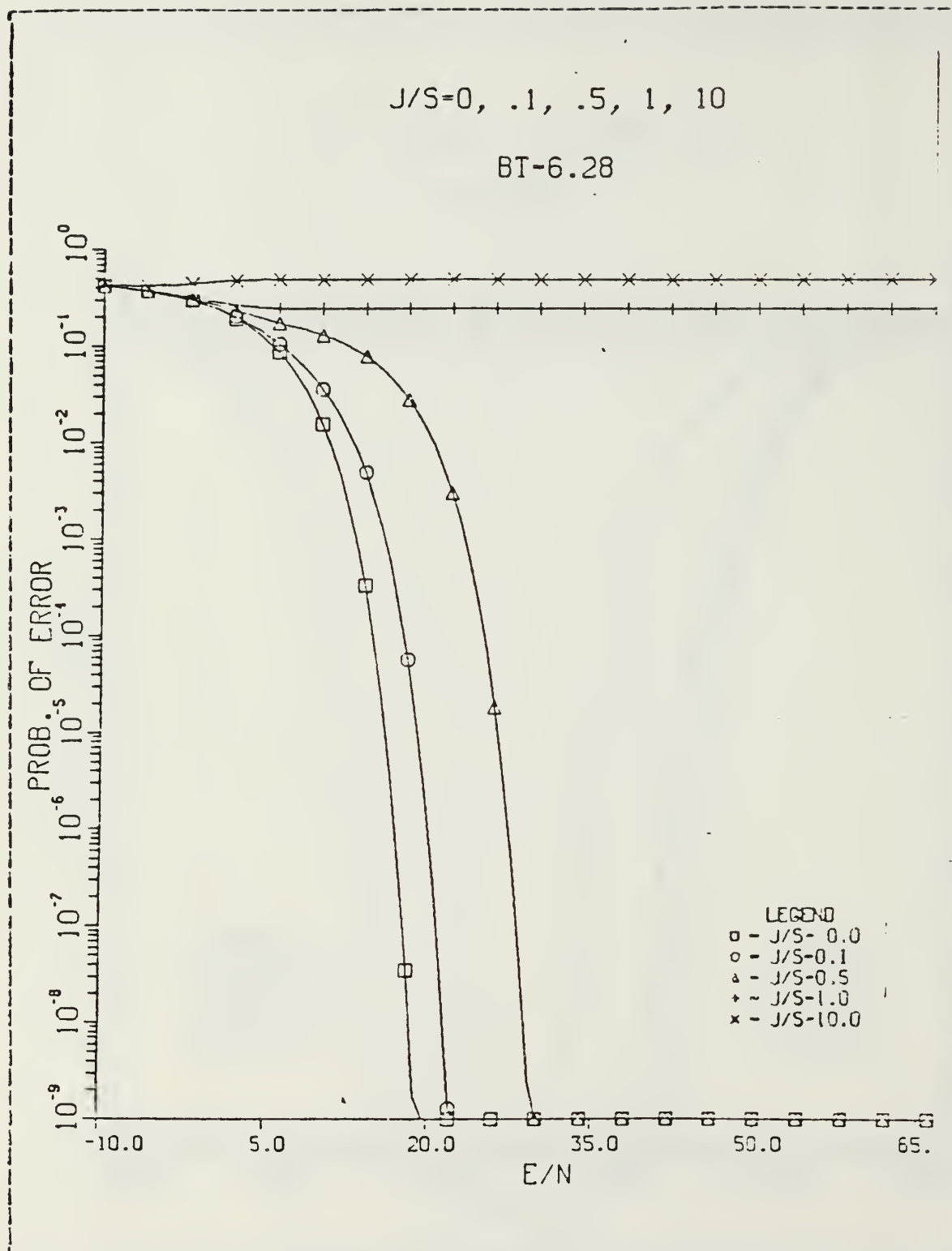
Figure A.6. Coherent PSK Receiver with an Ideal
Front-End Filter, BT = 6.28

104
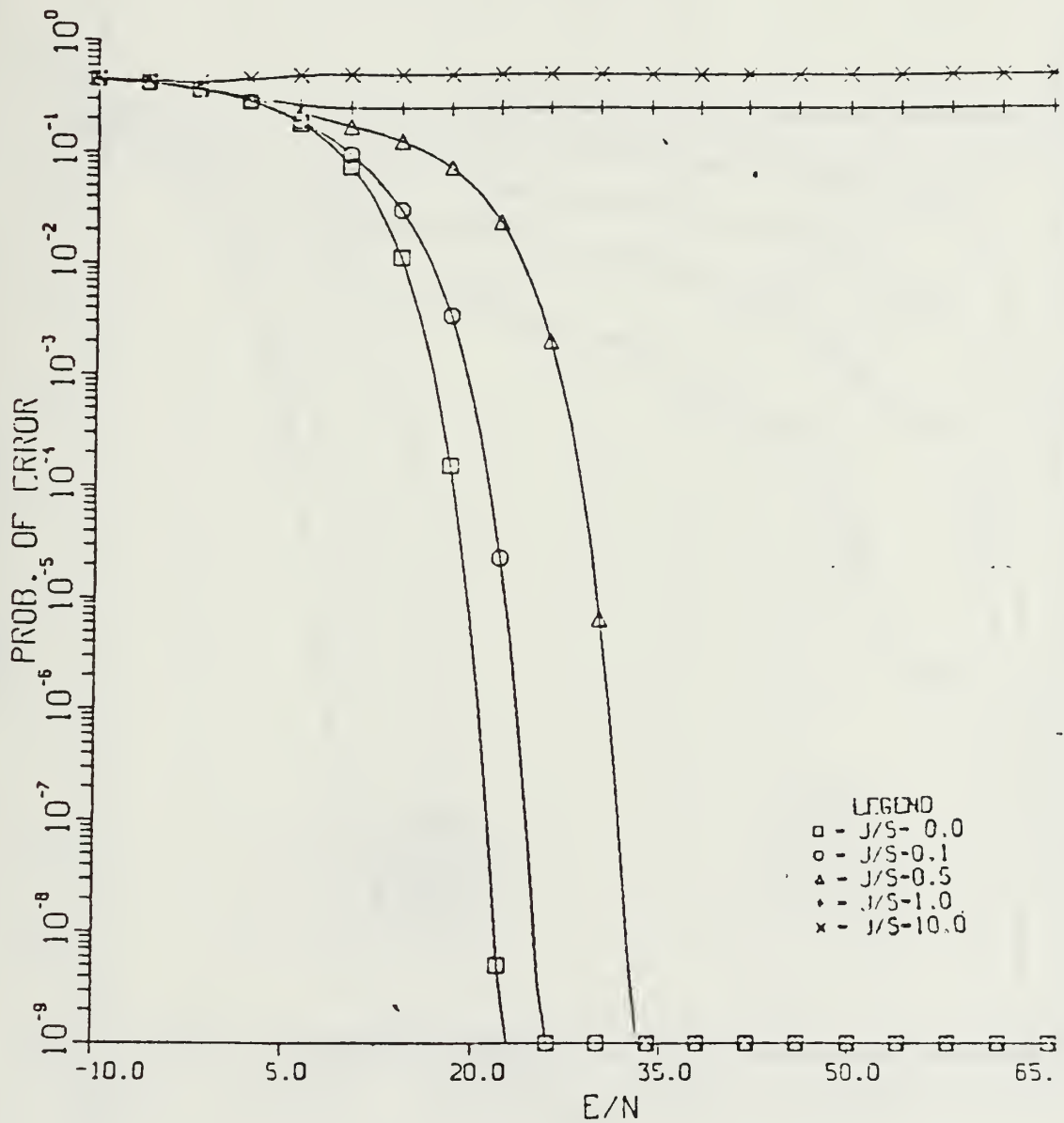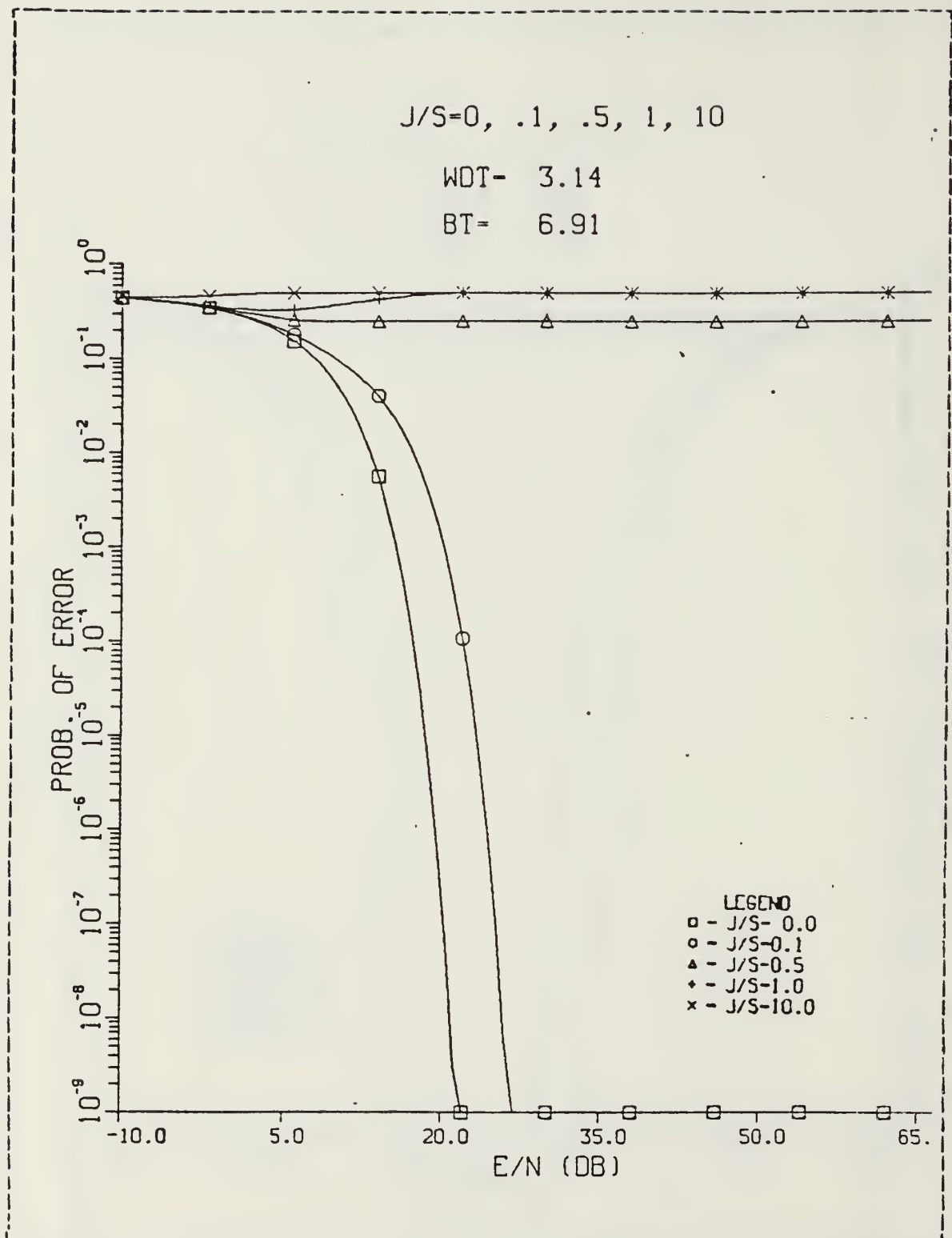
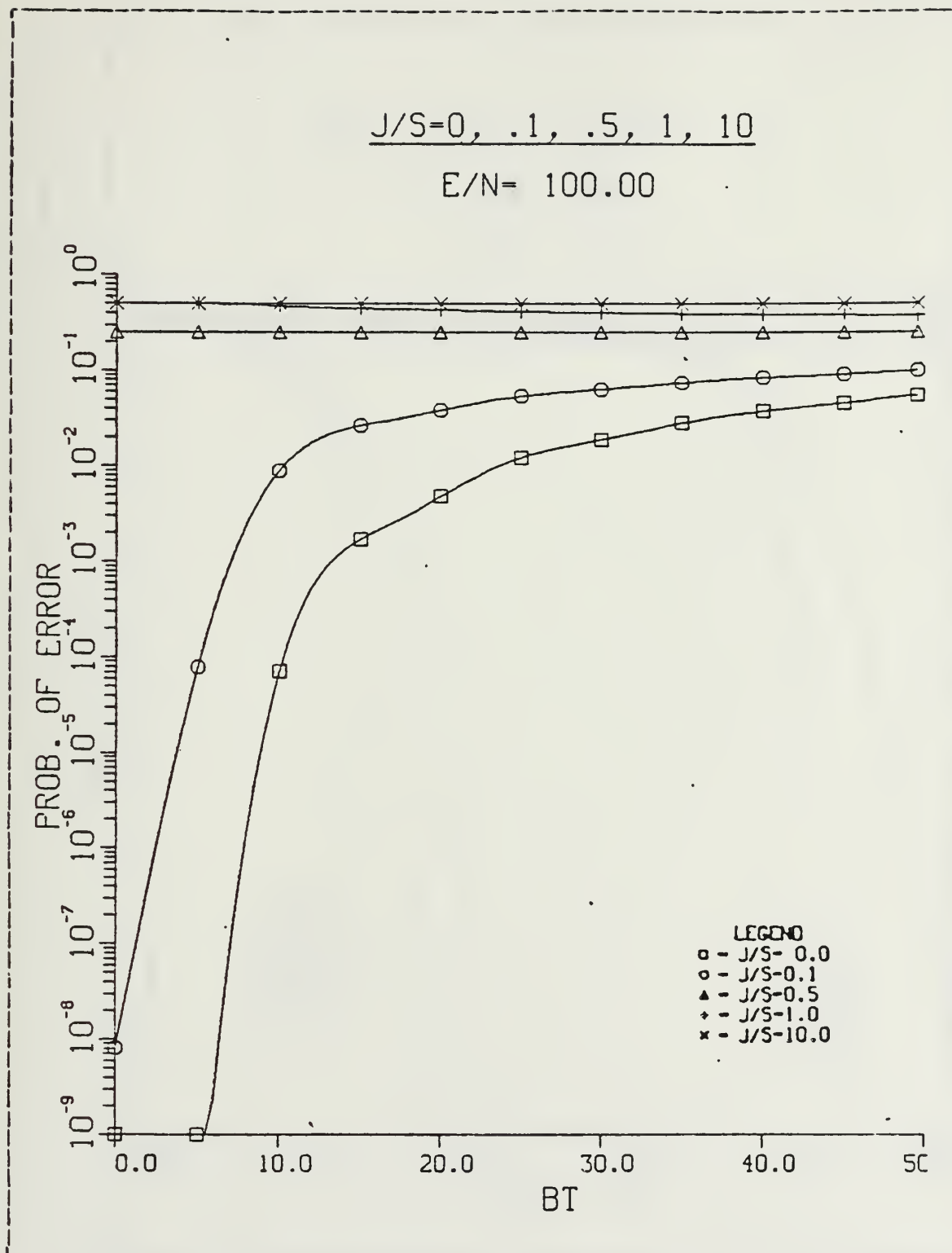Figure A.7. Coherent PSK Receiver with an Ideal
Front-End Filter, BT = 12.56
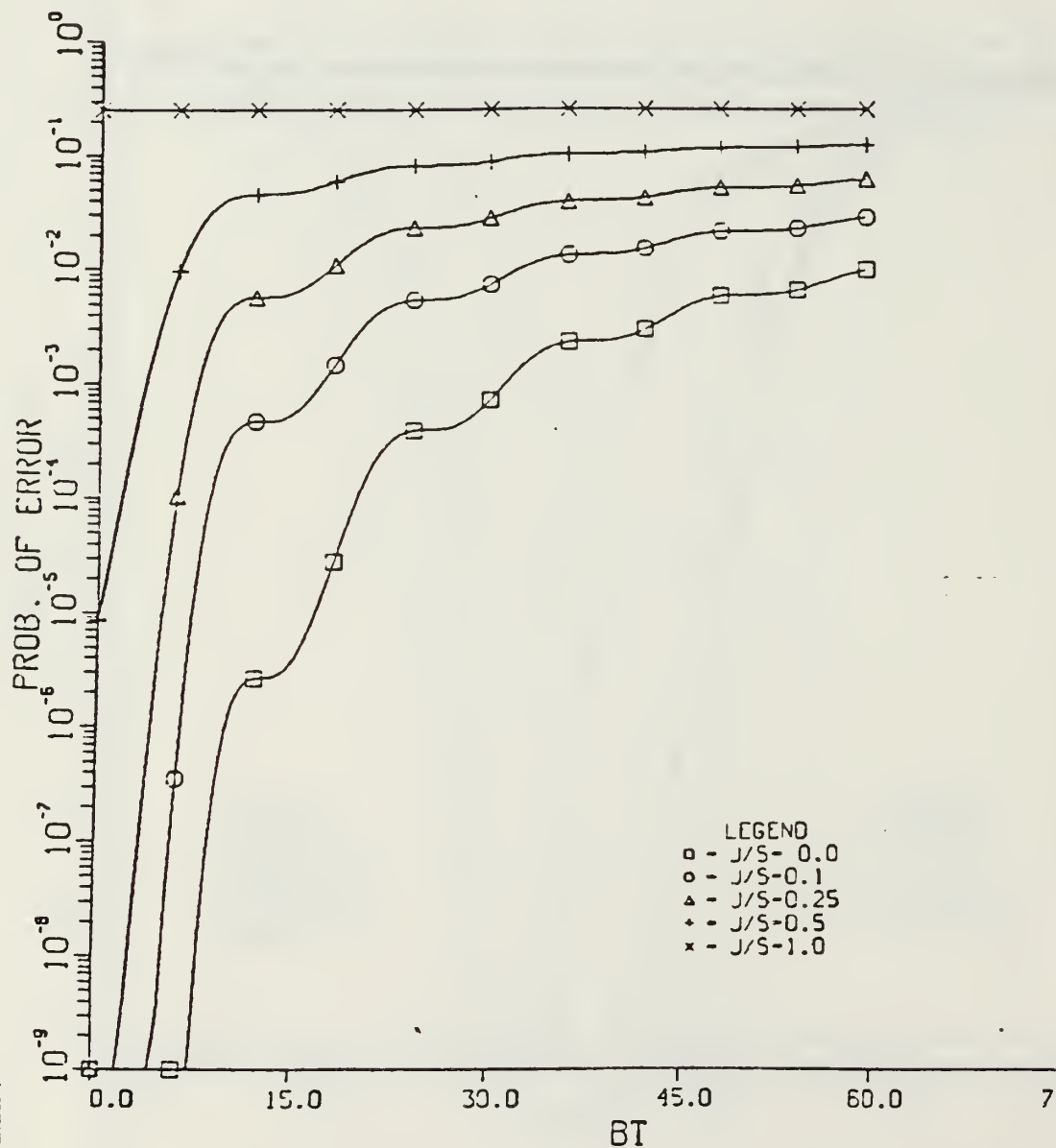
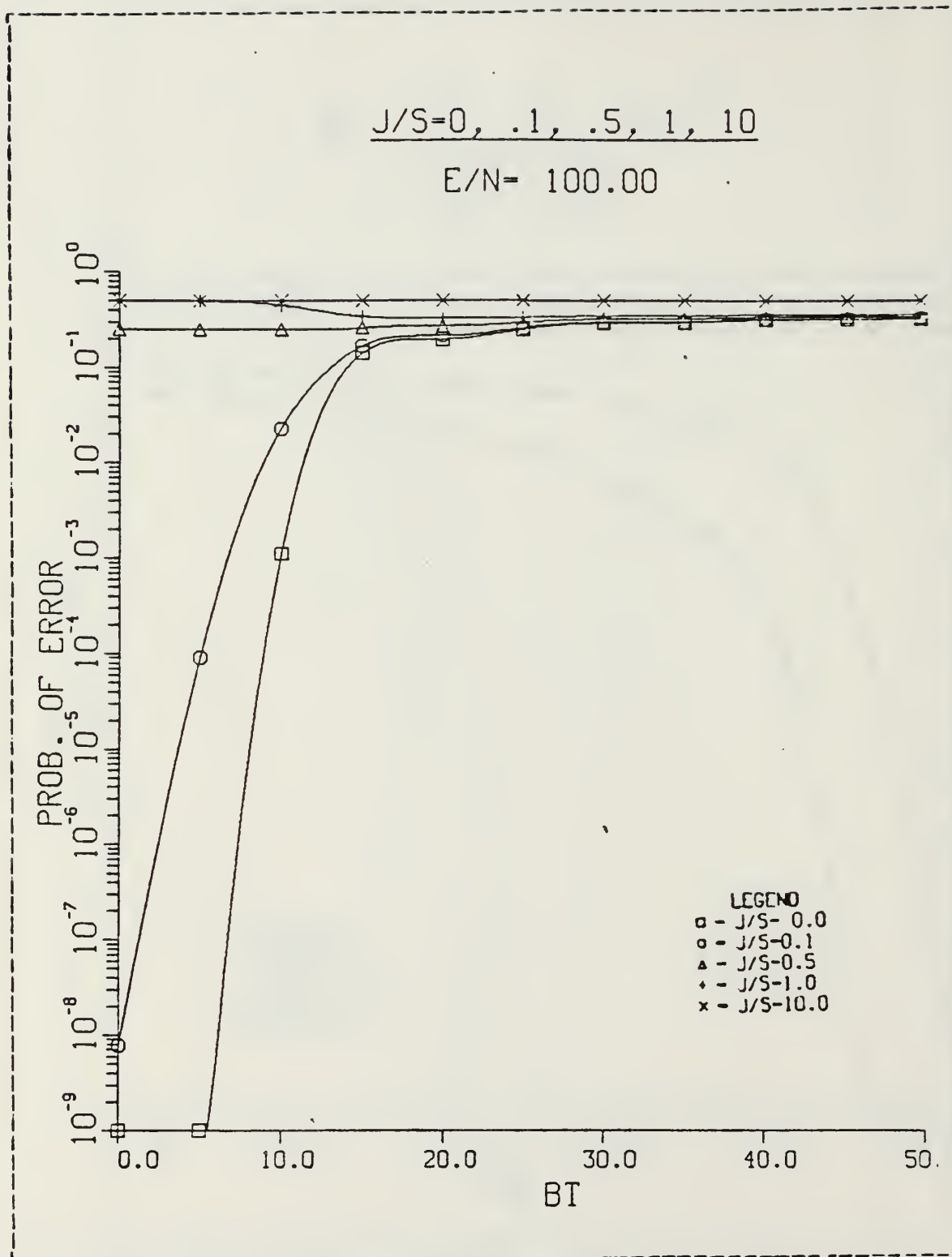Figure A.8. Coherent PSK Receiver with an Ideal
Front-End Filter, E/N = 100

106
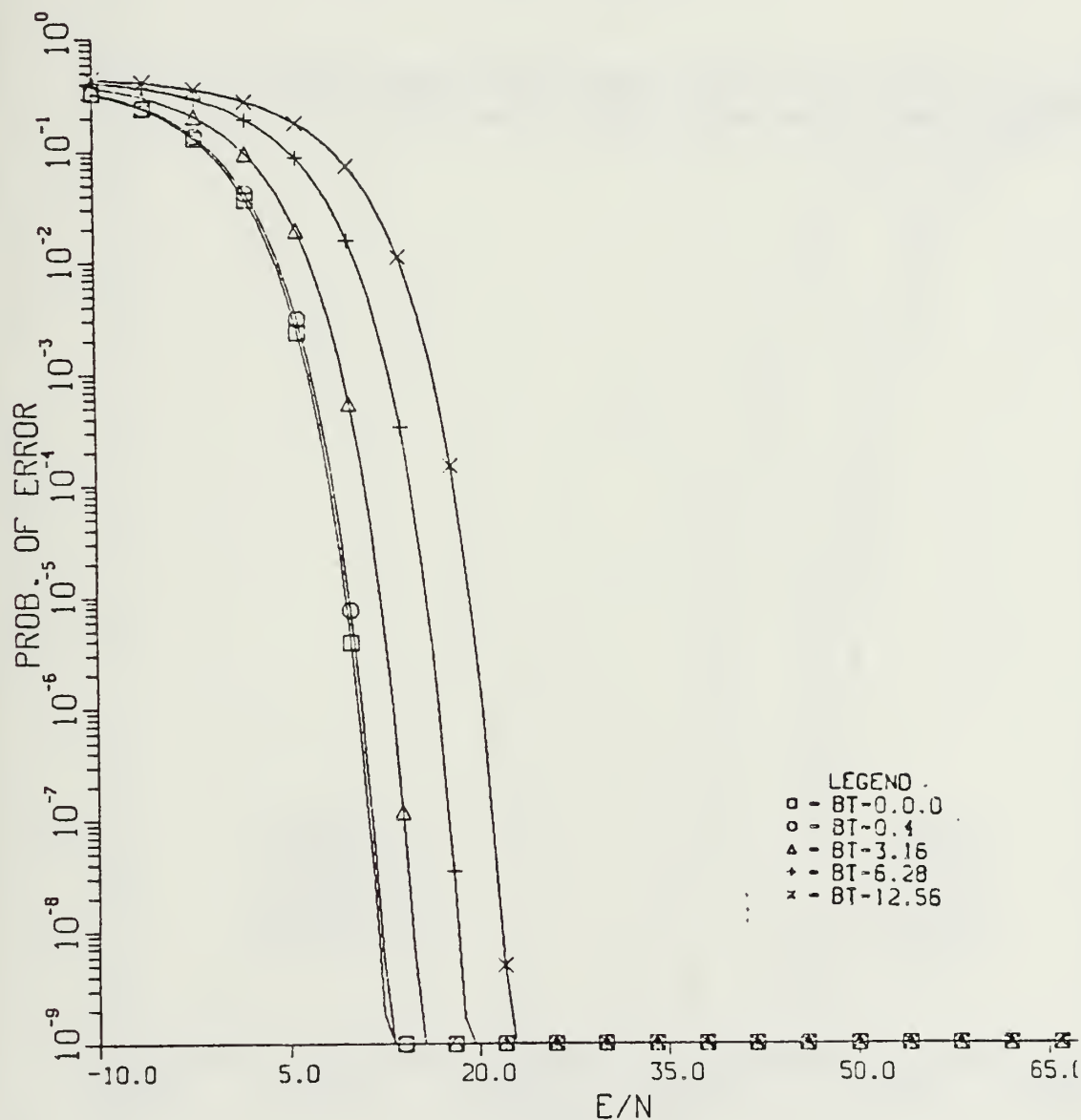
Figure A.9.   Coherent PSK Receiver with an Ideal
Front-End Filter with Variable BT

107
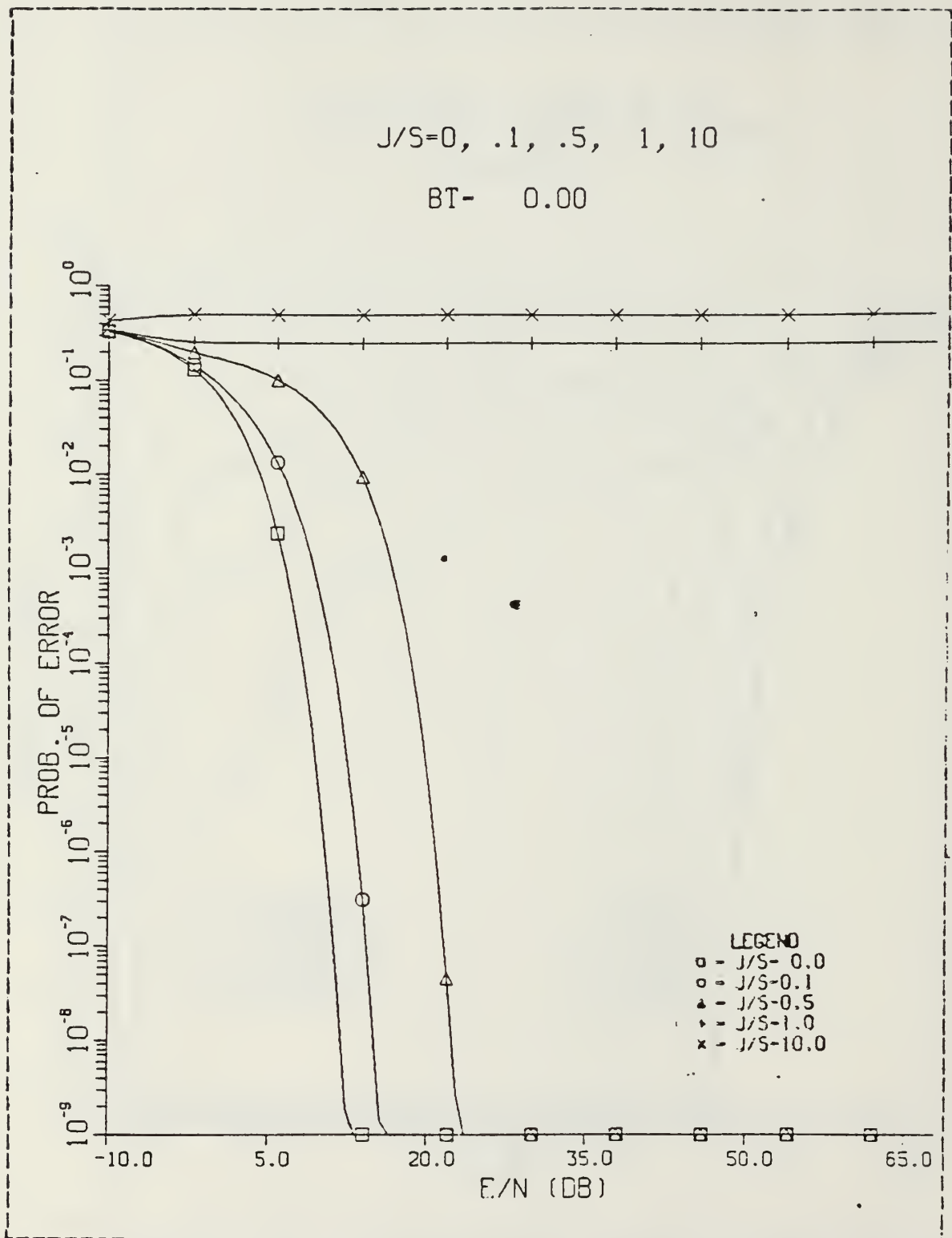
Figure A.10.   Coherent PSK Reciver with a Second
Order Front-End Filter (w/BT = 0.0)

108
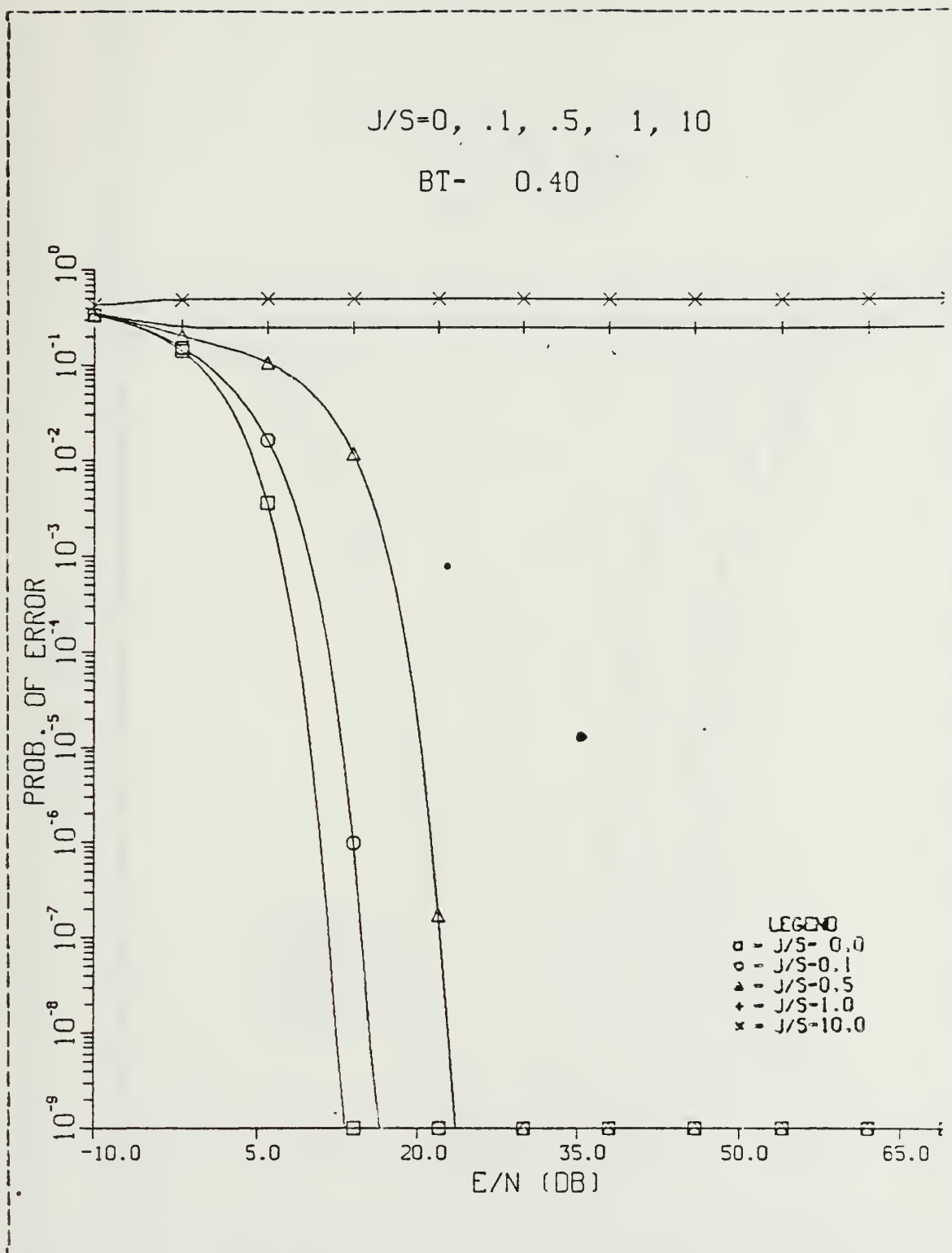
Figure A.11. Coherent PSK Receiver with a Second
Order Front-End Filter (w/BT = 0.4)

109
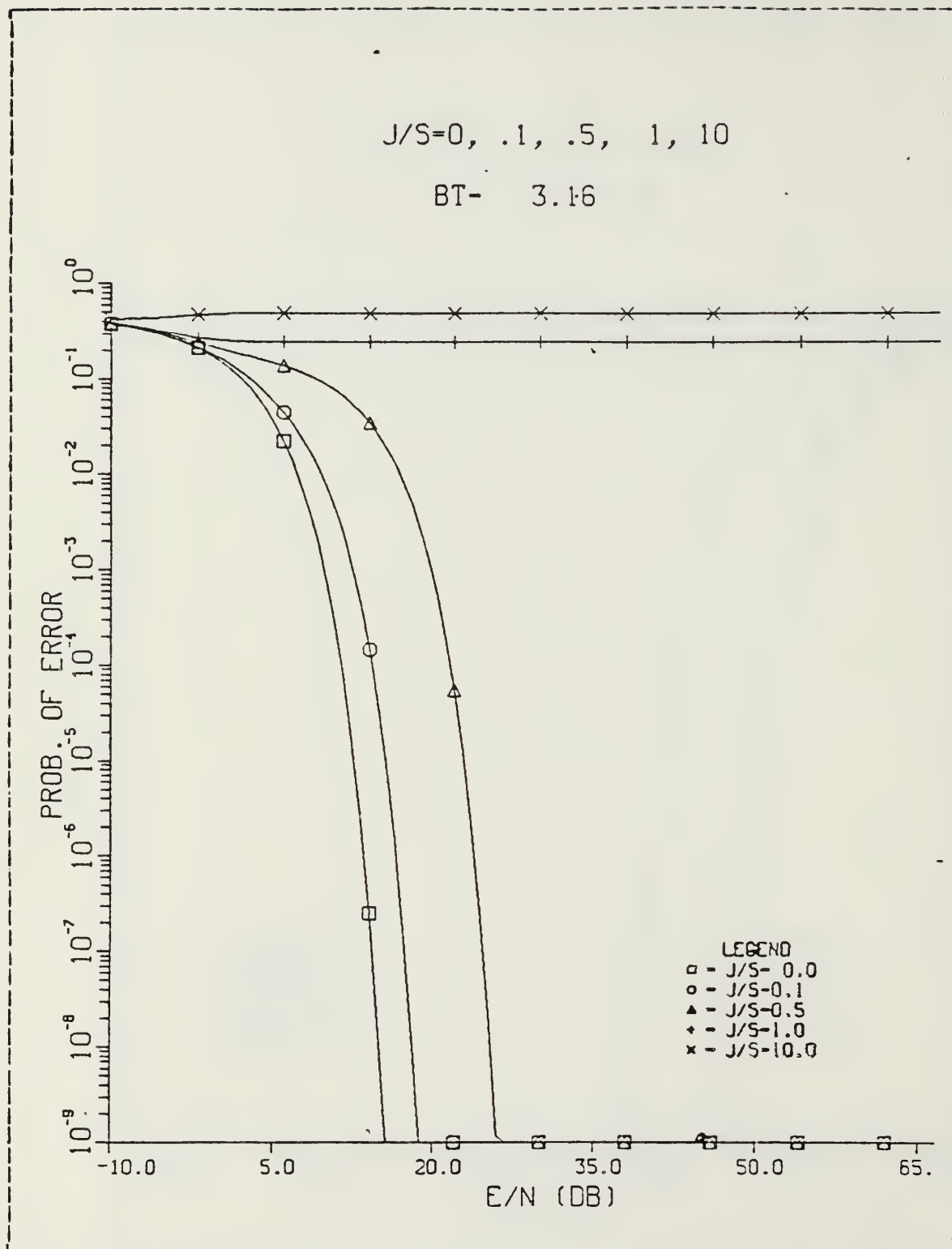
Figure A.12.   Coherent PSK Reciver with a Second
                Order Front-End Filter (w/BT = 3.16)

110
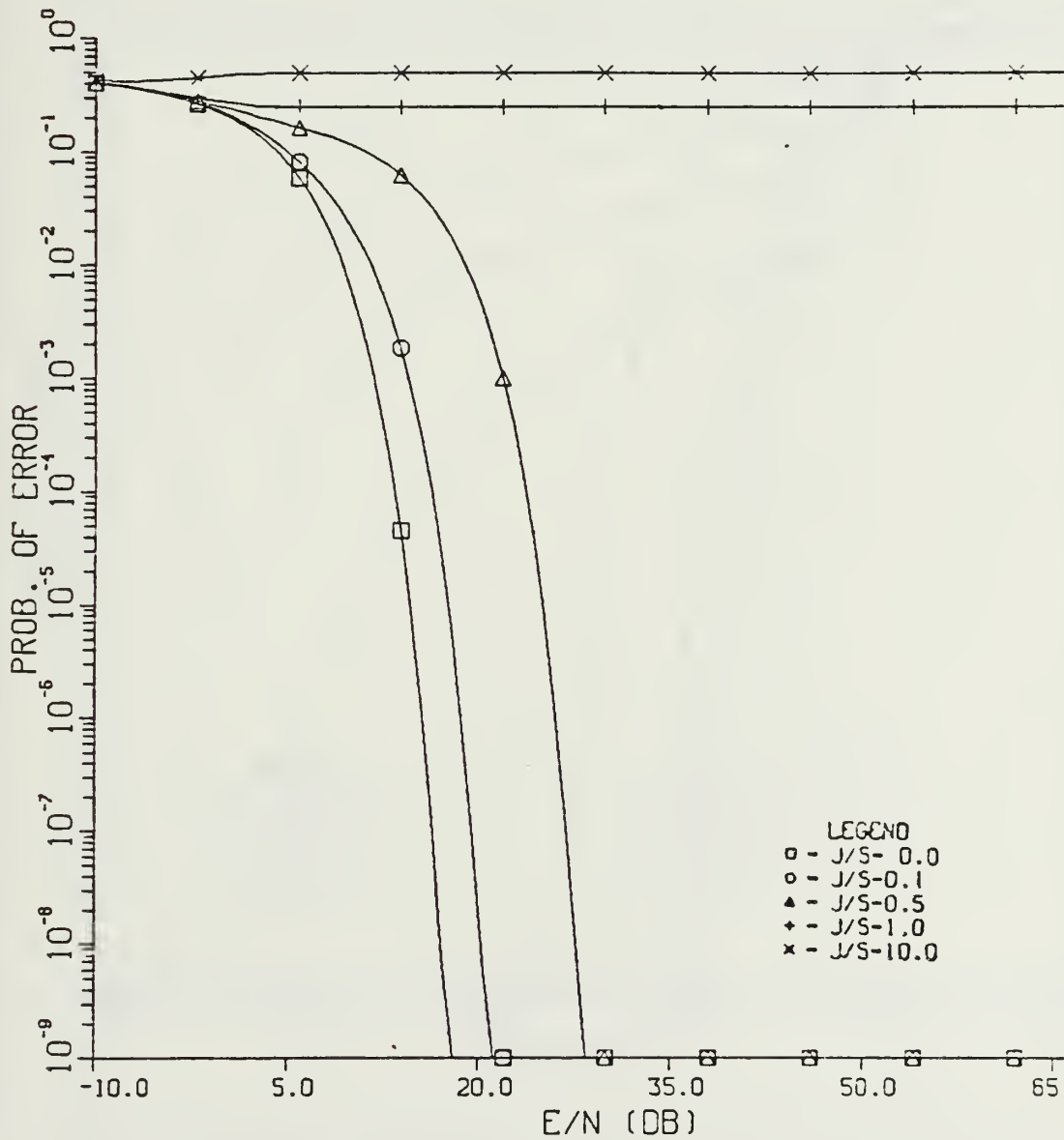
Figure A.13. Coherent PSK Receiver with a Second
Order Front-End Filter (w/BT = 6.28)

111
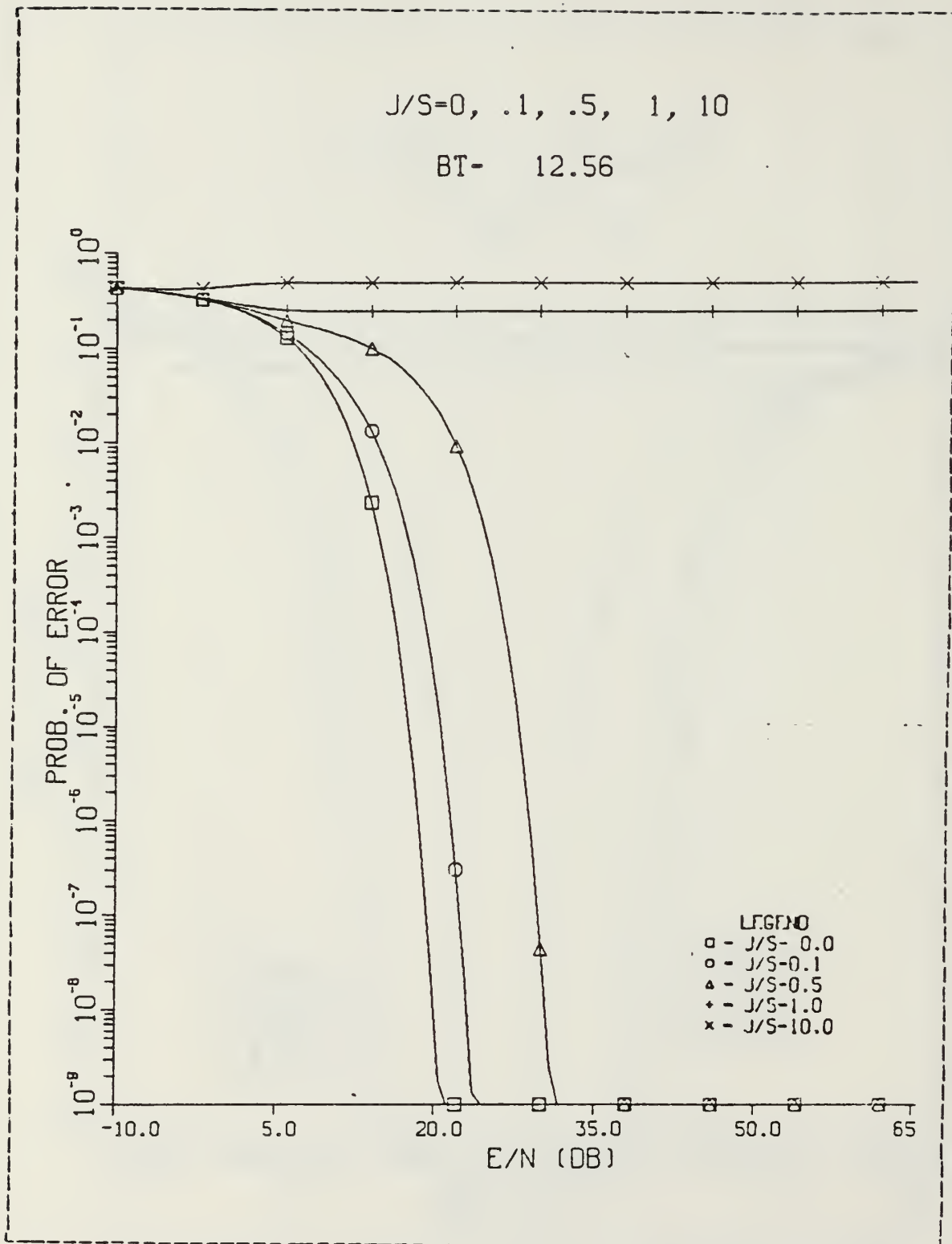
Figure A.14.   Coherent PSK Receiver with a Second
                Order Front-End Filter (w/BT = 12.56)

112
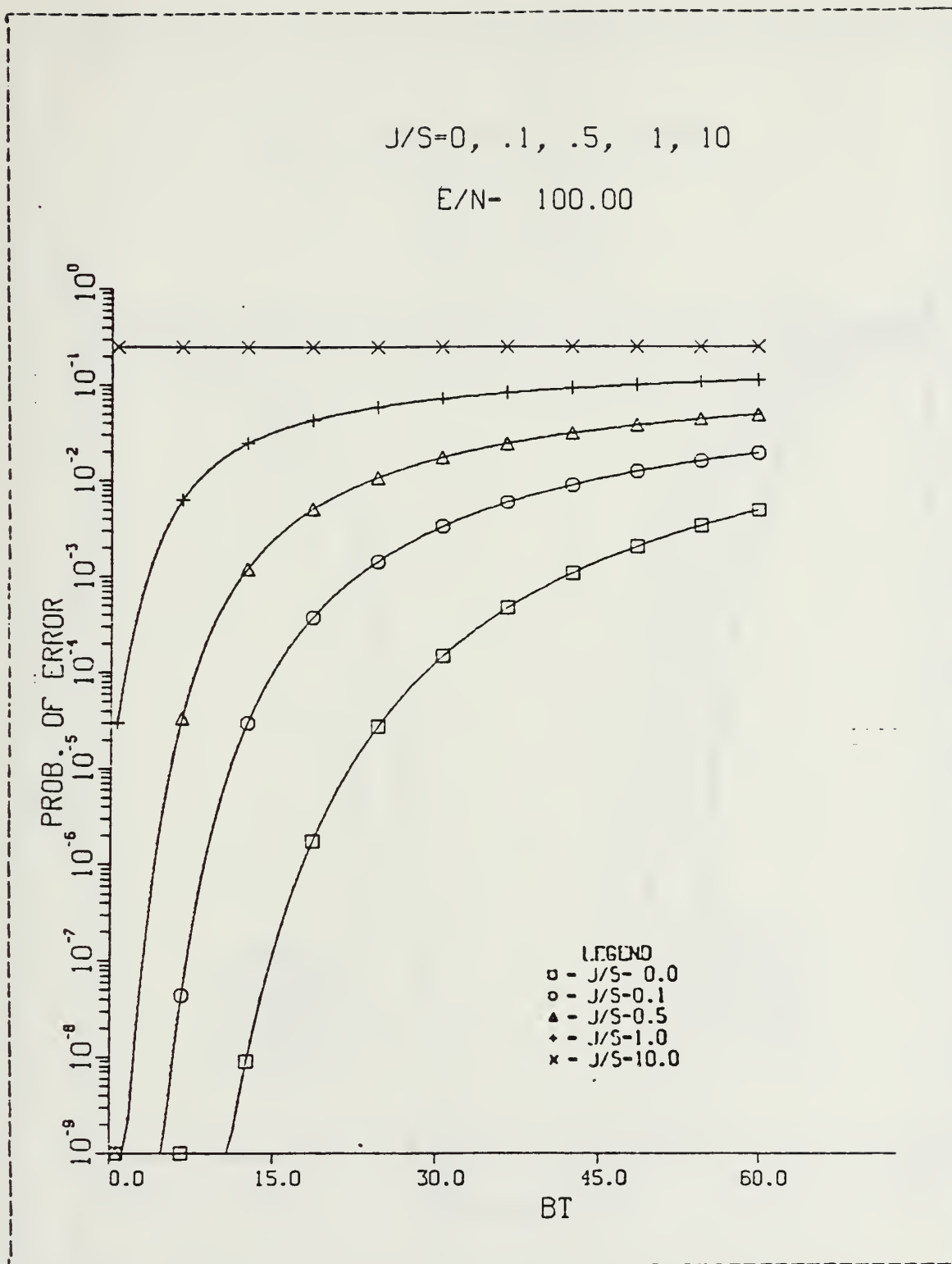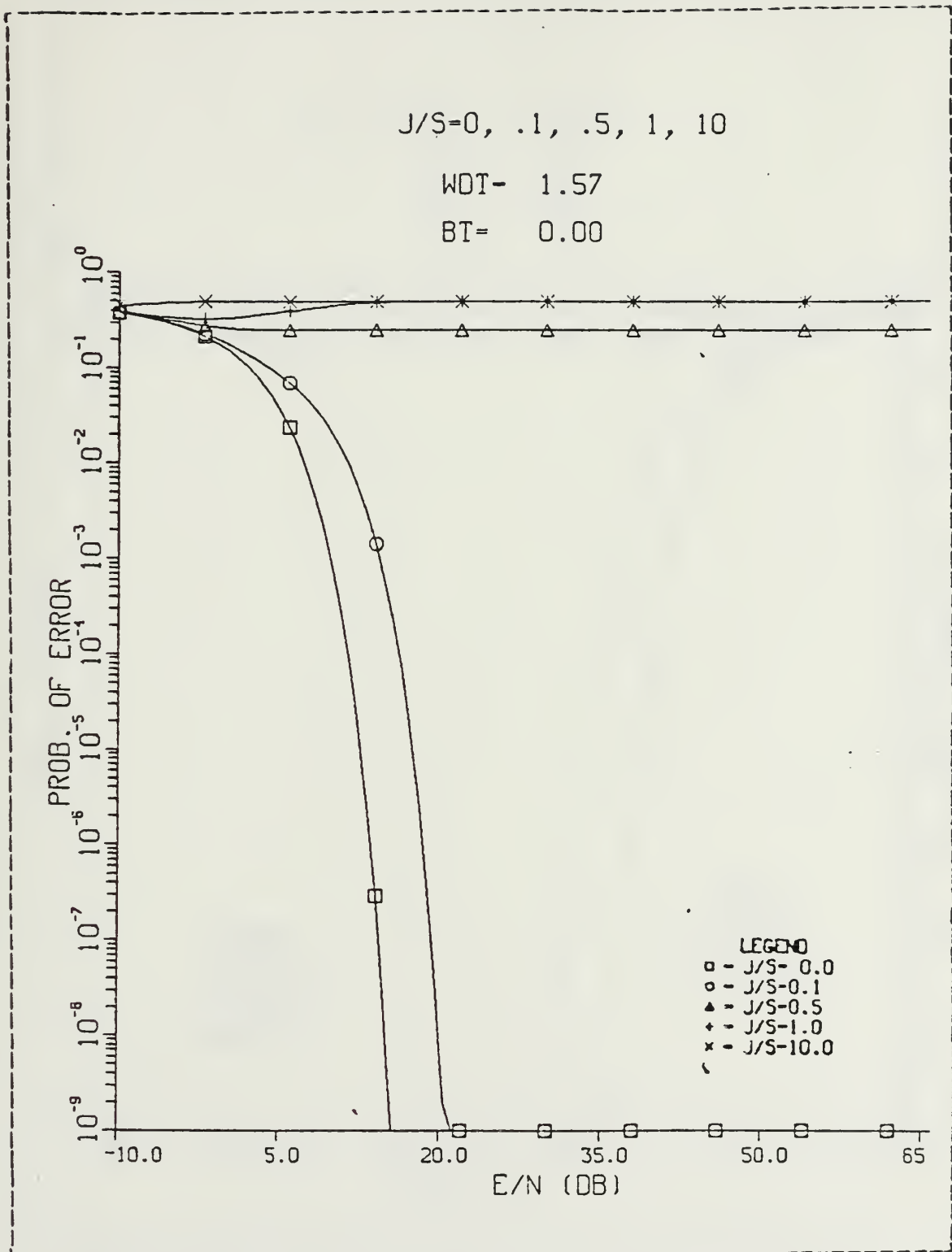
Figure A.15.   Coherent PSK Receiver with a Second
Order Front-End Filter (E/N = 100)

113

Figure A.16.   Coherent PSK Receiver with a Second
Order Front-End Filter (w/various BT)

114

Figure A.17.   Coherent FSK Receiver with an Ideal
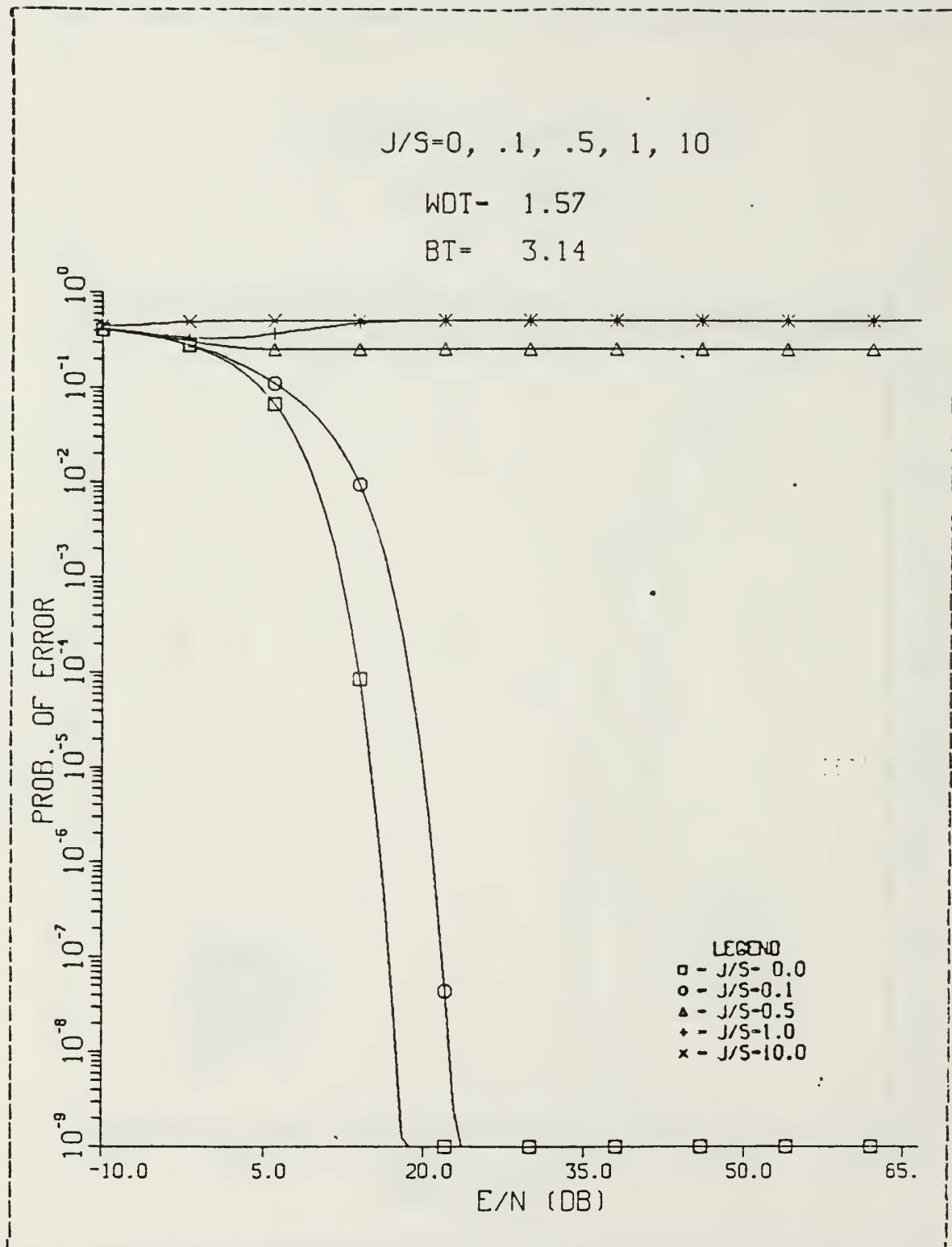   Front-End Filter, WdT = 1.57, BT = 0.00

115

Figure A.18. Coherent FSK Receiver with an Ideal
Front-End Filter, WdT = 1.57, BT = 3.14
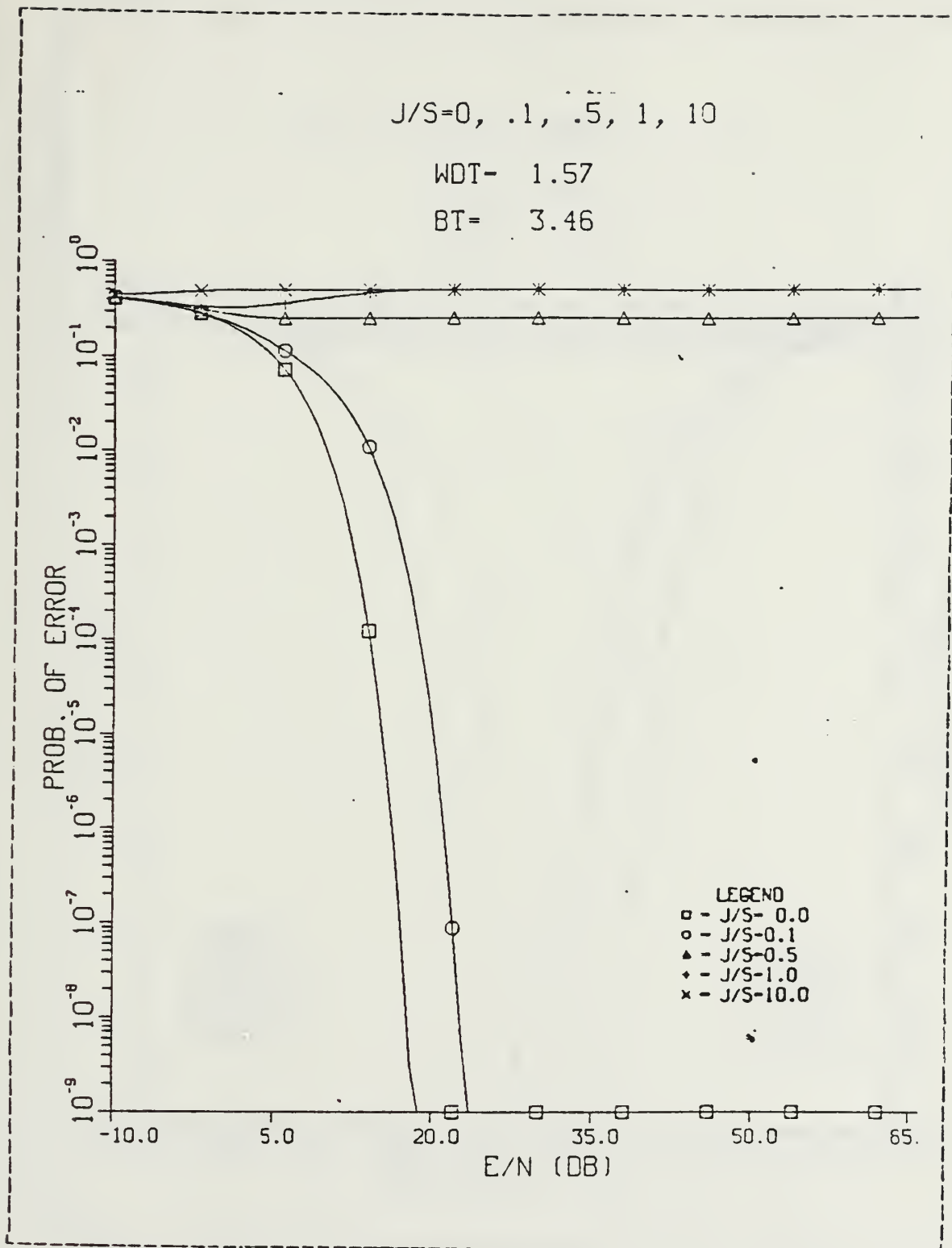
116

Figure A.19. Coherent FSK Receiver with an Ideal
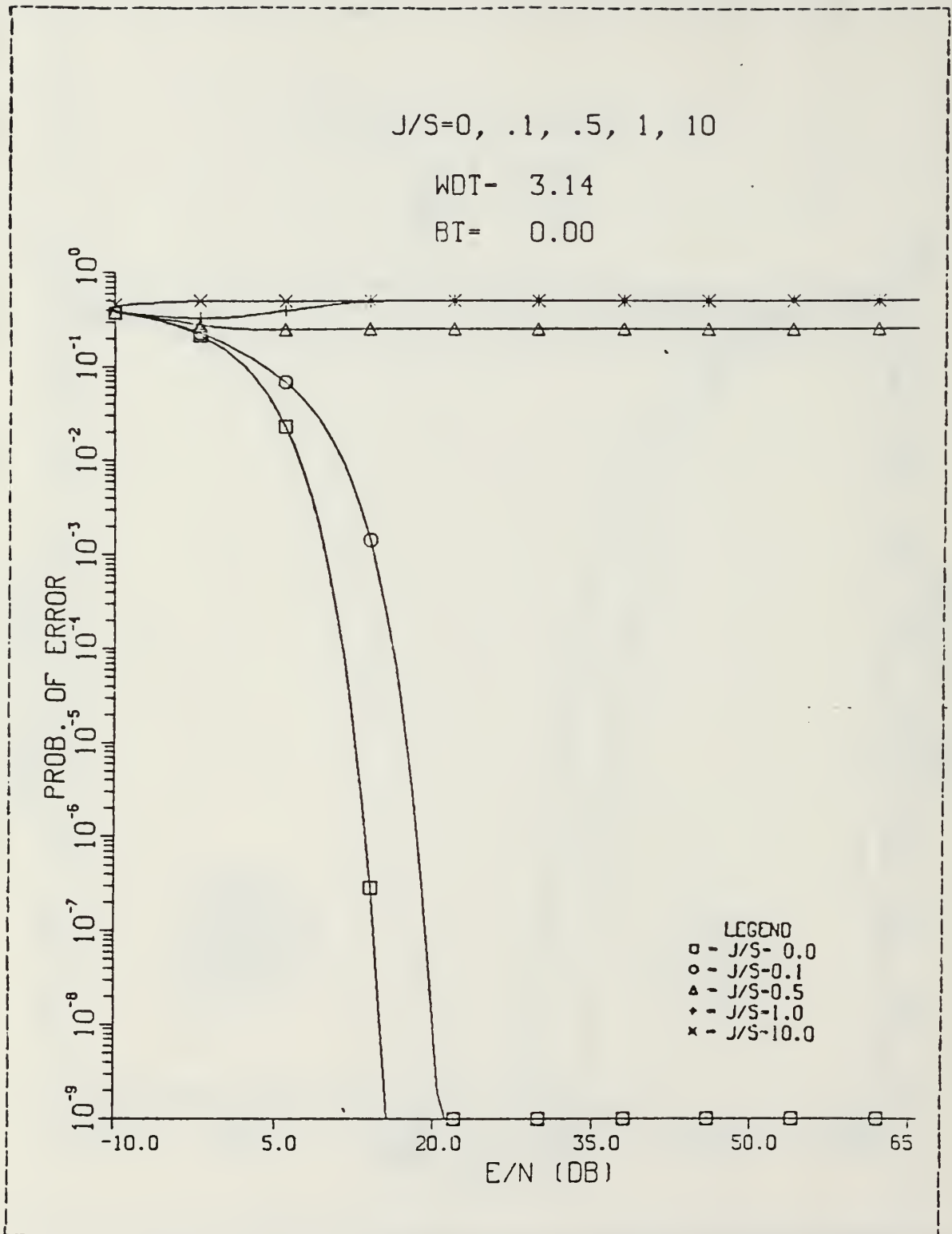Front-End Filter, WdT = 1.57, BT = 3.46

117

Figure A.20.   Coherent FSK Receiver with an Ideal
             Front-End Filter, WdT = 3.14, BT = 0.00

118

Figure A.21.   Coherent FSK Receiver with an Ideal
               Front-End Filter, WdT = 3.14, BT = 6.28

119

Figure A.22. Coherent FSK Receiver with an Ideal
Front-End Filter, WdT = 3.14, BT = 6.91

120

Figure A.23.   Coherent FSK Receiver with an Ideal
                Front-End Filter, WdT = 1.57, E/N = 100

121

Figure A.24. Coherent FSK Receiver with an Ideal
Front-End Filter, WdT = 3.14, E/N = 100

122

Figure A.25. Coherent FSK Receiver with a Second
Order Front-End Filter, WdT = 1.57, BT = 0.00

123

Figure A.26. Coherent FSK Receiver with Second Order
Front-End Filter, WdT = 1.57, BT = 3.14

Figure A.27. Coherent FSK Receiver with a Second
Order Front-End Filter, WdT = 1.57, BT = 3.46
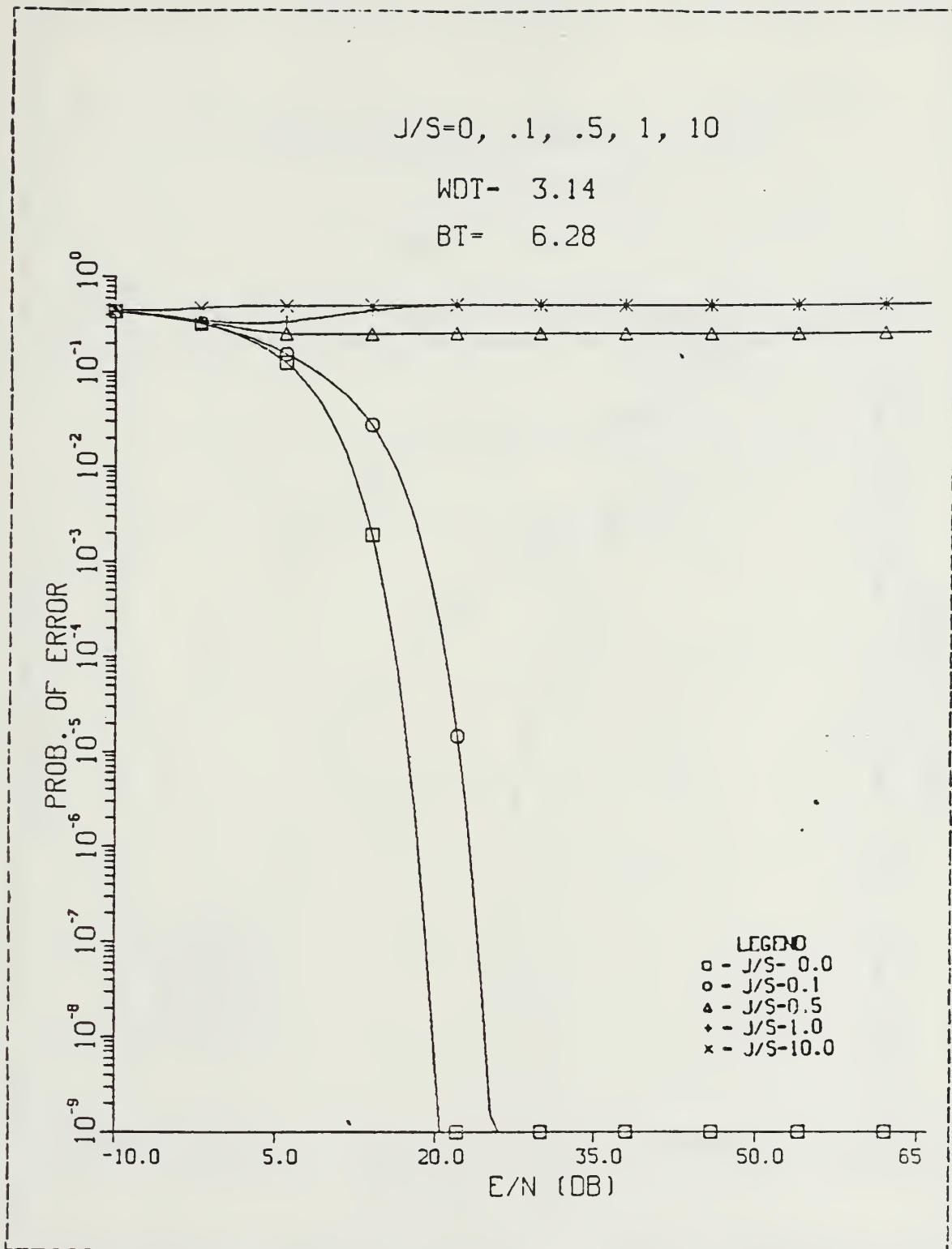
125

Figure A.28.   Coherent FSK Receiver with a Second Order
Front-End Filter, WdT = 3.14, BT = 0.00

126

Figure A.29.   Coherent FSK Receiver with a Second Order
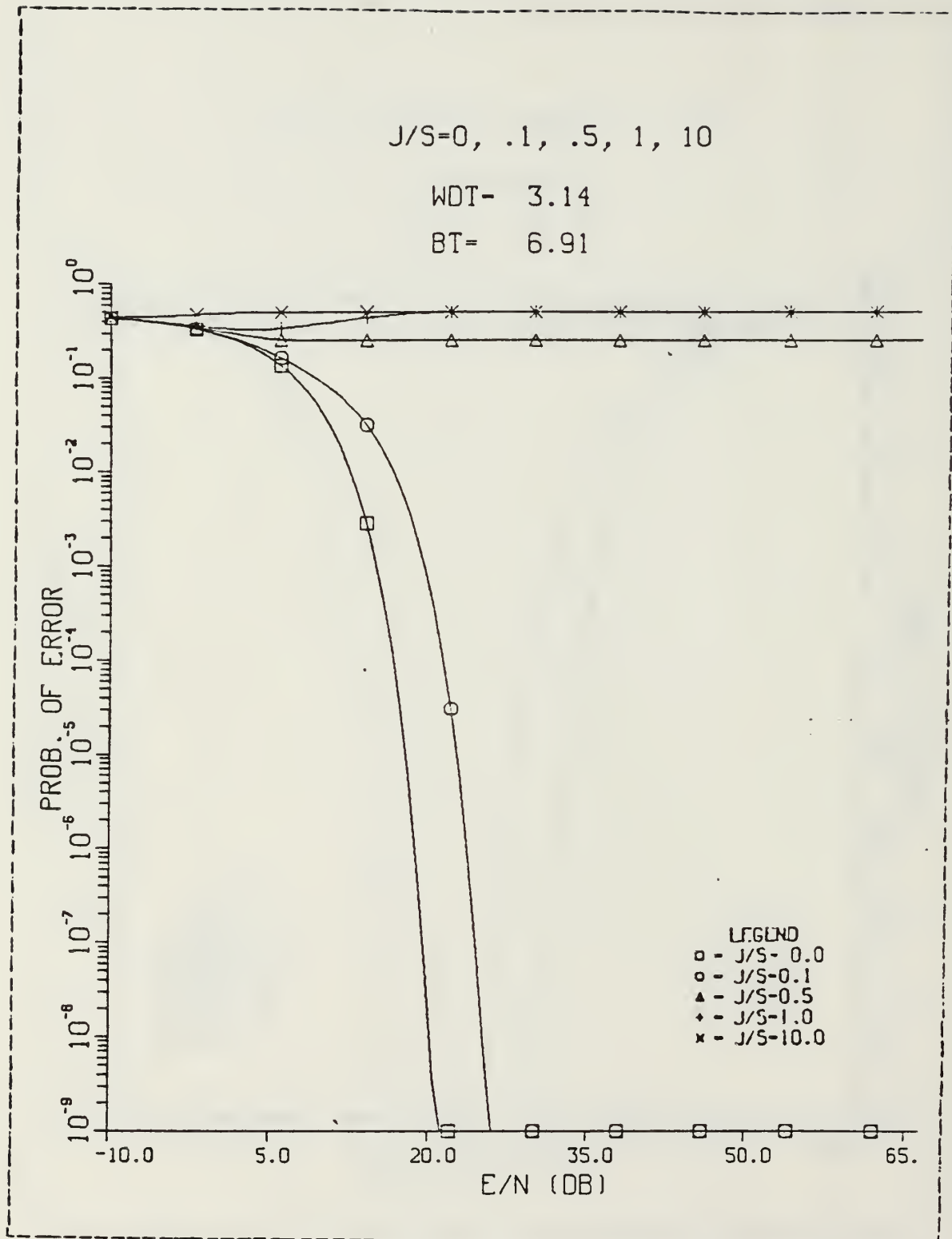   Front-End Filter, WdT = 3.14, BT = 6.28

127

Figure A.30.   Coherent FSK Receiver with a Second Order
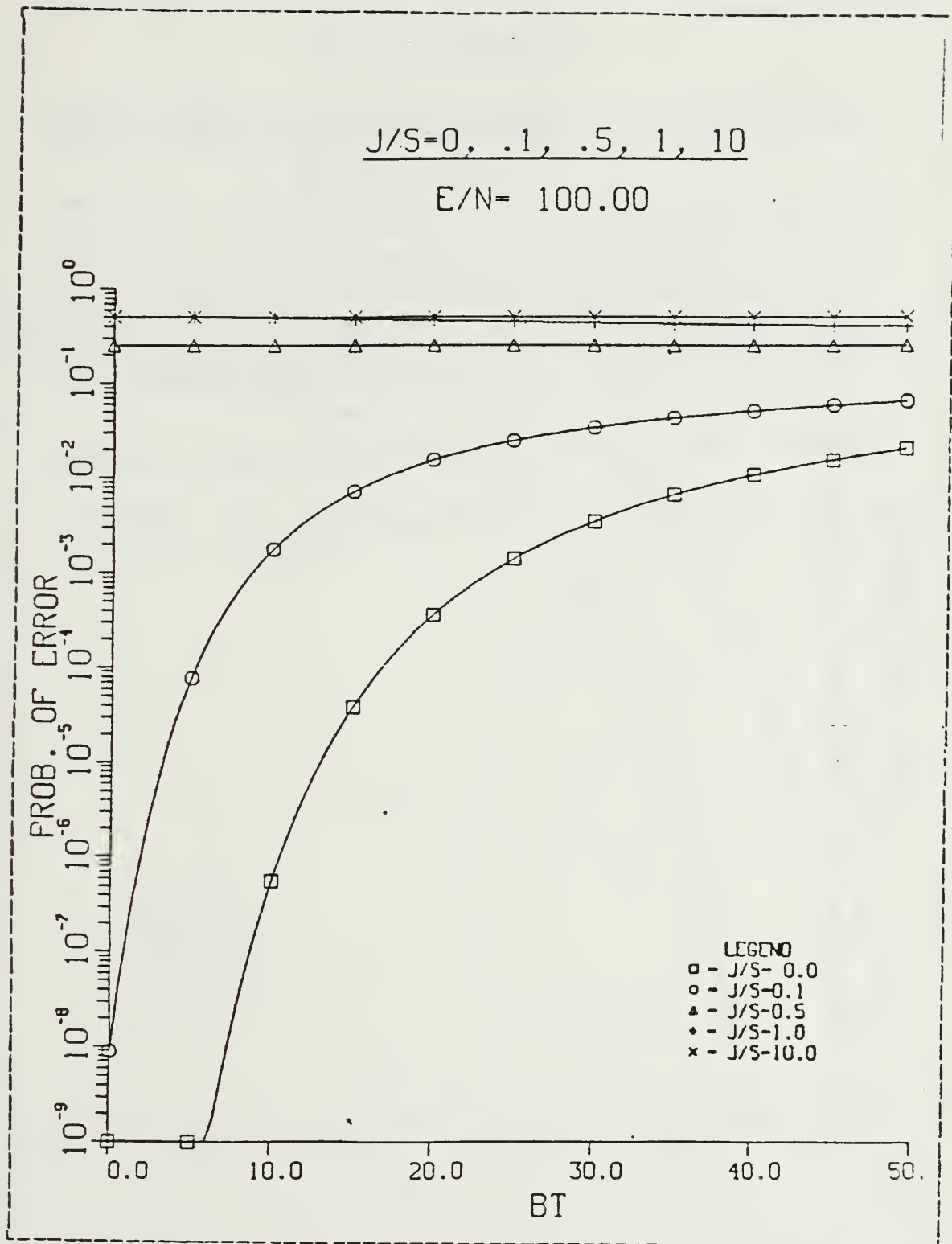   Front-End Filter, WdT = 3.14, BT = 6.91

Figure A.31. Coherent FSK Receiver with a Second Order
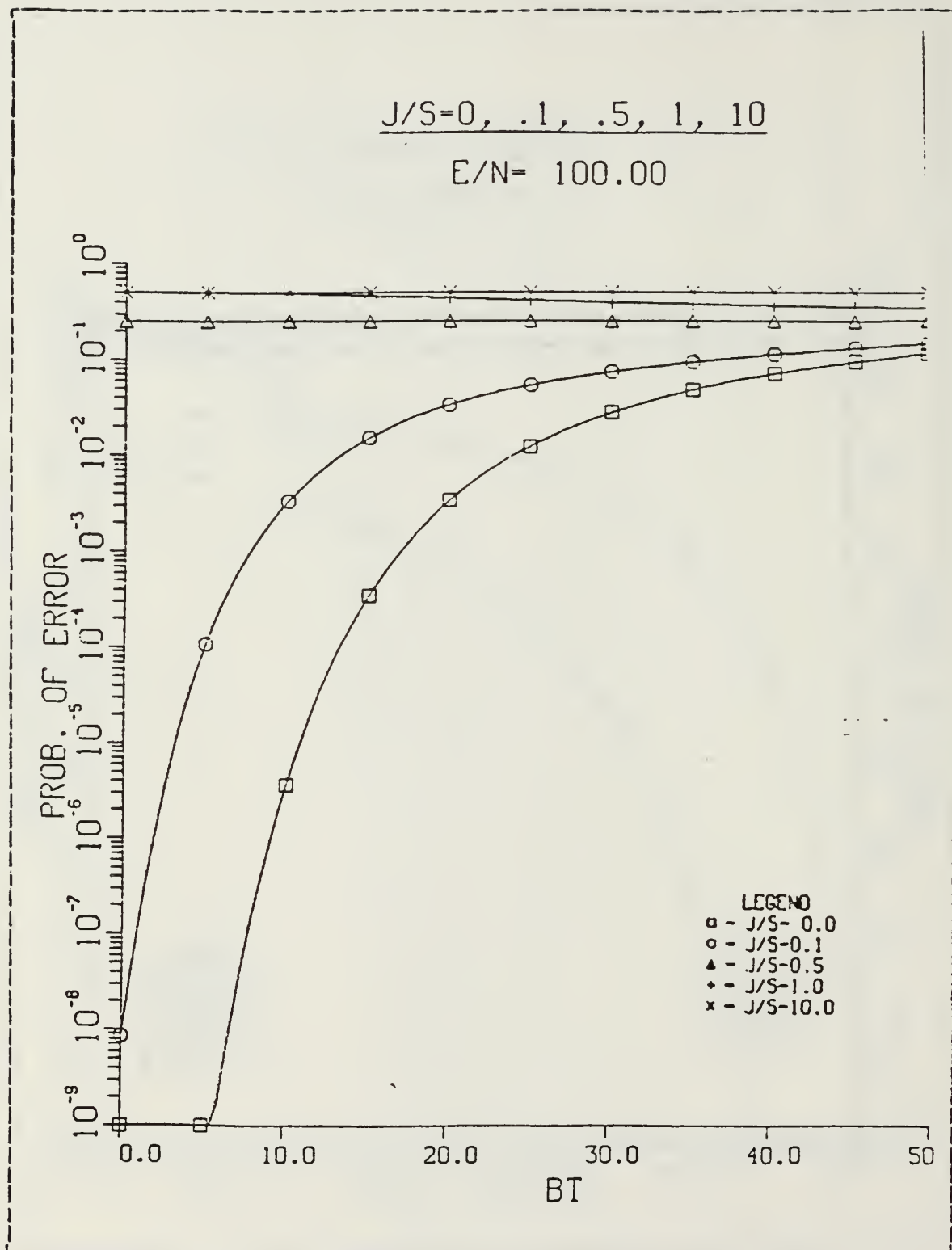Front-End Filter, WdT = 1.57, E/N = 100

Figure A.32. Coherent FSK Receiver with a Second Order
Front-End Filter, WdT = 3.14, E/N = 100

130

LIST OF REFERENCES

1. Srinath, M. D., Rajasekaran, P. K. An Introduction to Statistical Signal Processing with Applications, John Wiley and Sons, 1979.

2. Bukofzer, D. Final Report for Research Contract No. 5156-5160, "Performance of Optimum and Suboptimum Incoherent Digital Communications Receivers in the Presence of Noise and Jamming," February 1984.

3. Farwell, F.T., An Analysis of Digital Coherent Receivers in a Jamming Environment, Master's Thesis, Naval Postgraduate School, Monterey, California, 1984.

4. Torrieri, D.J. Principles of Military Communications Systems, Artech House Inc., 1981.

5. Gagliardi, R.M. Introduction to Communications Engineering, John Wiley and Sons, 1976.

INITIAL DISTRIBUTION LIST

No. Copies

1. Defense Technical Information Center 2
   Cameron Station
   Alexandria, Virginia 22304-6145

2. Library, Code 0142 2
   Naval Postgraduate School
   Monterey, California 93943-5100

3. Department Chairman, Code 62 1
   Department of Electrical and Computer
       Engineering
   Naval Postgraduate School
   Monterey, California 93943-5100

4. Prof. D. Bukofzer, Code 62Bh 5
   Naval Postgraduate School
   Monterey, California 93943-5100

5. Prof. S. Jaurequi, Code 62Ja 2
   Naval Postgraduate School
   Monterey, California 93943-5100

6. Naval Air Test Center 3
   Systems Engineering Test Directorate
   Electronic Warfare and Reconnaissance
       Branch
   Patuxent River, Maryland 20670
   (Attn: D. Macone Sy-92B)

7. VAQ-129 1
   Naval Air Station
   Whidbey Island
   Oak Harbor, Washington 98278
   (Attn: LCDR J. Powell)

8. CPT Ang Bing Ning 1
   C/o Naval Plans Department
   Hq RSN, MINDEF
   Tanglin, Singapore 1024
   Republic of Singapore